POLITECNICO DI TORINO
ESCUELA TÉCNICA SUPERIOR DE INGENIEROS INDUSTRIALES DE MADRID

MASTER OF SCIENCE IN AUTOMOTIVE ENGINEERING

ACADEMIC YEAR 2018/2109

MASTER’S THESIS

SUSPENSION DESIGN FOR A FSAE ELECTRIC VEHICLE

CANDIDATE
MARCO MATTANA

TUTORS
ANDREA TONOLI
FCO JAVIER PÁEZ AYUSO

To my parents, who never stopped believing in me, who allowed me to do everything.

To Martina, who has been with me throughout this time,
always trusting in my potential, even more than myself.

To the people I met in Erasmus, who made me enjoy myself,
learn and kept me company during my studies abroad.

To my friends, who believe in me as if I was their brother.

To Madrid, the city that made me discover a new side of myself.

To 2019, the most incredible and important year of my life, in which I really grew up.

To me, that I have achieved my goal. The first of many.

Ai miei genitori, che non hanno mai smesso di credere in me, che mi hanno permesso tutto.

A Martina, che mi ha accompagnato in tutto questo tempo,
sempre confidando nelle mie potenzialità, anche più di me stesso.

Alle persone che ho conosciuto in Erasmus, che mi hanno fatto divertire,
imparare e che mi hanno tenuto compagnia durante gli studi all'estero.

Ai miei amici, che credono in me come fossi il loro fratello.

A Madrid, la città che ha fatto scoprire un novo lato di me.

Al 2019, l'anno più incredibile e importante della mia vita, nel quale sono realmente cresciuto.

A me, che ho raggiunto il mio obiettivo. Il primo di tanti.

ABSTRACT

In order to conclude my university experience in the best possible way, I decided to spend the last semester of the second year of the magistral abroad, namely in Madrid. Here I had the opportunity to study in Spanish and carry out the activity of my project in the INSIA car investigation centre, perhaps the best in Iberian territory.

Here I met Professor Javier Páez, head of the racing team of the *Universidad Politécnica de Madrid*, who allowed me to deepen one of the topics that interests me most for my future work.

Having said that, the thesis, as you can already understand, is focused on the design and development of the suspensions of the future electric vehicle UPM Racing, which you will see racing in the competition of 2020. The aim is to create an optimal geometry that is adapted to the needs of the competition, justifying the choices made.

It should be noted that this project does not aim to create the final geometries for this vehicle but must be seen as a starting point for the actual design. There are many points of improvement for the suspensions, but this requires the organization and work simultaneously with the different groups of the team, such as dynamic vehicle, chassis, cost analysis, and so on.

To start this project, we relied on previous work done by other guys for their theses, in which, similarly to this, they designed and developed the suspensions of the relevant years.

Starting from the combustion vehicle and using the Adams/Car software, the work was resumed to be reanalysed and to identify the necessary improvement points. In fact, initially, the kinematics of these two suspensions are analysed, placing in the graphs the variations of the main parameters to be studied, and not their absolute values, which will be set according to the track and the preferences of the pilot.

Subsequently, this geometry is modified as if the vehicle were electric: this will be the starting point for the design of the final model of the suspension. Also in this case, the kinematic behaviour is analysed and compared with the previous one.

Once this is done, it is the turn of the final model. Initially, the factors of the previous model are defined that need to be modified, in order to get as close as possible to the real conditions. In fact, the following are modified: rear track width, to make room for the batteries; the characteristic and dimensions of the tyres, with the coefficients for Pacejka's magic formula, identified thanks to the work of a guy from UPM; the wheelbase is increased, according to the needs of the team; finally, the actual space occupied by the electric motor, which will be installed in the wheel, is considered.

Again, the kinematic analysis is carried out and then the dynamic one. In particular, critical load cases that may occur in the competition tests are analysed: braking, longitudinal and lateral accelerations and combined situations. From these, it will be possible to evaluate the forces acting on the joints and, consequently, to understand whether the material chosen for the individual components is sufficient to bear the load on them.

There are many possible improvements to this project, which can be used as a starting point for further development.

CONTENTS

ABSTRACT I

CONTENTS III

LIST OF FIGURES VII

1. INTRODUCTION 1
  - 1.1 Previous projects 1
  - 1.2 Objectives of the project 1
  - 1.3 Methodology 2

2. FORMULA SAE COMPETITION 3
  - 2.1 History of *FSAE* competition 3
  - 2.2 Competition 3
  - 2.3 Safety tests 4
  - 2.4 Static events 5
  - 2.5 Dynamic events 5
  - 2.6 UPM Racing 6
  - 2.7 FSAE General Vehicle Design Regulations 7
    - 2.7.1 General design requirements 8

3. SUPENSIONS 9
  - 3.1 Function 9
  - 3.2 Suspension elements 11
    - 3.2.1 Elastic elements 11
    - 3.2.2 Dampers 11
    - 3.2.3 Clamping and guiding elements 11
    - 3.2.4 Knuckle 11
    - 3.2.5 Hub 12
    - 3.2.6 Oscillating arms 12

3.2.7 Spherical joints 12
3.2.8 Rocker 12
3.2.9 Anti-roll bar 13
3.3 Suspension geometries 13
3.3.1 Rigid suspensions 13
3.3.2 Semi-independent or semi-rigid suspensions 14
3.3.3 Independent suspensions 15
4. VEHICLE DYNAMICS 19
4.1 Vehicle models 19
4.1.1 Kinematic steering (low-speed cornering) 19
4.1.2 Bicycle model (high-speed cornering) 20
4.1.3 Rigid-vehicle model (3 d.o.fs.) 21
4.1.4 Complete model (10 d.o.fs.) 23
4.2 Induced steering 24
5. MAIN SUSPENSION PARAMETERS 27
5.1 Kinematic parameters 27
5.1.1 Wheelbase 27
5.1.2 Track width 28
5.1.3 Camber angle 29
5.1.4 King-pin axis 29
5.1.5 Mechanical trail 30
5.1.6 Scrub radius 30
5.1.7 Caster angle 31
5.1.8 Toe angle 32
5.1.9 Instant centre of rotation (IC) 32
5.1.10 Roll centre 32
5.1.11 Anti-features 33
5.1.12 Ackermann steering 34
5.2 Dynamic parameters 35
5.2.1 Spring rate, $\boldsymbol{KS}$ 35

5.2.2 Wheel rate, $\boldsymbol{KW}$ 35

5.2.3 Motion ratio, $\boldsymbol{MR}$ 35

5.2.4 Tire radial stiffness 36

5.2.5 Side slip stiffness 36

5.2.6 Natural frequency of the sprung mass 37

5.2.7 Damping coefficient 38

5.2.8 Anti-roll bar stiffness 38

6. SUSPENSION DESIGN 39

6.1 Recommended values 39

6.1.1 Wheelbase 39

6.1.2 Track 40

6.1.3 Roll centre 40

6.1.4 Camber angle 40

6.1.5 Caster angle 41

6.1.6 King-pin inclination 41

6.1.7 Scrub radius 42

6.1.8 Toe angle 42

6.1.9 Anti-features 42

6.2 Suspension’s kinematics design 42

6.2.1 Front-view design 42

6.2.2 Side-view design 44

6.3 Suspension’s dynamics design 46

7. ANALYSIS OF SUSPENSION MODELS 49

7.1 Petrol vehicle 49

7.1.1 Geometries 49

7.1.2 Kinematic analysis 51

7.1.3 Definition of improving points 61

7.2 Electric vehicle 62

7.2.1 Geometry 62

7.2.2 Kinematic analysis ... 64
7.2.3 Comments ... 73
7.3 Comparison ... 74
7.3.1 Front suspension ... 74
7.3.2 Rear suspension ... 76
8. FINAL SUSPENSION MODEL FOR THE 2020 UPM RACING ELECTRIC VEHICLE 79
8.1 Requirements for the electric vehicle ... 79
8.1.1 Electric engine ... 79
8.1.2 Rear track ... 80
8.1.3 Wheelbase ... 80
8.1.4 Tire characteristic ... 80
8.2 Final geometry ... 81
8.2.1 Front suspension ... 81
8.2.2 Rear suspension ... 82
8.2.3 Full vehicle ... 83
8.3 Kinematic behaviour ... 84
8.3.1 Front suspension ... 84
8.3.2 Rear suspension ... 89
8.3.3 Comments ... 93
8.4 Dynamic behaviour ... 94
8.4.1 Motion ratios ... 94
8.4.2 Stiffness ... 95
8.4.3 Damping ... 96
8.4.4 Analysis ... 97
8.5 Analysis of forces ... 99
8.5.1 Braking ... 100
8.5.2 Lateral acceleration ... 101
8.5.3 Accelerating in a curve ... 102
8.5.4 Braking in a curve ... 104

8.5.5 Forces on components ... 106
9. CONCLUSIONS ... 109
10. BIBLIOGRAPHY ... 111
10.1 Books ... 111
10.2 Thesis projects and documents ... 111
10.3 Internet sites and videos ... 112
11. ANNEX ... 113
11.1 Suspension hardpoints ... 113
11.1.1 Petrol vehicle ... 113
11.1.2 Electric vehicle ... 113
11.1.3 Final model – 2020 single seater ... 114
11.2 MATLAB scripts ... 114
11.3 Tire model ... 116
11.4 Electric engine technical drawings ... 117

LIST OF FIGURES

Figure 1. FSAE skidpad layout. ... 5
Figure 2. UPM 13C single seater for the 2017 Silverstone competition. ... 6
Figure 3. UPM 03E electric single seater for the 2018/2019 season. ... 7
Figure 4. Vehicle ISO reference system. ... 10
Figure 5. Shock-absorber. ... 11
Figure 6. Knuckle, hub and brake disk. ... 11
Figure 7. Spherical joint. ... 12
Figure 8. Rockers (in gold). ... 12
Figure 9. Anti-roll bar ... 13
Figure 10. Rear rigid-axle suspensión for a rear-wheel-drive vehicle. ... 14
Figure 11. "De Dion" suspension model. ... 14
Figure 12. McPherson suspension. ... 16

Figure 13. Double-wishbone suspension. 16
Figure 14. Multi-link suspension of a Porsche 993. 17
Figure 15. Kinematic steering model. 19
Figure 16. Bicycle model for high-speed cornering. 20
Figure 17. Understeer and oversteer. 20
Figure 18. Curvature gain typical plot. 21
Figure 19. Rigid-model refernce system. 21
Figure 20. Wheel reference frame. 22
Figure 21. Trend of the derivatives of stability. 22
Figure 22. Root locus example. 23
Figure 23. Reference frame of the complete model. 23
Figure 24. Toe characteristics as function of the tie-rod design. 25
Figure 25. Dimensions and forces acting on a vehicle. 28
Figure 26. Camber angle convention. 29
Figure 27. King-pin geometry. 30
Figure 28. Scrub radius definition. 30
Figure 29. Caster angle convention. 31
Figure 30. Toe angle convention (plan view). 32
Figure 31. Position of the instant centre of rotation. 32
Figure 32. Position of the instant centre of rotation and, consequently, of the roll centre.. 32
Figure 33. Side-view instant centre of rotation. 34
Figure 34. Ackermann geometry. 34
Figure 35. Different steering configurations. 34
Figure 36. Simple explanation of the motion ratio (a). 36
Figure 37. Typical side forcé characteristic. 37
Figure 38. Camber change rate. 42
Figure 39. Front-view design scheme. 44
Figure 40. Anti-feature characteristic angles. 45
Figure 41. Rear frequency increased by 10%. 46
Figure 42. Damping influence on the frequency response. 48
Figure 43. Representation of the four in-wheel electric motors. 79
Figure 44. Model adaptation to find the Pacejka characteristic coefficents. 80
Figure 45. Second-type motion ratio simplification. (b). 94
Figure 46. NTNU rear suspension layout, with the Z-type anti-roll bar. 95
Figure 47. Static vehicle equilibrium. 96
Figure 48. Internal view of the Ohlins TTX25 mk2 damper. 96
Figure 49. (a) Front rocker and push-rod geometry. (b) Front spring delta displacement. (c) Front motion ratio variation. 98

Figure 50. (a) Rear rocker and push-rod geometry. (b) Rear spring delta displacement. (c) Rear motion ratio variation. 99

1. INTRODUCTION

1.1 Previous projects

In the past years, Daniel and Ángel, two students at *Universidad Politécnica de Madrid*, in their end-of-grade work, began working on the competition cars of the corresponding years, looking for the optimum geometry for their suspensions. Daniel focused mainly on the rear suspension, while Ángel worked on both suspensions.

Another useful work has been done by Miguel, that found an approximation of the tire characteristic curves by changing the coefficient that are embedded in the Pacejka's model.

Similarly, this project is focused on finding the optimal geometries for the two suspensions of the electric single seater designed for the 2020 competition. It has been developed by creating a new suspension geometry that will be used as a starting point for the new season.

1.2 Objectives of the project

The aim of this project is to design the front and rear suspension of an electric single-seater vehicle, as mentioned above, of the FSAE type, using the ADAMS/CAR software.
The steps that will be followed will be:

1) Initial training in the use of the ADAMS/CAR software.
2) Adaptation of the 2012 general model incorporated in ADAMS/CAR to the single seater combustion vehicle existing in the UPM RACING equipment.
    a) Modification of the suspension geometry with the data provided by the existing combustion vehicle.
    b) Kinematic analysis of the suspension geometry provided.
    c) Analysis of the adequacy of the suspension geometry design. Definition of improvement points.
3) Modification of the geometry as if the previous model was electric.
4) Determination of general design parameters of the 2020 UPM electric single seater.
5) Adaptation of the last geometry to the new requirements of the electric vehicle.
6) Dynamic analysis of the electric single seater vehicle in competition tests.
7) Results and conclusions.

1.3 Methodology

Pre-training and acknowledgement of the working environment:

- Study of the literature;
- Information collection, schematization and know-how synthesis;
- Adaptation to the UPM Racing environment and learning how to use the software.

ADAMS/CAR modelling and kinematic analysis:

- Modelling of combustion-vehicle geometries (1);
- Kinematic analysis of geometry (1);
- First modelling of the final geometry (2);
- Kinematic analysis of geometry two (2);
- Analysis and comparative study of the kinematic behaviour of both models.

Final geometry modelling:

- Identification of the new requirements;
- Adaptation of geometry (2) to the requirements (3);
- Kinematic analysis of geometry (3);

ADAMS/CAR dynamic analysis:

- Calculation of forces in the different tests;
- Achievement of joint forces and elaboration of the load notebook;
- Computation of forces acting on the suspension components.

2. FORMULA SAE COMPETITION

Formula SAE® is an automobile competition between teams of university students at an international level, encouraging the application of technical knowledge in engineering through a competition where team members design, build, implement and compete with a single-seater vehicle in static and dynamic events.

2.1 History of *FSAE* competition

The first edition of Formula Student dates from 1981, after the suppression of the competition Mindy SAE that organized asphalt races with Briggs & Stratton engines of 5 HP. Driven by the University of Texas student body, participation in this first Formula SAE hosted a competition between four universities: Stevens Institute (NJ), University of Cincinnati (OH), University of Tulsa (OK) and University of Cincinnati (OH).

In 1983 the Briggs & Stratton class was eliminated, a common engine for all single seaters. Likewise, it was in 1984, the last year in which the UT would host the event, when the organization began to impose restrictions on manoeuvrability and resistance combined in a single race, as the contingent teams prioritized efficiency to fuel economy. This led to the 1985 decision by Professor Bob Woods of the University of Texas at Allington to undertake the drafting of a new regulation and scoring system that would include static events as part of the format.

Over the years, the competition continued to boom, and it was in 1998 when it was held for the first time in Europe, specifically in the United Kingdom and organized with IMeche. More than 400 people from the sector and the media attended this edition.

Some recent milestones that should be noted is the appearance of the hybrid mode in 2003 (Hybrid Formula), with similar tests, but with different powertrain, since the single-seater had to accommodate a dependence on electric batteries complemented by the four-stroke combustion engine. The electric vehicle mode became a reality in 2013.

2.2 Competition

The competition consists of two disciplines: ***static events*** and ***dynamic events***. They test the aesthetics and design of the vehicle, as well as its acceleration, braking, cornering stability and the characteristics of its dynamic behaviour.

The team with the highest score according to the above requirements will win the edition. It should be noted that in addition to these events, **safety tests must be passed** to be able to circulate on track, because if they are not passed, this would mean immediate disqualification from the championship.

Static events have a maximum score of 325 points, while dynamic events have a score of 675. Both have a maximum total score of 1000 points. Below is a table specifying the main events as well as the maximum possible rating for each.

	Test	***Scores***	***Total score***
Static events	*Engineering design*	150	325
	Cost and manufacturing analysis	100	
	Presentation	75	
Dynamic events	*Acceleration*	100	675
	Skidpad	75	
	Autocross	125	
	Endurance	375	
			Total: 1000 *points*

2.3 Safety tests

- *Technical & safety scrutineering.* Examiners inspect the vehicle to make sure it meets FSAE requirements thoroughly, including the pilot's equipment. One of the most rigorous checks in this last section is the verification that the pilot can leave the passenger compartment in less than 5 seconds, for safety reasons.
- *Tilt testing*. This test is performed where two requirements are to be verified by tilting a platform supporting the vehicle: the fluid requirement at 45° and the stability requirement at 60° inclination.
- *Brake test*. The braking capacity of the vehicle is evaluated, as well as the emergency stop. To pass this test, the car must be able to brake by simultaneously locking all four wheels and stop it in a straight line without deflecting, while the traction system is switched off. In addition, it is acceptable for the active light of the traction system to go out shortly after the vehicle has to come to a complete stop, as it can take up to 5 seconds to reduce the voltage of the traction system.
- *Noise testing*. Checks whether the vehicle complies with the relevant acoustic requirements contained in the FSAE regulation, with the sound intensity limit being 110 dB at maximum revolutions and 103 dB at idle (with the engine idling).

2.4 Static events

- *Engineering Design*. In this test it is judged how the design and the corresponding justification of it are related to the engineering knowledge that the students have received during their formative period. The team that obtains the proposal with the highest proportion between both aspects will receive the highest score.
- *Cost and manufacturing analysis*. The students of the team must answer to the jury justifying the costs and the manufacture of the vehicle. They must also provide a Cost Report, which will be evaluated for the accuracy and completeness of its contents.
- *Presentation*. The jury assesses the ability of the construction team to develop the single seater and whether the project can be marketed on the basis of its profitability and both economic and technical aspects.

2.5 Dynamic events

- *Acceleration*: It evaluates the acceleration capacity of the vehicle in a straight section of 75 m conveniently paved. The jury will measure the time it takes to travel this distance. Previously, the car will start from a distance of 0.3 m from the reference line, and the team will have to choose two pilots, each with two attempts. Critical factors in this test are the convergence of the rear wheels or the divergence in the front wheels, as well as the pressure in the tyres.

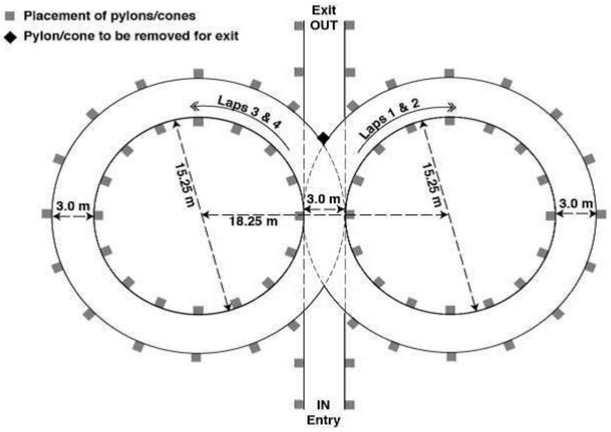

Figure 1. FSAE skidpad layout.

- *Skidpad*: This event makes it possible to assess the stability and dynamic behaviour of the single-seater in the curves of an 8-shaped circuit, which consists of two asphalted circular sections of constant radius of 12.25 m in diameter with a track width of 3 m. Both circular sections are spaced 18.25 m apart (distance measured between their centres). The entry and exit of the circuit take place at the intersection between the two circular routes. Aspects such as the camber angle on the wheels for the support in curves and the inflation pressure of the tyres have a considerable influence.
- *Autocross*: The single seater shall race the circuit in one lap, testing a combination of technical issues evaluated in previous tests, such as acceleration, braking and

turning capacity. The manoeuvrability of the vehicle will depend not only on whether the driver is sufficiently skilful, but also on the requirements of the layout, which in general does not allow average speeds of more than $50\,km/h$. The approximate length of the circuit is $800\,m$, with a minimum track width of $3.5\,m$, and includes straight and curved sections combined with Slalom delimited by cones.

- *Endurance*: This test measures efficiency, reliability and endurance on a $22-km$ track, with straight sections and twisty curves, always delimited by cones. In this event the change of pilot must be carried out, during a stop of $3\,min$ that will be carried out in the middle of the test. Due to the complexity of the circuit, single seaters usually register average speeds around $50\,km/h$, and do not usually exceed $100\,km/h$ during the course. Aspects such as the divergence of the front wheels, the convergence of the rear wheels, and the angles of fall of the same are critical to ensure a higher success rate in this event.

2.6 UPM Racing

At the end of 2003 both the *Escuela Técnica Superior de Ingenieros Industriales de la Universidad Politécnica de Madrid* (UPM) and the *Instituto Universitario de Investigación del Automóvil* (INSIA), in conjunction with the master's in automotive engineering of INSIA, formed the UPM RACING team, becoming the first Spanish representative in the Student Formula.

The team is made up of 50 students, which are renewed each season. It is a research and design project, through a methodology that puts into practice the training received by its members during the academic year both in degree and master, as well as some that allow the development of personal and professional skills of students.

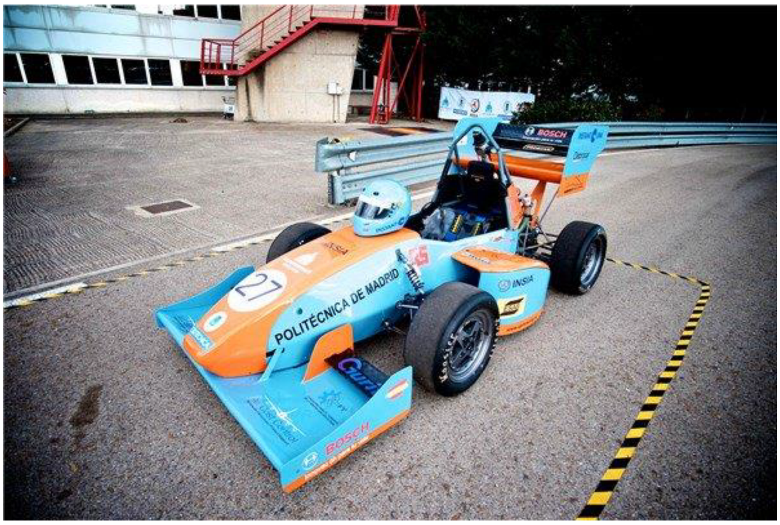

Figure 2. UPM 13C single seater for the 2017 Silverstone competition.

In 2012 the Polytechnic University was introduced in the Formula Student Hybrid competitions to develop the knowledge in this new technology both for the students of ETSII and the students of the specific master of INSIA.

In 2017, the Spanish team took part in the Silverstone circuit with a vehicle equipped with an 80 HP Yamaha engine, capable of accelerating from 0 to 100 km/h in just 4.0 seconds.

In the 2017/2018 season, UPM Racing is in the development phase of an electric vehicle.

In the 2018/2019 season, the team has finally developed his first electric vehicle, called *UPM 03E*.

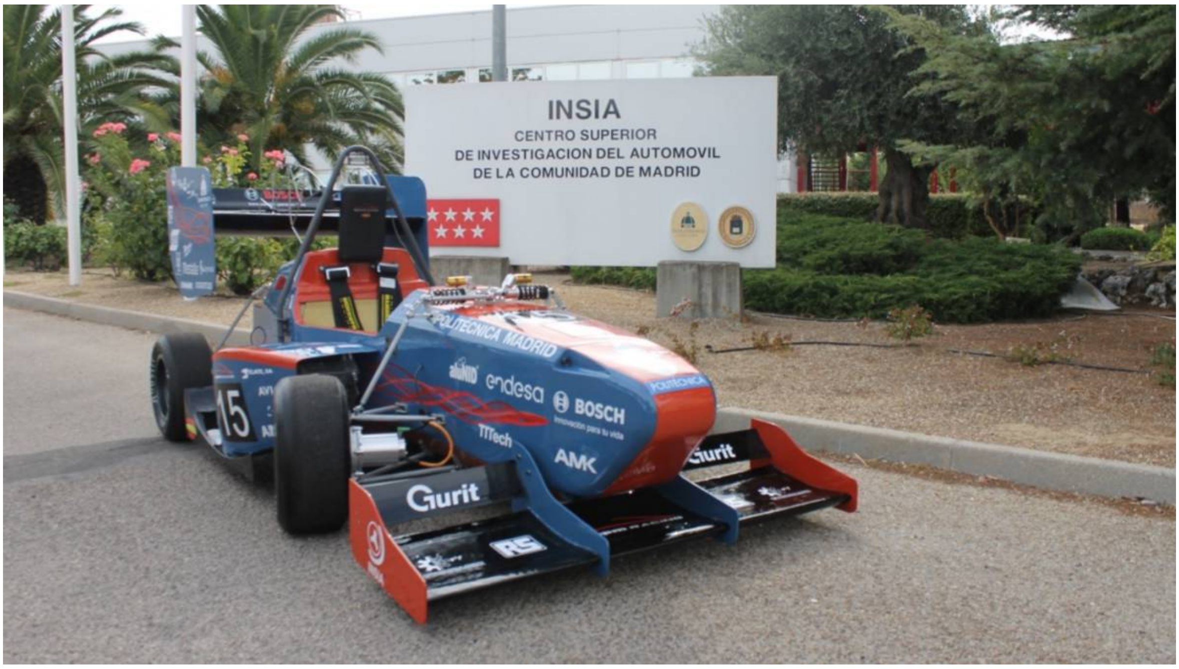

Figure 3. UPM 03E electric single seater for the 2018/2019 season.

2.7 FSAE General Vehicle Design Regulations

The purpose of the FSAE Regulations is the exhaustive compilation of the rules and regulations not only associated with the purely technical or engineering field, but also with the administrative disposition, these being the ones that govern the scoring method in each one of the aforementioned methods and the corresponding penalties.

The regulations explain the precepts to be taken into account for internal combustion vehicles "*PART IC - INTERNAL COMBUSTION ENGINE VEHICLES*" and for electric vehicles "*PART EV - TECHNICAL REGULATIONS - ELECTRIC VEHICLES*".

Also, the competition, through this code, allows some flexibility in terms of design on the part of the teams of students, although there are certain canons that limit the development phase of the single seater.

All the general technical aspects dealt with in section T "*GENERAL TECHNICAL REQUIREMENTS*" of the Formula Student 2019 Standard, most of which are relevant to the suspension of the vehicle.

2.7.1 General design requirements

2.7.1.1 *Wheelbase*

"The car must have a wheelbase of at least 1525 *mm. The wheelbase is measured from the center of ground contact of the front and rear tires with the wheels pointed straight ahead."*

2.7.1.2 *Vehicle track*

"The smaller track of the vehicle (front or rear) must be no less than 75% *of the larger track."*

2.7.1.3 *Suspension*

"The vehicle must be equipped with a fully operational suspension system with shock absorbers, front and rear, with usable wheel travel of at least 50 mm, with a driver seated.

Officials may disqualify vehicles which do not represent a serious attempt at an operational suspension system, or which demonstrate handling inappropriate for an autocross circuit.

All suspension mounting points must be visible at Technical Inspection, either by direct view or by removing any covers."

2.7.1.4 *Steering*

"The steering wheel must be mechanically connected to the front wheels.

Electrically actuated steering of the front wheels is prohibited.

Steering systems using cables or belts for actuation are not permitted."

2.7.1.5 *Ground clearance*

"Ground clearance must be sufficient to prevent any portion of the vehicle except the tires from touching the ground during dynamic events.

Intentional or excessive ground contact of any portion of the vehicle other than the tires will forfeit a run or an entire dynamic event."

2.7.1.6 *Wheels*

"The wheels of the car must be 203.2 *mm* (8.0 *inches) or more in diameter.*

Any wheel mounting system that uses a single retaining nut must incorporate a device to retain the nut and the wheel in the event that the nut loosens. A second nut ("jam nut") does not meet these requirements."

3. SUPENSIONS

3.1 Function

The basic function of the suspension system is to allow the relative movement of the wheels towards and away from the body.

The basic functions assigned to it in the vehicle are as follows:

- ***Driver comfort.*** Absorbs ground irregularities. In competition vehicles this is a secondary function as the suspension is more rigid and reduces the vibrations of the cabin to a lesser extent.
- ***Vehicle load support.*** Every vehicle is made up of the Suspended Mass and the Non-Suspended Mass. The suspension system is in charge of mechanically joining and transmitting the efforts between both parts. The Suspended Mass (or sprang mass) is formed by all the elements whose weight is supported by the chassis, this includes the engine, body, pilot, fuel tank... The Unsuspended Mass (or unsprung mass) includes the wheel and all its attachments that are not inside the frame structure (suspension arms, brake discs...).
- ***Reduce the incidence of forces on the body.*** The suspension absorbs vibrations by means of a coaxial spring-shock system. Its presence reduces the magnitude of the forces transmitted from the pavement to the chassis. When dimensioning the structure of bars that forms the frame, bars of less resistance are required, therefore the possibility of manufacturing lighter cars appears, with the reduction in manufacturing costs and fuel savings that all this entails.
- ***Ensure wheel-ground contact.*** Because there is the possibility of relative movement between the wheels and the body, together with the presence of a shock absorber that is semi-compressed in static, the wheels can adapt to the unevenness of the asphalt surface, ensuring contact for as long as possible. When a wheel momentarily loses contact with the ground, there is no transmission of braking or traction forces from that wheel, as well as steering in the case of a front wheel. The consequence of this is a directional instability in the single seater caused by the yaw moment that appears.

- ***Increases stability.*** In addition to the yaw moment, pitch and roll moments appear on vehicles due to load transfer. The pitching moment appears as a consequence of the load transfer in the direction of travel. Possible causes are acceleration, braking, aerodynamic resistance or sloping tracks. This movement causes the compression of the suspension in one of the axles, and the extension in the other. The roll of the car is a consequence of the lateral force it experiences in a single seater (centrifuge, superelevation...). The centrifugal force is usually the greatest lateral force in Formula vehicles, developed during cornering. In this case there is a load transfer, but in a lateral direction, from the inner to the outer wheels. As a result, the inner suspension expands and the suspension on the outside of the curve is compressed. The deformation of the elastic elements of the suspension system absorbs a large part of this weight transfer, making the load distribution on the wheels more homogeneous, achieving a more stable single seater trajectory.

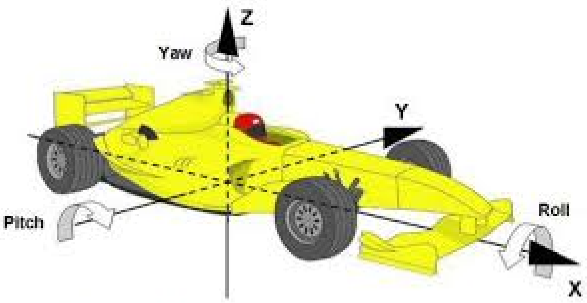

Figure 4. Vehicle ISO reference system.

- ***Improves directional behaviour.*** Facilitates the guidance of the vehicle by ensuring proper contact of the wheels with the pavement.
- ***Increases tyre grip.*** The dynamic behaviour of the spring-shock assembly has a marked influence on the efficient transmission of traction and braking forces. Ensuring tyre contact with the ground increases the average grip value.
- ***Maintain and adapt steering levels.*** The relative movement of the wheel with respect to the chassis causes the steering dimensions to vary during the wheel's trajectory in the expansion and compression movement. The suspension must be correctly studied and elaborated in order to control the modification of the steering dimensions and make the most of its advantages, in terms of adherence, stability and reduction of wear. Racing vehicles are designed with little height between the bottom of the chassis and the ground. In order to prevent the body from rubbing against the ground, more rigid suspension configurations are usually adopted, i.e. with less deformation of the elements. The rigidity of the suspension system is also required for a better adaptation to the irregularities of the terrain. Rider comfort is therefore sacrificed for better performance. It is also possible to include a system that limits the compression of the suspension (it must ensure the limits imposed by regulations), so that the chassis does not rub against the ground.

3.2 Suspension elements

Every suspension of a racing vehicle consists of the following basic elements:

3.2.1 Elastic elements

Whether helical springs, springs or torsion bars, the elastic elements are responsible for adapting the distance of the wheel with the body to compensate for unevenness of the ground and ensure contact with the running surface for as long as possible.

It also keeps the mass suspended at a certain height, preventing it from sinking, which would cause it to rub against the ground.

Greater rigidity of the suspension system worsens the comfort of the cab but improves the dynamic response of the suspension.

Figure 5. Shock-absorber.

3.2.2 Dampers

They're a fundamental part of the suspension. Their function is to dissipate in the form of heat part of the energy stored in the elastic element in the movements of expansion and compression. They therefore reduce oscillations, stabilising the car.

They can present different configurations: two or four ways, with dissipation at high and low speed, they can be hydraulic, elastic or pneumatic...

3.2.3 Clamping and guiding elements

They have the function of anchoring the knuckle to the wheel, and this set to the chassis. They are also in charge of fixing the trajectory of the wheel during the suspension travel, defining the degrees of freedom of the mechanism.

3.2.4 Knuckle

It is connected to the hub, which together with the bearings is the one that allows the rotation of this one. The knuckle is a key element of the suspension geometry, as it receives the forces from the spring-shock assembly and from the trapezoids in the case of the double trapezoid configuration. Likewise, the brake disc is coupled to the knuckle, being this the one that contains the brake calipers. In the case of the front axle, the stub axle will be attached

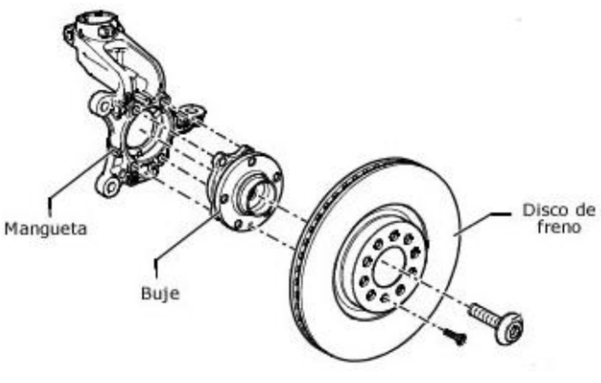

Figure 6. Knuckle, hub and brake disk.

to a steering bar, while in the case of the rear axle, it will be attached to the convergence stabilizer bar.

3.2.5 Hub

It is the element that carries the wheel and allows the wheel to rotate on its own axis. They are usually made of flexible material, such as rubber or different forms of polyurethane with the aim of minimizing vibration, wear and also achieve a lower rate of noise in the turn.

3.2.6 Oscillating arms

These are the elements that connect the knuckle to the chassis and allow the relative movement of the suspended mass with respect to the unsuspended mass. The pull-rod and push-rod systems also include elements such as the bars and the rocker arm, which transmit the forces of the wheel to the shock-absorbing spring assembly.

3.2.7 Spherical joints

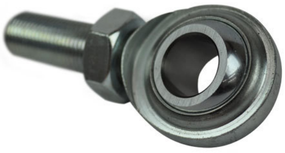

Figure 7. Spherical joint.

In order to avoid the transmission of torsional forces, the connection between the different elements is made by means of spherical plain bearings. They are connecting elements that allow all the relative turns between the two connecting bodies. The joints are not perfect, so sometimes they have dimensional gaps or incompatibilities that do not allow the complete rotation of the elements.

3.2.8 Rocker

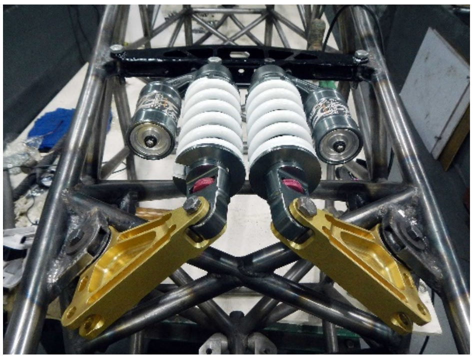

Figure 8. Rockers (in gold).

It is the element that joins the knuckle to the spring-shock assembly, supporting the efforts that the latter transmits to it. These efforts will depend on the pull-rod or push-rod configuration. This is usually located in the highest part of the body, with one of its anchors located at a point near the curved transition between the lateral part of the monocoque and the upper part where the spring-shock assembly is located. The other two points are connected to the shock absorber and the push-rod bar, respectively, allowing the transmission of forces bidirectionally, according to the load transfer on the axle.

3.2.9 Anti-roll bar

The mission of the anti-roll bar is to limit the inclination of the body when subjected to centrifugal forces (cornering). It is mounted by attaching the ends to each of the lower arms of the suspension of each wheel. In the conventional vehicles it is incorporated in the front part, but in the competition vehicles it is arranged in the front axle as in the rear one to improve the stability in curve.

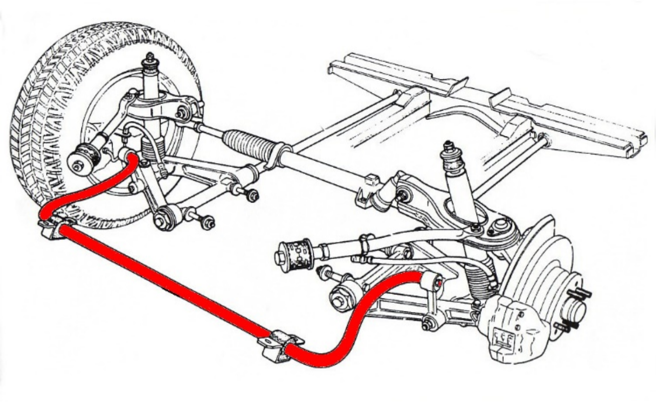

Figure 9. Anti-roll bar.

It can adopt different configurations: torsional bar, working by bending, which links the displacements of the two wheels of the axle, can also be independent. The configuration usually used on the front axle is the torsional bar. It is a U-shaped bar, joined by two tilting fixings to the chassis. Eventually a "Z" bar can be found when the elastic elements are aligned.

It is in charge of linking the movement of the two wheels of the same axle when their travel is asymmetrical. In this case, a torque is produced as a consequence of the difference in relative positions of the wheels with respect to the chassis. The torsional rigidity of the anti-roll bar reacts with a resistant moment opposite to that applied due to the asymmetrical vertical displacement of the wheels and reduces the inclination of the vehicle.

This bar has no function if the tyre displacement is symmetrical with respect to the ground: during pure vertical oscillations of this mass with respect to the unsuspended mass, it does not affect the rigidity of the suspension.

3.3 Suspension geometries

Next, the most common configurations used in competition vehicles, and which in some cases are common to commercial passenger cars, will be explained.

A first classification of suspension systems is related to the route of the same during the rebound of the wheel and its consequent displacement, being the possible typologies: *rigid*, *independent* and *semi-independent* suspension.

3.3.1 Rigid suspensions

It was the first suspension geometry used in vehicles. Although partially disused, this configuration is commonly used in industrial vehicles, buses and coaches, trucks and some SUVs and SUVs of considerable dimensions. However, a variant of this design is the well-known spring suspension system, which can incorporate a free play in the spring support to reduce the acceleration of the "rollover threshold".

The rigid bridge that joins the two wheels causes the vibrations and stresses that one of them suffers as a result of rolling to be transmitted to the one on the opposite side. Likewise, the weight of the unsuspended mass increases considerably, due to the presence of the rigid axle and the conical-differential group.

The tendency to oversteer is another of the opposing factors, which conditions instability in circulation. To stabilize the axle, a "Panhard" bar is usually used, which serves as a link between the axle and the frame and allows the existence of a single rolling centre.

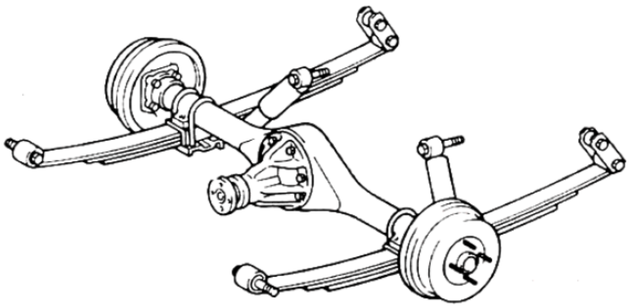

Figure 10. Rear rigid-axle suspensión for a rear-wheel-drive vehicle.

However, one of the advantages that can be deduced is the simplicity of its design and that certain parameters such as the drop angle or the tyre advance are not modified excessively during driving.

3.3.2 Semi-independent or semi-rigid suspensions

This configuration is very similar to that of the rigid bridge, with the exception of less vibration transmission with the incorporation of an additional arm and a conical-differential group that is not integrated in the axle, but is connected directly to the frame, separating the motor function and the function of the suspension system.

Some of the variants of this design are the "Dion" axle suspension and the torsional axle suspension.

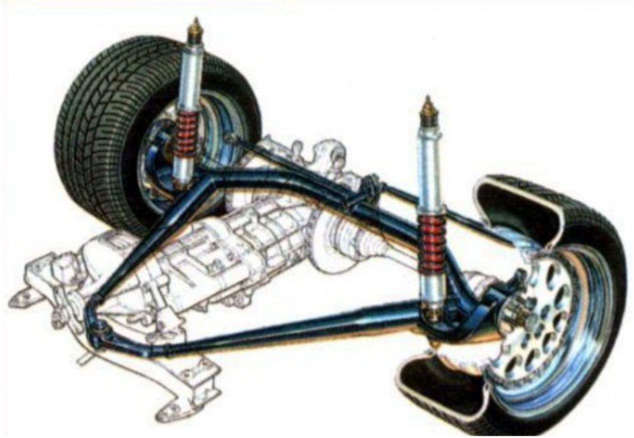

Figure 11. "De Dion" suspension model.

In the suspension with "Dion" axle, articulated supports join the wheels and the conical-differential group, and if the axles transmit the turn to the wheels. The Dion tube is a crossbeam that joins the wheels of the same axle and that allows longitudinal slides, as well as a lower weight of the unsuspended mass due to its greater lightness.

Torsion axle suspension is commonly used on the rear axle and with front-wheel drive vehicles. The operation of this bar has been explained in the previous section.

3.3.3 Independent suspensions

It is the most widely used suspension model today (in particular, the only one on the steered wheels) and the one used in the design of race cars. It stands out fundamentally by the optimization of the response of the vehicle in the section of the comfort and to level of stability in front of vibrations. This is achieved with a lower unsprung weight, ensuring possible changes induced in the parameters of the wheel during wheel rotation.

The only apparent disadvantage is the greater structural complexity of the geometry, which means greater maintenance of the system.

Some of the main variants of the independent suspension model are described below:

- Oscillating axle suspension;
- Suspension of pulled arms;
- McPherson suspension;
- Double-wishbone suspension;
- Multi-link suspension.

3.3.3.1 Oscillating axle suspension

It is a system very similar to the semi-rigid, being the most basic of the types of independent suspension. This consists of a central articulation close to the middle plane of the monocoque, and on which the semi-axles attached to the wheel oscillate. The final assembly incorporates two spring-shock telescopic assemblies to filter the rebound.

One of the main disadvantages is that the camber angle is significantly affected during cornering. As an alternative, it is possible to superimpose the differential group on the central articulation and place the two axles on each shaft, which also favours the axial displacement of the transmission shaft.

3.3.3.2 Suspension of pulled arm

This configuration has two longitudinally arranged support elements or "arms", which are attached to the frame and by the other to the wheel hub. This arrangement is more focused on urban use, as vibrations are not managed very effectively.

If the axle is a traction axle, the differential group is anchored to the frame. In any case, the wheels are "pulled" or dragged by the longitudinal arms that pivot in the anchorage of the monocoque.

The fundamental difference between the different variants of this suspension model lies mainly in which is the axis of rotation of the trailed arm in the anchorage to the frame and which is the elastic element that is used, being these springs and torsion bars essentially. The longitudinal arms can pivot on an axis of rotation perpendicular to the longitudinal plane of the vehicle, or on oblique axes to the same, this last variant being known as "semi-travelled arms".

3.3.3.3 McPherson suspension

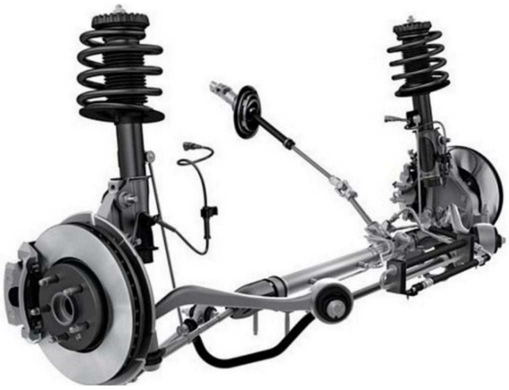

Figure 12. McPherson suspension.

Developed by Earle S. McPherson, a Ford engineer from whom it receives its name, this is one of the most commonly used suspension systems on the front end (commonly used on this axle), although it can also be used on the rear end. This independent configuration is commonly used in most commercial vehicles, due to its simplicity of manufacture and maintenance, its low cost and its small size.

The McPherson suspension has only one swing arm, connected to the frame structure by elastic bearings at one end, and to the knuckle. The latter is attached in its upper anchorage to the vertical shock absorber. In this case, the shock absorbers are bolted directly to the monocoque or to the body of the vehicle, so they must have a certain rigidity in that area to avoid breakage or fatigue damage. In this way, you can transmit the vibrations correctly, although under high stresses or demanding turning situations, noise or vibrations may appear.

3.3.3.4 Double-wishbone suspension

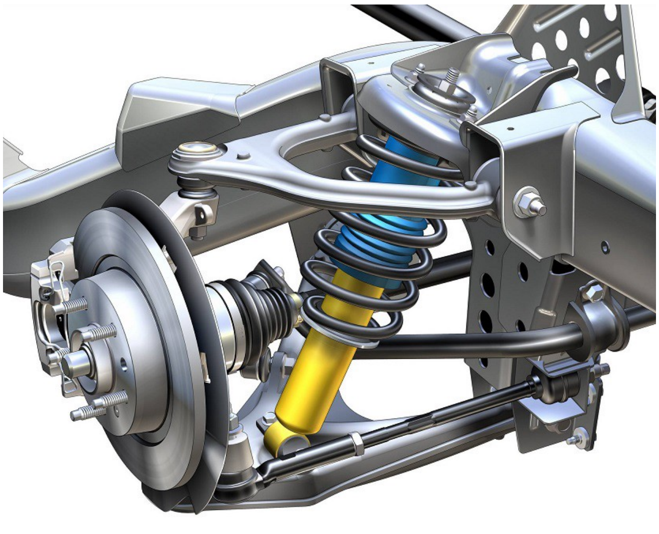

Figure 13. Double-wishbone suspension.

This is the suspension model used for the majority of the single seaters, both on the front and rear axles.

The parallelogram is made up of two A-arms, one upper and one lower, and each of them is made up of two articulated arms. Both arms are joined to the monocoque through pivots or kneecaps, and close the parallelogram joining both in an anchorage in the upper part of the knuckle. The articulated union of the latter and the A-arms is carried out through spherical ball-and-socket joints that allow the orientation of the wheel.

A rocker arm is the one that transmits the efforts between the wheel and the coaxial shock absorbers of helical and hydraulic telescopic spring type by means of an oscillating bar, called push-rod. The system also has a convergence stabiliser bar (in the case of the front axle) or a steering bar (in the case of the rear axle).

This is a geometry oriented to competition vehicles, as it allows a better dynamic response, as it offers greater rigidity and inclination of the suspension.

3.3.3.5 Multilink suspension

Multi-link suspensions are based on the same basic principle as the geometry of the deformable parallelogram suspension, so the design continues to consist of two transverse arms, the knuckle and the frame itself. The fundamental difference with respect to the suspension in double A-arms is the incorporation of elastic anchors by means of sleeves or rubber plugs to receive the vibrations. Furthermore, in this system, the upper part is screwed to the chassis turret.

This new configuration therefore makes it possible to modify the fundamental parameters of the wheel, such as drop or convergence, in the most appropriate way with regard to stability and driving comfort depending on traffic conditions, so that the longitudinal and transverse dynamics are not compromised and can be configured in isolation or independently.

The use of multi-link suspension is usually attached to the suspension of high-end sport cut vehicles on one or both trains. For a suspension to be considered multi-link, it must consist of at least three arms. Some of them have variants of the main model, such as the threaded body suspension, which offers the possibility of adjusting the height and hardness, or focused on competition vehicles, which have an expansion vessel for the lubricant.

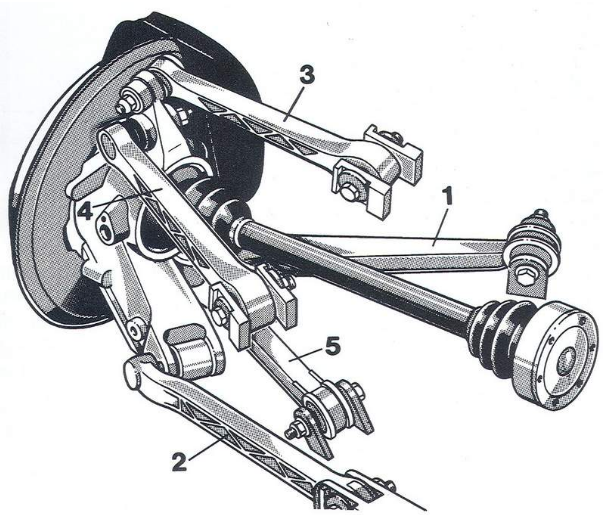

Figure 14. Multi-link suspension of a Porsche 993.

4. VEHICLE DYNAMICS

The dynamics of the vehicle intervenes when it is necessary to change trajectories. The contact and exchange of forces takes place thanks to the tyres: it is important to have a model of the vehicle in order to study them and understand how the vehicle behaves.

4.1 Vehicle models

There are different models for the study of a vehicle, depending on the completeness and complexity that the analysis requires. Subsequently, the different models used will be introduced, differentiated by the number of degrees of freedom.

4.1.1 Kinematic steering (low-speed cornering)

This model can be used if the change of trajectory occurs very slowly, so that the vehicle only behaves kinematically. In this way, the speed of each wheel remains in the equatorial plane of the wheels, without angles of drift, while the speed of the vehicle is perpendicular to the radius of curvature.

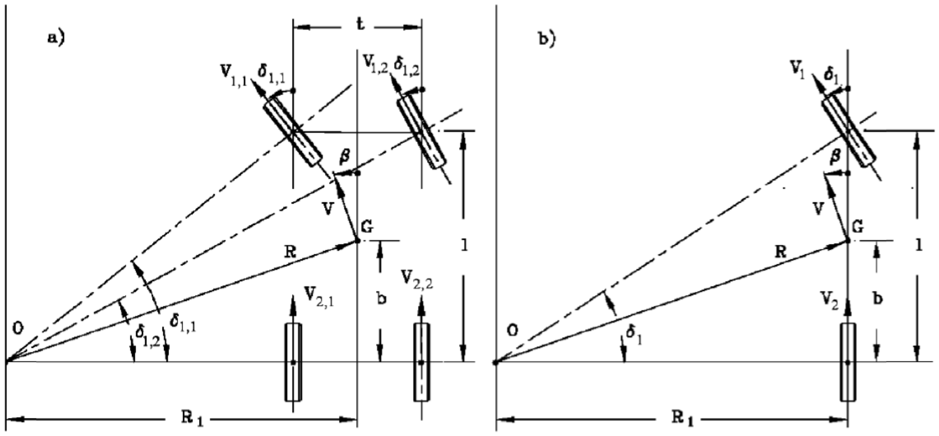

Figure 15. Kinematic steering model.

The condition to be fulfilled is as follows:

$$\begin{cases} \tan \delta_1 = \dfrac{l}{R_1 - \dfrac{t}{2}} \\ \tan \delta_2 = \dfrac{l}{R_1 + \dfrac{t}{2}} \end{cases}$$

If the steering angle is very small, it can be assumed that the two wheels move through parallel arcs, so the model can be simplified to the *bicycle model* shown below.

$$\frac{t}{2} \ll R_1 \approx R \rightarrow \tan\delta_1 = \frac{l}{R} = \tan\delta_2$$

4.1.2 Bicycle model (high-speed cornering)

The bicycle model (also called *monotrack model*) can be used when the radius of curvature is very high ($R \gg l$), assuming that it is driven at a constant speed and without taking into account aerodynamic effects. With these assumptions, a steady state manoeuvre can be analysed.

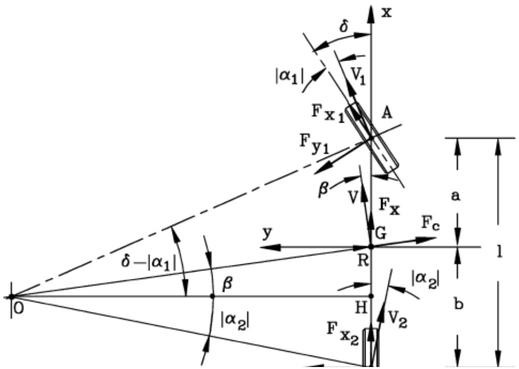

Figure 16. Bicycle model for high-speed cornering.

In the case of high speeds, the drift angle of the wheels (and consequently of the vehicle) is taken into account. In this case, the centre of the curvature can be found by the intersection of lines perpendicular to the individual speeds of the wheels.

By adding the forces in the model and developing the calculations, it is possible to calculate the *curvature gain*.

$$\frac{1}{R \cdot \delta} = \frac{1}{l} \cdot \frac{1}{1 + \frac{MV^2}{l^2} \cdot \left(\frac{b}{C_1} - \frac{a}{C_2}\right)}$$

The equation can also be written as $\frac{1/R}{\delta}$, i.e. curvature between steering angle. With a certain rotation angle, information about the curvature is obtained. This is important to know the behaviour of the vehicle and is a function of tyre characteristics and speed.

In particular, you can see whether the vehicle has oversteering or understeering characteristics by focusing on the factor in brackets:

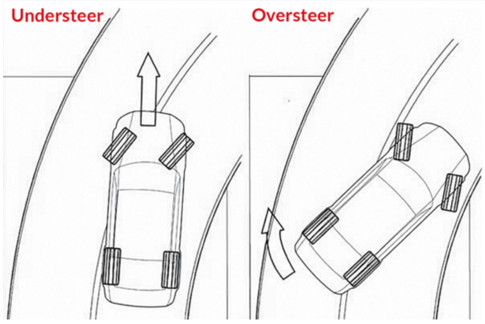

Figure 17. Understeer and oversteer.

- $> 0 \rightarrow$ ***Understeer.*** If the speed increases, the denominator increases, then the ratio decreases. This means that the curvature $1/R$ will increase with the turning angle δ constant or, in the same way, for the same curvature a greater turning angle is needed.
- $< 0 \rightarrow$ ***Oversteer.*** On the contrary, the relationship increases.
- $= 0 \rightarrow$ ***Neutral steer.*** In this case, the vehicle is perfectly balanced: this condition coincides with the previously explained kinematic turn.

The really important parameters to define this behaviour are C_1 and C_2. Increasing C_1, for example, the vehicle will have a direct characteristic towards oversteer; the opposite for C_2.

In fact, these values may vary depending on the load transfer from one side of the vehicle to the other as it turns. Specifically, when the tyre becomes saturated, it is no longer capable of satisfying the "demand" for lateral force, so the overall stiffness value of the axle decreases, modifying the character of the vehicle.

In other ways, these values are also modified by changing the stiffness of the springs and/or stabilizer bars, which will modify the load transfers between sides, by not allowing the tires to become saturated or yes on an axle.

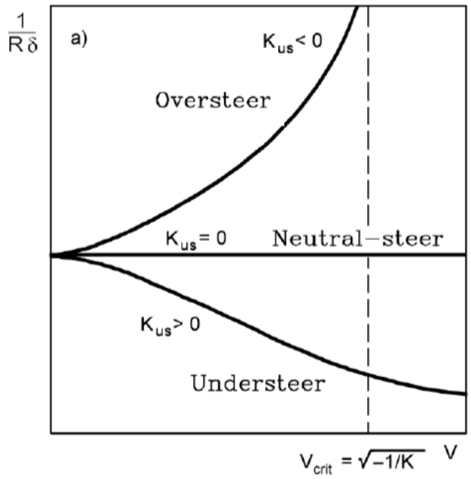

Figure 18. Curvature gain typical plot.

4.1.3 Rigid-vehicle model (3 d.o.fs.)

This model, unlike the previous one, is implemented to also study transient conditions. The vehicle is still rigid: neither wheels nor suspensions are considered, which greatly simplifies the model.

The main concept, used for both the 3-d.o.f. model and the 10-d.o.f. model, is to simplify the equations by writing them with respect to the non-inertial reference system (of the moving vehicle).

Its variables then are $\begin{cases} u \\ v \\ r = \dot{\psi} \end{cases}$ and identify the three d.o.fs. of the system.

Using the formula of relative movements between systems it is possible to find the forces acting on the complete vehicle:

$$\left(\frac{d\overline{V}}{dt}\right)_{inercial} = \left(\frac{d\overline{V}}{dt}\right)_{no\ inercial} + \overline{\Omega} \times \overline{V}$$

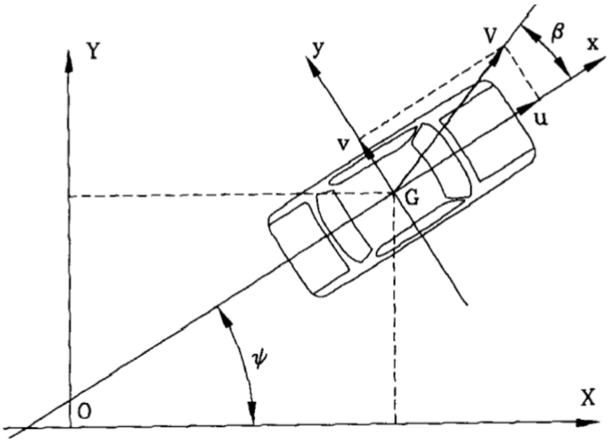

Figure 19. Rigid-model refernce system.

where $\overline{V} = \begin{Bmatrix} u \\ v \\ 0 \end{Bmatrix}$ is the vehicle speed vector and $\overline{\Omega} = \begin{Bmatrix} 0 \\ 0 \\ r \end{Bmatrix}$ is the rotation speed vector of the reference system.

For a correct analysis, it is necessary to study the individual tyres, which are solely responsible for the exchange of forces between the vehicle and the ground. Considering a local reference system, it is possible to calculate the side slip angle for each tyre and consequently, assuming that the lateral force produced is maintained in the linear range (small side slip angles).

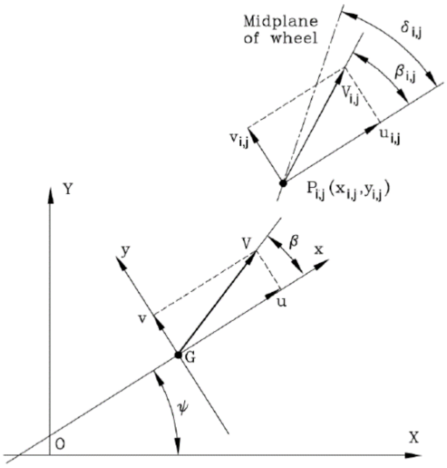

Figure 20. Wheel reference frame.

Geometrically it will be possible to define the drift angle as $\alpha_i = \beta_i - \delta_i$, where β is the drift angle of the vehicle and δ the steering angle; following the calculations, finally the lateral forces F_y acting on the two axles will be obtained, assuming that there are no differences of δ (and therefore of α) between the two wheels and considering the rigidity to the lateral slide C of the axle.

$$\begin{cases} F_{y1} = -C_1 \cdot \alpha_1 = -C_1 \cdot \left(\beta + \dfrac{a \cdot r}{V} - \delta\right) \\ F_{y2} = -C_2 \cdot \alpha_2 = -C_2 \cdot \left(\beta - \dfrac{b \cdot r}{V}\right) \end{cases}$$

where a and b are the wheelbases from the centre of gravity of the vehicle.

By adding the aerodynamic effect and external forces, it is finally possible to write the equations of the dynamic behaviour of a rigid vehicle.

$$\begin{cases} m \cdot V \cdot (\dot{\beta} + r) + m \cdot \dot{V} \cdot \beta = Y_\beta \cdot \beta + Y_r \cdot r + Y_\delta \cdot \delta + F_{y,ext} \\ J_r \cdot \dot{r} = N_\beta \cdot \beta + N_r \cdot r + N_\delta \cdot \delta + M_{z,ext} \end{cases}$$

where the terms Y_β, Y_r, N_β and N_r depend on speed and are called "stability derivatives". They are precisely defined:

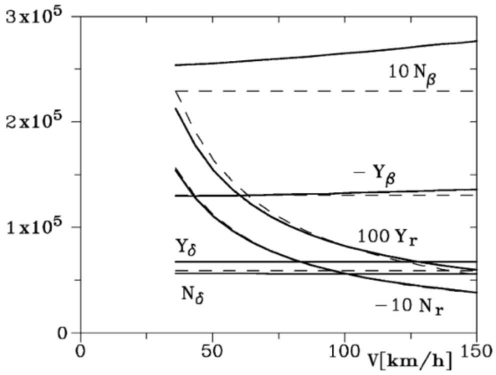

Figure 21. Trend of the derivatives of stability.

$$Y_\beta = -(C_1 + C_2) + \frac{1}{2}\rho S (C_y)_\beta V^2$$

$$Y_r = -\frac{1}{V}(C_1 a - C_2 b)$$

$$Y_\delta = C_1$$

$$N_\beta = -C_1 a + C_2 b + (M_{z1})_\alpha + (M_{z2})_\alpha + \frac{1}{2}\rho S (C_{Mz})_\beta$$

$$N_r = \frac{1}{2}(-C_1 a^2 - C_2 b^2 + (M_{z1})_\alpha a - (M_{z2})_\alpha b)$$

$$N_\delta = C_1 a - (M_{z1})_\alpha$$

Since β and r are actually *pseudo-coordinates*, it would be better to write these two equations in state-space, in order to analyse the system's own values and understand whether the vehicle is stable or not. Solutions can be real or complex conjugated and, if the real part is positive, the system will be unstable. This can be collected in a graph called root locus where all solutions are put.

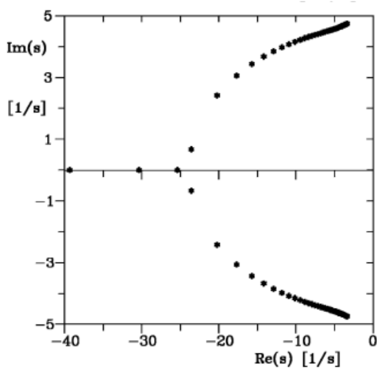

Figure 22. Root locus example.

4.1.4 Complete model (10 d.o.fs.)

The rigid-vehicle model is well suited to analyse the macroscopic performance of the vehicle, but it is not satisfactory for higher design stages. The dynamic behaviour of the vehicle is defined by some characteristics that can be studied with a simplified model and others, like comfort, that require a complete model.

So, it is necessary to add some degrees of freedom, up to 10 or 14:

- 6 of the body;
- 4 of the relative motion of the wheel with respect to the body;
- 4 of the wheel rotations.

Consider that now the body is compliant, as well as wheels, thus roll motion must be analysed.

To create a model, again it is useful to move from the inertial reference frame to a moving, non-inertial reference frame. In this case, this one is aligned with the roll axis of the body and it is centred in its centre of mass: a rotation matrix is needed.

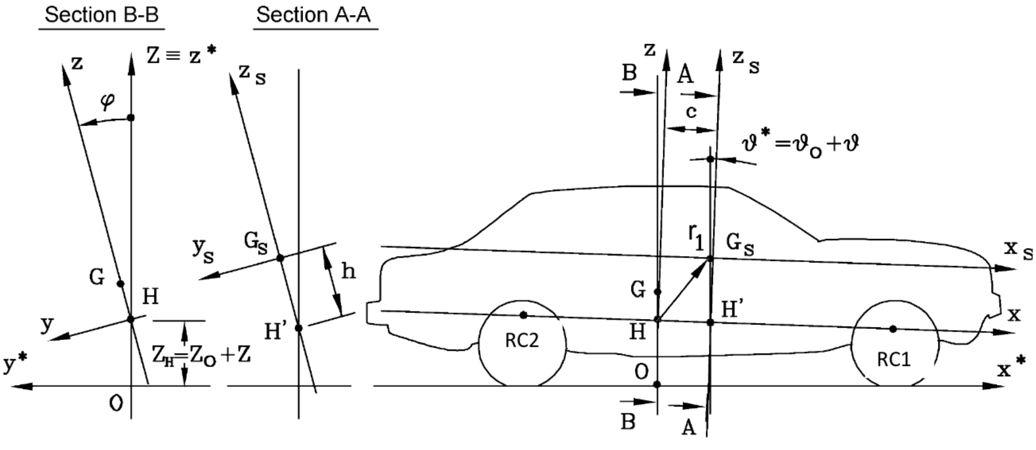

Figure 23. Reference frame of the complete model.

Once done this translation, it is just a matter of correctly write the equations by using the Lagrangian approach:

$$\frac{d}{dt}\left(\frac{\partial \mathcal{L}}{\partial \dot{q}}\right) - \left(\frac{\partial \mathcal{L}}{\partial \dot{q}}\right) + \frac{\partial F}{\partial \dot{q}} = \frac{\partial \delta L}{\partial \delta q}$$

Where $q = \begin{Bmatrix} x^* \\ y^* \\ Z \\ \psi \\ \phi \\ \theta \\ z_i \\ \phi_i \end{Bmatrix}$ includes the variables of the system, $\mathcal{L} = T - U$ is the Lagrangian operator (T kinetic energy, U potential energy), F are all the dissipative forces and δL is the virtual work.

After all the calculations, what will be left are a series of equations (10, one per each variable) that can be decoupled between handling and comfort only if four assumptions are carried through the computation:

1. The speed V is known, as in the previous model;
2. Angles are small: roll ϕ, pitch θ and yaw rate $\dot{\psi}$ are small, thus side slip angles α and β are small;
3. Body is symmetric, no differences between left and right;
4. The characteristics of the suspension are linear, for both spring and damper.

$$\left\{ \begin{array}{c|c} x^* & y^* \\ \theta & \phi \\ Z & \psi \\ z_1 & \phi_1 \\ z_2 & \phi_2 \end{array} \right\}$$

On the left there are all the variables related to the *comfort*, while on the right there are the ones of the *handling* description. This is telling that the two behaviours can be studied separately and independently from each other's.

Furthermore, a little simplification can be made if the roll motion of the axles is considered negligible compared to body roll, since tire stiffness is way bigger than suspension one. This is called ***Segel model*** and allows to analyse handling performances by using only 3 d.o.fs.

4.2 Induced steering

One of the effects that is also considered in the complete model is the roll steering, or undesired steering. It is a steering effect that most type of steering and suspension systems cannot avoid. The reason is that if the wheel steer when it runs over an obstacle or when the car rolls in a turn, the car will travel on a path non desired by the driver.

If the effect is to steer the front wheel out of the turn, it reduces the lateral force improving the understeer; in the case of rear wheels, it is the opposite: it is needed to steer the wheels towards the turn centre to have understeering effect. Its presence can be noticed in the following formula:

$$\delta_i = \delta_{i,true} - \left(\frac{\partial \delta_i}{\partial \phi}\right)\phi$$

Roll steer is function of suspension geometry and steering system geometry. It should be taken into account that each suspension has an instant axis of rotation and it is requested that the tie rod has to correct this effect by setting the proper point of rotation and length. Specifically, there exist three main set-ups, according to the required characteristic.

If the tie-rod connection is following the same path of the suspension joint and it is aligned with the instant centre of rotation of the suspension, the effect of undesired steering in null or minimum.

If the connection on the body is lowered or increased (thus the tie-rod is not aligned with the IC), a linear characteristic is obtained. The effect that is proposed in the figure is of enhancing understeering behaviour, since the wheels toe towards the external of the curvature.

In the case that the tie-rod is shorter, it results in a non-linear characteristic of this effect, which is totally undesirable.

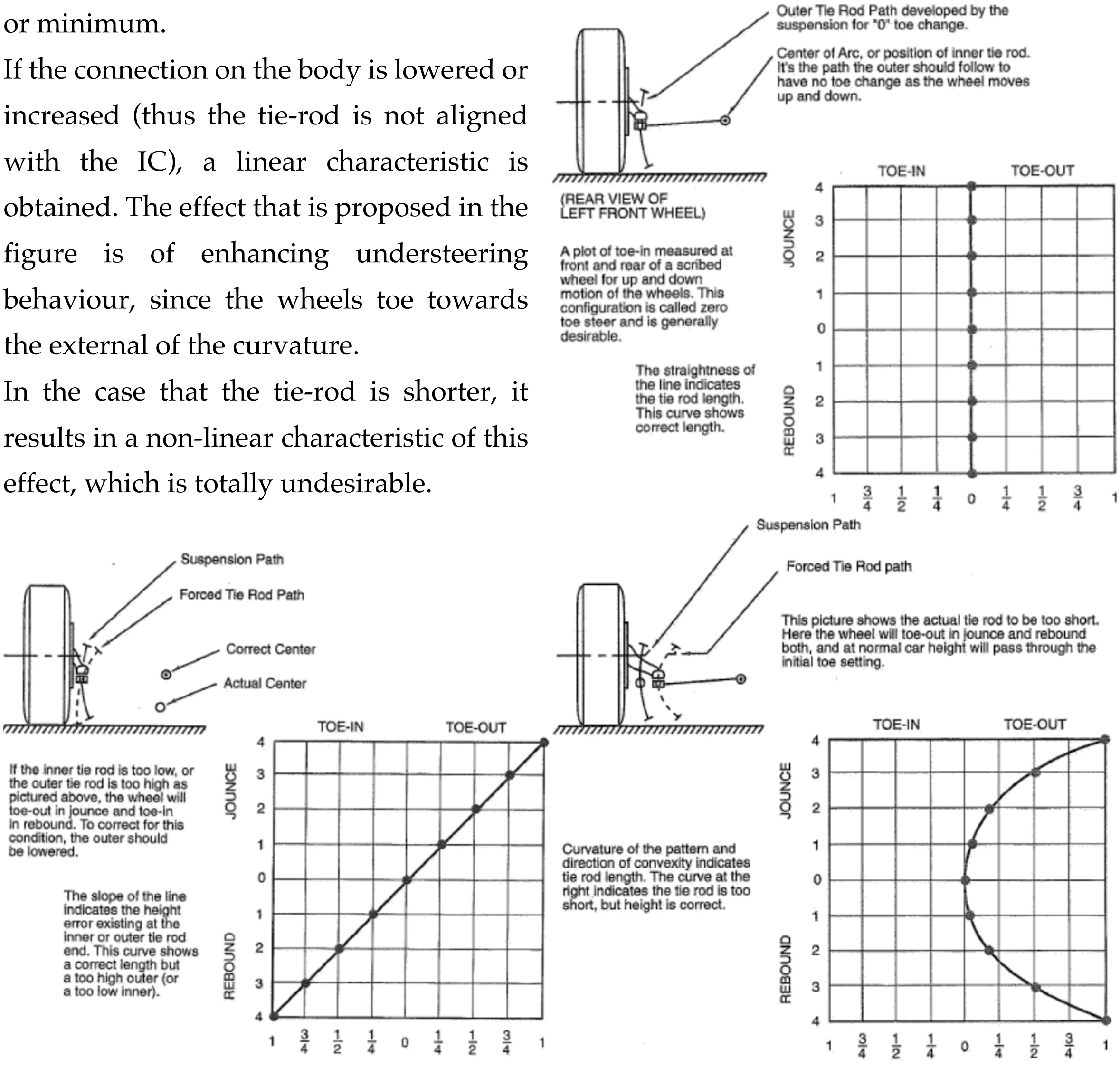
Outer Tie Rod Path developed by the suspension for "0" toe change.
Center of Arc, or position of inner tie rod. It's the path the outer should follow to have no toe change as the wheel moves up and down.
(REAR VIEW OF LEFT FRONT WHEEL)
TOE-IN
TOE-OUT
JOUNCE
REBOUND
4
3
2
1
0
1
2
3
4
1
3/4
1/2
1/4
0
1/4
1/2
3/4
1
Suspension Path
Forced Tie Rod Path
Correct Center
Actual Center
Suspension Path
Forced Tie Rod path

A plot of toe-in measured at front and rear of a scribed wheel for up and down motion of the wheels. This configuration is called zero toe steer and is generally desirable.

The straightness of the line indicates the tie rod length. This curve shows correct length.

If the inner tie rod is too low, or the outer tie rod is too high as pictured above, the wheel will toe-out in jounce and toe-in in rebound. To correct for this condition, the outer should be lowered.

The slope of the line indicates the height error existing at the inner or outer tie rod end. This curve shows a correct length but a too high outer (or a too low inner).

This picture shows the actual tie rod to be too short. Here the wheel will toe-out in jounce and rebound both, and at normal car height will pass through the initial toe setting.

Curvature of the pattern and direction of convexity indicates tie rod length. The curve at the right indicates the tie rod is too short, but height is correct.

Figure 24. Toe characteristics as function of the tie-rod design.

5. MAIN SUSPENSION PARAMETERS

As mentioned above, the purpose of the suspension is to facilitate the work done by the tyres and to allow predictable body behaviour to ensure the driver's control of the car. Moreover, the geometry of any wheel and the suspension system around it determines the linear and angular trajectories that the wheel and tyre will follow when it moves from its static position, either by the effect of road irregularities on the unsprung mass or by the movement of the suspended mass due to both lateral and longitudinal load transfers.

For this reason, the design of the suspension system geometry consists of first choosing the type of suspension to be used (which is given by the characteristics mentioned earlier), and then selecting the locations of the pivot points and anchorages, the absolute and relative lengths and inclinations of the links and bars, and the dimensions of the wheelbase.

The main factors affecting this system can be classified into two possible areas of behaviour: ***kinematic*** and ***dynamic***.

5.1 Kinematic parameters

The kinematic study of the vehicle aims to ensure the largest area of contact of the tyre with the asphalt under any driving condition, so it focuses on the relative geometric position of the suspension elements and the wheels of the single seater. These are explained in the following sections.

5.1.1 Wheelbase

The wheelbase is the distance measured longitudinally between the front and rear axles of a vehicle.

This parameter is particularly important for longitudinal load transfer, due to acceleration and braking processes, the greater the wheelbase, the smaller the wheelbase. The weight distribution in the axles will also depend on the distance from the centre of gravity of the car to each of the axles, which influences the tractor effort and braking developed in each wheel.

Also, the greater the distance between the axles, the slower the response of the vehicle in a curve, and also affects the speed at which the resonance of the suspension is produced (that is, the speed at which the movement of the suspensions of both axles after negotiating a bump is coupled and the car rebounds), causing an oscillation in motion of the vehicle that becomes uncontrollable. A bigger wheelbase makes this speed higher.

The vertical force acting on the front and rear wheels is then calculated in an acceleration process, taking into account a simplified model of a vehicle with mass m, moving with an a_x acceleration in the direction of travel:

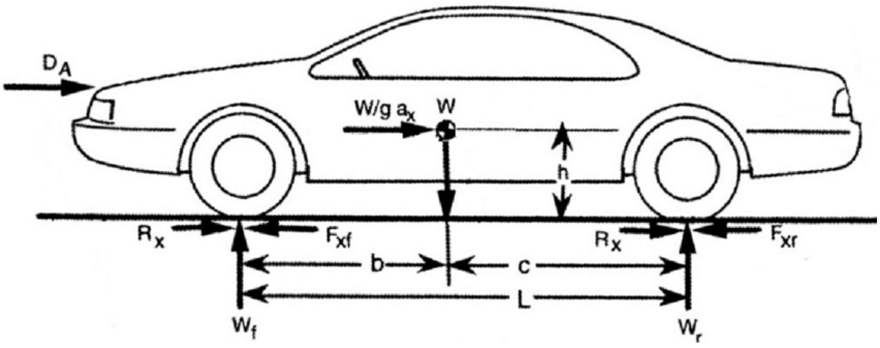

Figure 25. Dimensions and forces acting on a vehicle.

Taking into account the distance b between the centre of gravity and the centre of the front axle in the longitudinal direction, and a height h of the centre of masses, the force acting on each wheel shall be:

$$F_{z1} = h \cdot a_x \cdot m + (1 - b) \cdot m \cdot g$$

$$F_{z2} = h \cdot a_x \cdot m + b \cdot m \cdot g$$

where F_{z1} is the vertical force on the front wheels and F_{z2} is the vertical force on the rear wheels.

5.1.2 Track width

The track is the distance between the wheel centres of the same axle. This factor is of great importance for lateral load transfer, due to the centrifugal acceleration of the vehicle that occurs in the passage through the curve, which will be lower the greater the track. Furthermore, the track also affects the "vehicle rollover threshold", i.e. the condition in which the lateral acceleration reaches the maximum value that the vehicle can tolerate without tipping over or, in other words, the a_y value for which the single seater provides the maximum net moment of reaction to the rollover.

The value of the net reaction moment, for a vehicle with axle weight P and track width value B, the value of the net reaction moment is (M_{yr}):

$$M_{yr} = P \cdot \frac{B}{2}$$

As far as limitations are concerned, the current regulation states that the smallest section in the *SkidPad* circuit must not be less than 3 m and in the Autocross and Endurance circuits is greater than 3.5 m.

However, the total load transfer depends not only on the wheelbase, but also on the grip capacity of the tyre to the running surface, creating a larger contact footprint, or on the use of the stabiliser bar integrated into the chassis.

5.1.3 Camber angle

The camber angle (γ) is the angle formed by the median plane of the wheel and the angle normal to the running surface, from an elevated view of the vehicle.

The convention of signs corresponding to the angle of fall establishes that this is negative when the upper part of the wheels of the same axle is at a smaller distance between them than the part that is in contact with the profile of the road. Therefore, a positive camber angle would make the parts of the wheel that rest on the tread shorter than the top of them. If the camber is neutral ($\gamma = 0$), the middle planes of both wheels remain parallel in their static position.

A negative camber allows to maximise the grip of the tyres in the curve, favouring a better traction. However, the interior of the shoulders of both tires suffers a greater tension in straight traffic, including greater wear inside the rims and a greater likelihood of overheating in the blocks and nerves of the tread. When the camber tends to be positive, the wear is less, although the vehicle reduces its ability to take curves.

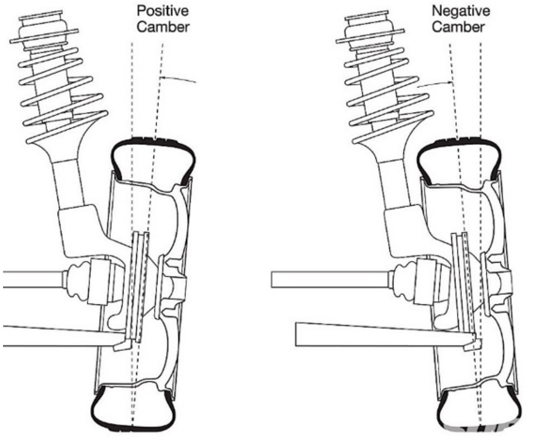

Figure 26. Camber angle convention.

Moreover, for different normal load values, a greater drop angle tends to favour greater lateral thrust and greater tyre drop rigidity. The designation commonly used to name this tyre variable is IA (inclination angle).

5.1.4 King-pin axis

The king-pin axis is the axis determined by the line connecting the Upper Ball Joint (UPB) and Lower Ball Joint (LBJ) anchor points to the knuckle. This axle does not necessarily pass through the centre of the wheel or the centre of the contact track from a side view of the vehicle.

The angle formed by this axle with respect to the normal to the contact surface, from a front view of the wheel in the direction of movement, is known as king-pin inclination. This parameter must be taken into account if tight turns occur, as it causes the wheel to tilt positively if the tilt angle of the centre pivot is positive.

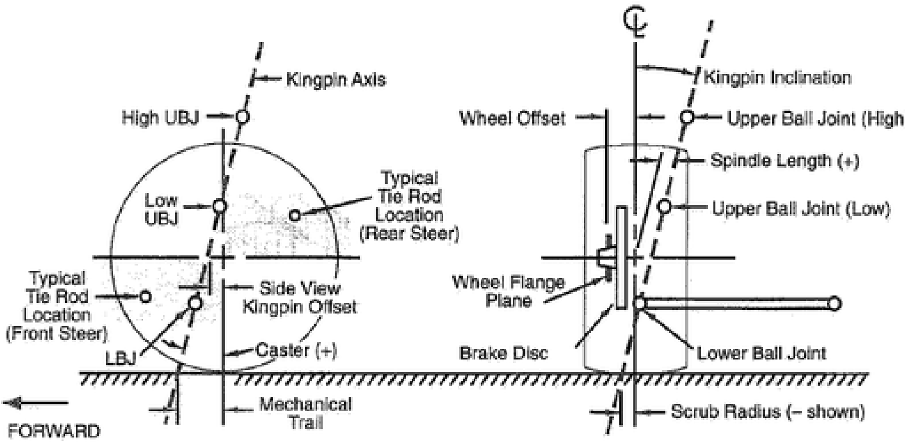
Kingpin Axis
High UBJ
Low UBJ
Typical Tie Rod Location (Rear Steer)
Typical Tie Rod Location (Front Steer)
Side View Kingpin Offset
LBJ
Caster (+)
Mechanical Trail
FORWARD
℄
Kingpin Inclination
Wheel Offset
Upper Ball Joint (High)
Spindle Length (+)
Upper Ball Joint (Low)
Wheel Flange Plane
Brake Disc
Lower Ball Joint
Scrub Radius (– shown)

Figure 27. King-pin geometry.

5.1.5 Mechanical trail

The mechanical trail is the distance between the cut point of the king-pin axle with the horizontal of the running surface and the cut with that surface of the vertical axle of the wheel, which passes through its centre, seen from the side. A greater mechanical advance requires a greater turning torque in the direction.

5.1.6 Scrub radius

Scrub radius is a term similar to mechanical advance, the first being identified with the distance between the cut point of the king-pin axle with the horizontal of the rolling surface and the cut with that surface of the vertical axis of the wheel, which passes through its centre, from a frontal view.

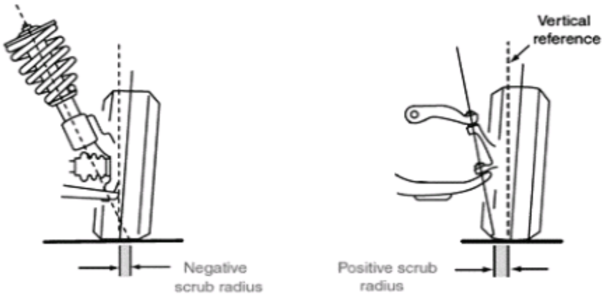
Vertical reference
Negative scrub radius
Positive scrub radius

Figure 28. Scrub radius definition.

If the braking or traction force is different on both sides, this will introduce a torque in the direction proportional to the scrub radius, which will require a response from the driver on the steering wheel.

- ***Positive.*** In a rear-wheel drive vehicle with a positive scrub radius, forward movement of the vehicle and friction between the tire and the road causes a force that tends to move the front wheels toe-out, keeping the vehicle straight forward. During braking, in any type of driving, if the braking effort is greater on one side of the vehicle than on the other, the positive braking radius will cause the vehicle to turn to the side with the greatest effort, requiring much greater driver involvement and also competition.
- ***Zero.*** Keeping the scrub radius small will make the car easier to drive at low speeds. It also reduces the risk that loss of traction on a wheel during braking will cause the car to change direction. If the scrub radius is small, then the contact patch is rotated

into place when parked, which requires much more effort. The advantage of a small scrub radius is that the steering becomes less sensitive to braking inputs. However, a zero-scrub radius, in hard braking conditions, makes the suspension unstable due to the variation in road conditions created by the variation in the amount of torque (both positive and negative) around the steering axle. Therefore, a certain amount of scrub radius, positive or negative, is preferred. Having a small amount of scrub radius under heavy braking generates a small amount of torque on a predictable side. Although this torque is not desirable, it is predictable and is not mainly due to changes in road conditions, which makes steering smoother.

- ***Negative.*** An advantage of a negative scrub radius is that the geometry naturally compensates for split braking or failure in one of the braking circuits. Vehicles with a diagonally spaced brake system have a negative scrub radius integrated into the steering geometry. If half the braking system fails, then the vehicle will tend to climb in a straight line. The negative scrub radius also provides a central point direction in the event of tyre deflation, which provides greater stability and steering control in this emergency situation. If you hit stagnant water at speed on one side of the car, with a negative scrub radius, the torque in the direction will move you away from the puddle, which balances the dragging effect on that side.

5.1.7 Caster angle

The forward angle is the angle formed by the king-pin axis and the vertical axis perpendicular to the contact footprint, from a side view of the vehicle.

A negative caster angle would cause the anchorage point of the lower trapeze to be behind the vertical axis, following the direction of movement.

The caster angle must be studied so that, if this takes very high values, it can cause harmful effects on the steering system and generate oversteer problems when taking a curve. The caster has a positive effect on straight stability, as it induces a self-linear effect on the tyres (i.e. a resistant moment is created in the steering wheel when driving around bends, and at the exit of this helps to reduce the turning of the wheels).

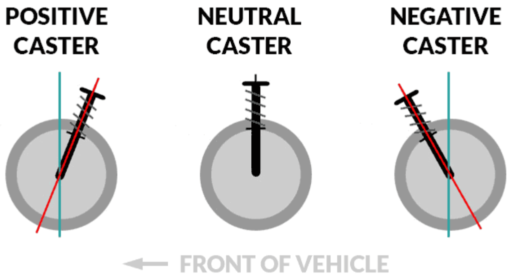

Figure 29. Caster angle convention.

5.1.8 Toe angle

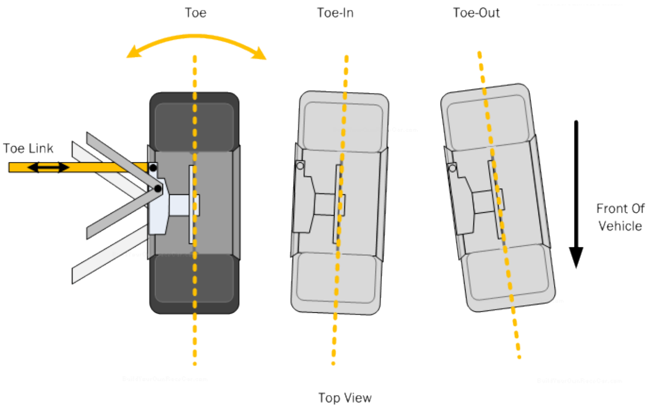

Figure 30. Toe angle convention (plan view)

The convergence angle (or toe angle) is the angle formed between the median plane of the wheel and the longitudinal median plane of the vehicle, seen in plan. The convergence is negative when the median planes of both wheels converge at a point ahead of the axle that joins them (toe-in); and is positive in the opposite case, that is, they diverge (toe-out). It is a parameter that has a special impact on tyre wear, as well as on vehicle guidance.

5.1.9 Instant centre of rotation (*IC*)

The instantaneous centre of rotation is defined as the point at which the wheel and the knuckle will rotate when the suspension moves, so as changes occur in the suspension geometry as a function of traffic incidents, this point will move at the same time.

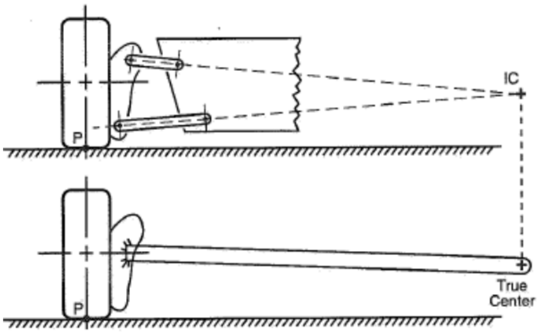

Figure 31. Position of the instant centre of rotation.

The estimation of the instantaneous centre of rotation is purely geometric and is carried out with respect to the front view of the single seater. If we take the middle line of the upper trapeziums in lower and both are prolonged until converging in a point, this point of cut will represent the IC. Its incidence in the behaviour of the vehicle is not trivial, because if it is near the wheel, it will lead to a greater variation of the fall in front of the movement of the suspension, while, if this distance increases, the variation will be smaller.

5.1.10 Roll centre

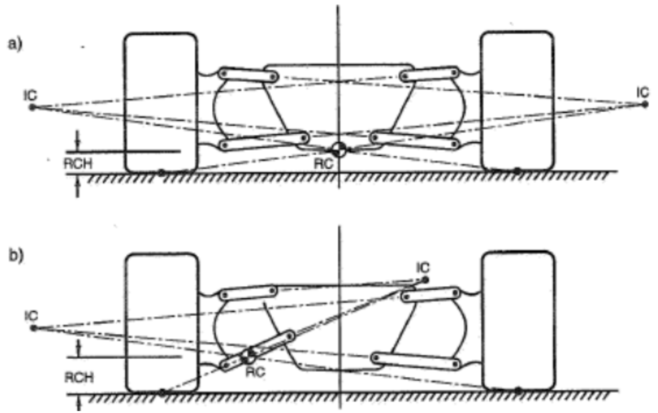

Figure 32. Position of the instant centre of rotation and, consequently, of the roll centre.

The rolling centre is understood as an ideal point at which, given a lateral force F_y applied, there would be no rolling of the suspended mass relative to the unsuspended mass. The rolling centres of the front and rear axle define the rolling axis of the suspended mass and precisely with respect to this axle there will be the movement of this mass, produced exclusively by a rolling torque.

The definition of this point, like that of the instantaneous centre of rotation, is made geometrically, and is determined as the intersection of the lines joining each instantaneous centre of rotation with the midpoint of contact of the tyre tread with the ground.

It should be noted that one of the most relevant points regarding the study of the location of the rolling centre is its position with respect to the ground and its relative position with respect to the centre of gravity.

In the first case, if the RC is close to ground level, but above it, the lateral force generated by the tyre causes a moment on the IC, which pushes the wheel towards the surface (downwards), lifting the sprung mass. This effect is known as Jacking. However, if the wheel is below ground level, this can also compromise the stability of the vehicle; this is because the greater the distance in the vertical between the centre of roll and the centre of masses, the greater the rolling torque that the car suffers from lateral disturbances.

5.1.11 Anti-features

Anti-effects in a suspension model describe the coupling or relationship between the vertical and longitudinal forces supported by the car and the sprung and unsprung mass. These characteristics are only present during the transient processes of acceleration and braking, and depend on the inclination of the swing arm, the height of the centre of gravity and the position of the IR from a side and front view, so they do not affect the load transfer during a stationary state. These anti-features are anti-dive, anti-squat and anti-lift.

The anti-features change the amount of load passing through the springs and the angle of inclination of the car and are quantified as a percentage. As an example, a front axle with 100% anti-dive will not deviate during a braking process, so there will be no load transmission along the springs; whereas if a front axle with 0% anti-dive will deviate depending on the load transferred through the springs, that will be a function of their rigidity.

The definition of each of them is stated in the following lines:

- ***Anti-dive***: reduces the deflection of the front skirt during braking;
- ***Anti-squat***: reduces the elevation of the rear axle during braking (due to a possible pitching moment);
- ***Anti-lift***: reduces the pitching movement of the rear spoiler when accelerating.

The calculations of anti-dive, anti-squat and anti-lift are performed differently depending on whether or not the trapezes support the driving torque or the braking torque on the disc. In the first case, they are calculated according to the location of the instantaneous centre of rotation in relation to the point of contact with the ground. If they do not react to such stresses, they are calculated according to the position of the IC in relation to the wheel centre.

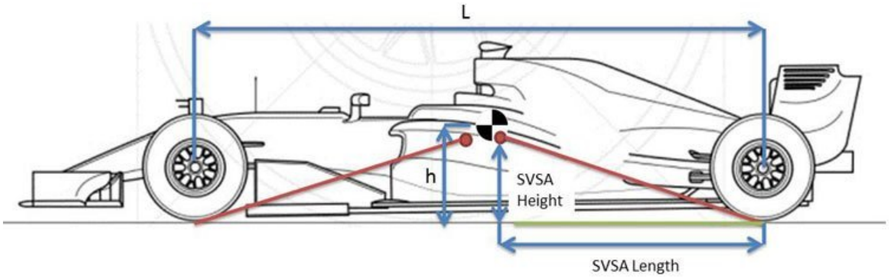

Figure 33. Side-view instant centre of rotation.

5.1.12 Ackermann steering

Ackermann geometry for steering is especially useful when the vehicle is exposed to negligible centrifugal force value, these are conditions assimilable to virtually zero tyre drift angles, negligible load transfer between tyre wheels and relatively low speeds.

This system therefore imposes a minimum slip between the tyre and the asphalt, which forces all the wheels of the car to be oriented in such a way that they move along a path with a common instantaneous centre of rotation (IC).

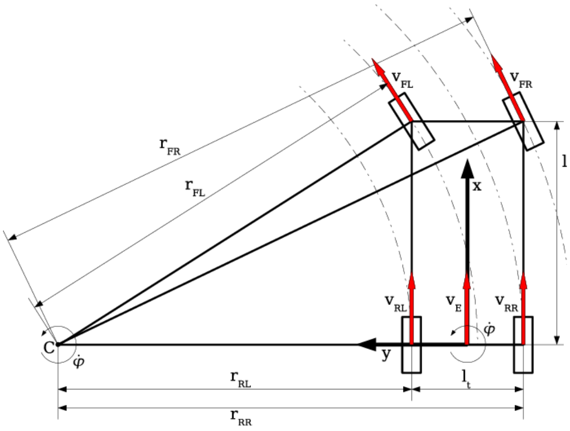

Figure 34. Ackermann geometry.

However, when high lateral forces occur, it is more convenient to implement a parallel or inverted Ackermann geometry for the steering system. Using low-speed steering geometry on a racing vehicle would cause the internal tyre curve to tend to much higher slip angles than necessary and this would only result in increases in tyre temperature, as well as the car slowing down due to the drag induced by that slip angle. Therefore, single seaters competing in the Formula Student format often use parallel steering or even revert to Ackermann.

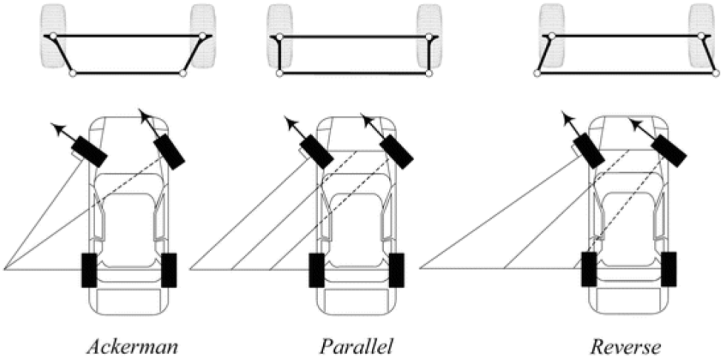
Ackerman Parallel Reverse

Figure 35. Different steering configurations.

5.2 Dynamic parameters

5.2.1 Spring rate, K_S

In the shock absorber used in the suspension system, a helical spring is used, which is an element capable of deforming a given length or deflection x before a given force F acting on it. The mathematical relation that relates both parameters is expressed through a physical law, which is *Hooke's law of elasticity*.

$$F = -k \cdot x$$

where k is the proportionality factor that is characteristic of the spring under consideration, and which more specifically is defined as the spring constant. The minus sign of the previous expression indicates that the force exerted by the spring goes in the opposite direction to the deformation suffered by it.

For a pneumatic-spring system of a suspension constituted by two springs of constants K_1 and K_2, these will be placed in series and the total proportionality constant will be the sum of the two constants. For two springs located in parallel, the total constant will be the sum of the inverse of both constants.

5.2.2 Wheel rate, K_W

It is the stiffness of the unsuspended mass, which differs from the stiffness of the spring due to the spring-beam-push-rod arrangement, which induces a displacement ratio described in the following paragraphs. This parameter is calculated taking into account the stiffness constant of the suspension system or spring (K_{sp}) and the stiffness of the tyre (K_n):

$$K_W = \frac{K_n \cdot K_{sp}}{K_n - K_{sp}}$$

This assumption is based on the 2 d.o.fs. vibrational model of a quarter of a vehicle, which allows approximate fundamental frequencies to be obtained by disregarding the damping and making a simplification, which consists of assuming that the suspended mass is much larger than the unsprung mass. If the opposite were assumed (i.e. the unsprung mass is much greater than the sprung mass), the stiffness of the wheel would be calculated from the serial association of the stiffness of the suspension system and the stiffness of the tyre.

5.2.3 Motion ratio, MR

This parameter represents the relationship between the vertical displacement of the wheel and the compression or extension of the spring-shock assembly. In fact, it is equivalent to the quotient between the travel speeds of the wheel and the shock absorber.

$$MR = \frac{Wheel\ displacement}{Spring\ displacement}$$

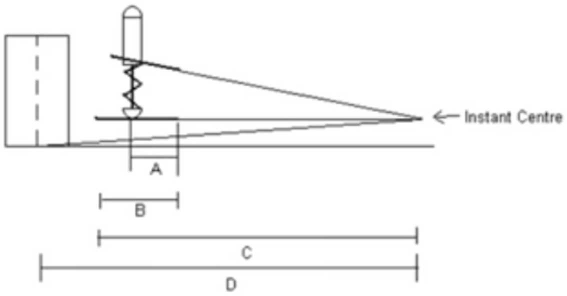

Figure 36. Simple explanation of the motion ratio (a).

This parameter, usually required in the vehicle geometry technical data sheet, is particularly important for the dimensioning of the spring-shock assembly, as well as when calculating the forces transmitted through the push-rod or pull-rod bar and how these affect the forces on the wheels.

From the figure, it is possible to approximate the motion ratio as $MR = {}^{A}/_{B} \cdot {}^{C}/_{D}$: this is the first type of motion ratio. The second one will be explained in Chapter 8.

Moreover, it is possible to calculate the spring constant K_s taking into account the stiffness of the wheel and the displacement ratio: $K_s = K_w \cdot MR^2$

Therefore, if the displacement ratio is greater than 1, then the stiffness of the spring must be greater than the stiffness of the wheel.

5.2.4 Tire radial stiffness

Refers to the ability to absorb irregularities in the road, taking into account its elastic behaviour in a vertical direction. Together with the equivalent damping coefficient, it allows the tyre to be modelled and the influence of its behaviour on the suspension design to be studied. The stiffness of the tyre depends on the type, load conditions and inflation pressure, and certain design parameters.

Radial stiffness is defined by the following expression:

$$K_z = \frac{\partial F_z}{\partial Z}$$

For radial and diagonal tyres, the deformation curves are almost linear, except for relatively small values of load and pressure, so it is generally accepted that the stiffness is usually independent of the value of the load. If it is of the inflation pressure, where it shows a proportionality dependence. In general, diagonal tyres tend to have between 20% and 30% more stiffness than belts, although the latter can increase this factor by 5% by using a metal belt instead of a textile belt.

Within the design parameters, using stiffer sidewalls, a smaller angle between cords, increasing the modulus of elasticity of the fabrics and increasing the number of fabrics allow the stiffness of the tyre to be increased.

5.2.5 Side slip stiffness

Side slip stiffness is the parameter that shows the variation of the transverse force developed in the contact track with the drift angle, without considering the influence of the wheel drop angle. It is therefore defined with the derivative of this lateral force with respect to the drift angle, for a value of this angle $\alpha = 0$.

$$K_\alpha = \left(\frac{\partial F_y}{\partial \alpha}\right)_{\propto=0}$$

The side slip angle is defined as the angle formed by the direction of the contact track and the plane of the wheel, which are not collinear when the car goes through a curve, due to the elastic conception of the tyre itself.

This angle increases as a consequence of the increase in the transverse force supported by the tyre. For small values of the drift angle (i.e. less than 4° or 5°), the relationship between the two parameters is practically linear, as the lateral accelerations are small and so is the tyre-ground slip in that area.

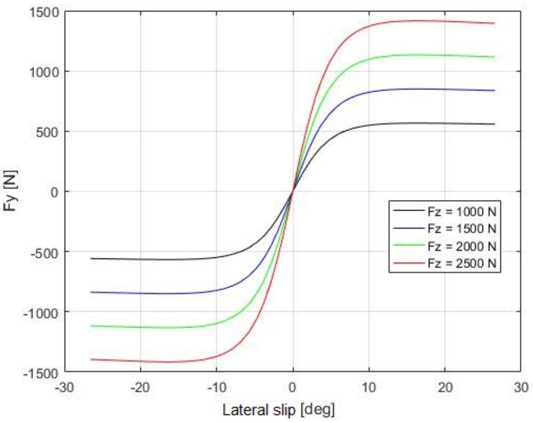

Figure 37. Typical side forcé characteristic.

For higher values of this angle, the slope of the curve decreases, establishing a lateral force value that coincides with the grip limit available in that direction, causing the wheel to skid.

Side slip stiffness is a factor that depends on the structural and geometric characteristics of the tyre, inflation pressure, normal load conditions and temperature, camber value and lateral load transfer between wheels.

5.2.6 Natural frequency of the sprung mass

It is the frequency of oscillation of the sprung mass due to a transient excitation, motivated by the expansion and compression of an elastic element. It is the inverse of the period (T) and is measured in *Hertz* (Hz). If a mass is excited with a periodic force of the same frequency, the oscillations that take place as a sub-damped system have great amplitude, all the greater when the system is little damped.

In fact, the stiffness of the spring is directly related to the oscillation, being this one of greater frequency when the constant of stiffness is greater. A lower value of this constant will ensure a longer period of time to complete the rise and fall of the sprung mass. The relationship between the frequency of oscillation and the stiffness constant of the wheel is determined by the following mathematical expression:

$$f_n = \frac{1}{2\pi} \cdot \sqrt{\frac{K_w}{M}}$$

M being the total sprung mass, or in this case, that corresponding to the mass suspended over a quarter of a vehicle (corresponding to a wheel). In competition, the natural frequency of oscillation can reach 6 Hz.

The weight distribution is greater in the rear than in the front, due to the set of batteries located in the rear, so the frequency will be higher in the front than in the rear of the single seater.

5.2.7 Damping coefficient

In relation to what has been said in the previous section, the study of the oscillation of the elements belonging to the suspended mass must integrate the damping coefficient ζ, the value of which is stated in the following formula:

$$\zeta = \frac{1}{2} \cdot \frac{C}{\sqrt{K_w \cdot M}}$$

where the value of M is the total mass supported by a wheel and C is the damping constant of the spring. The value of the damping coefficient makes it possible to classify the system as follows:

- If $\zeta = 1$, the system is critically damped.
- If $\zeta < 1$, the system is underdamped (most common).
- If $\zeta > 1$, the system is overdamped.

5.2.8 Anti-roll bar stiffness

It is the parameter that relates the torque (or bending moment, according to the design) to which the bar is subjected and the angle of rotation of the same at that moment. Its value may not be constant and is a function of the dimensions of the bar, that is, the diameter of the section and its length.

As has already been mentioned in previous lines, the design of the current suspension geometry does not have a stabiliser bar, so it is essential to obtain an approximate calculation of the total stiffness to swing of the suspension to evaluate the need to incorporate it. These data will be highlighted for the possibility of being designed in the future by the member of the team in charge of this activity.

6. SUSPENSION DESIGN

There are several factors to consider when designing a suspension. First of all, you need to identify the geometry you want to adopt, so you can follow a series of steps that allow you to get all the desired features.

Obviously, the first part of the design is to define the kinematic behaviour of the suspension, and then follow by studying the dynamic behaviour of the vehicle.

The procedure used to define kinematic characteristics is the following:

- Design of the oscillating arms in front view, to identify the centre of instantaneous rotation, then the centre of roll and the walking camber angle;
- Design of the oscillating arms in lateral view, to identify the centre of instantaneous rotation and define the "anti-features";
- Modify the anchors on the sleeve to obtain the desired king-pin axis, scrub radius and forward angle;
- Control of the tie rod / caster rod to obtain a desired variation of the;
- Overall optimization.

Then, it is necessary to define the suspension dynamic parameters, by following these steps:

- Definition and design of the spring motion ratio;
- Choice of the proper spring available from the list;
- Definition and design of the anti-roll bar motion ratio;
- Compensation of the wheel stiffness with the proper anti-roll bar stiffness;
- Choice of the damping characteristic available from the list.

6.1 Recommended values

Of course, it will be necessary to set values with which the suspension will then be designed. These values are different depending on the vehicle you are designing and, therefore, it is necessary to identify the recommendations for racing vehicles.

6.1.1 Wheelbase

Mandatorily $>\ 1525\ mm$; most common during competition between $1530 - 1650\ mm$.

6.1.2 Track

The track may be different on the front axle and on the rear axle but must comply with the restriction imposed by the FSAE regulation, which stipulates that the vehicle's shortest track must be at least 75% of the wheelbase.

The track is of particular importance in the study of vehicle lateral dynamics, as the tipping limit speed (V_{lv}) is directly proportional to the square root of the track. For a curve of radius R and inclination α, and a car of track B and centre of mass height h, the speed limit mentioned above is: $V_{lv} = \sqrt{gR\,\frac{B/_{2h}+\tan\alpha}{1-B/_{2h}\cdot\tan\alpha}}$.

6.1.3 Roll centre

In this case, it is necessary to analyse the height of the rolling centre and the lateral migration of this point with respect to the symmetry axis. During the turning of the vehicle, the centrifugal force applied in the centre of masses of the single seater generates a load transfer that is absorbed by the springs of the suspension system, compressing those of the outer wheel and extending those of the inner wheel.

There is also a rolling torque, which is directly proportional to the difference in height between the centre of gravity and the rolling centre. The greater this distance, the greater the rolling torque and therefore the greater the instability of the vehicle during traffic. If it is above ground level, then the Jacking effect is favoured, which is in any case undesirable for the behaviour of the single seater. It is therefore necessary to reach an intermediate point, usually slightly higher than the level of the running surface, in order to avoid accentuating one effect more than the other. It is common to use a value that is close to 50 mm at the front and it may be a bit higher at the rear.

On the other hand, the roll centre is located as close as possible to the longitudinal plane of symmetry of the vehicle, in order to avoid a different distribution of loads during the passage through the curve (i.e. a different distribution of weights between the entry and exit of the curve). In order to favour the handling of the load transfer at will, this can be done by varying the springs or with an adequate adjustment of the stabilising bar.

6.1.4 Camber angle

It is recommended that the camber be negative on both the front and rear axle wheels. Usually, the camber angle is between $-1°$ and $-3°$, so that there is greater grip, which ensures greater transversal force. In general, the coefficient of friction tends to be higher when the camber is negative, evolving increasingly until a value close to $-3°$, from which it begins to decrease.

It should be noted that the evolution of the coefficient of friction with the camber angle is slightly different for front and rear tyres, since, despite the same trend, rear tyres tend to have a better grip. In order to configure the camber angle in the design of the geometry, it is established by giving the given inclination with respect to the horizontal to the axle of the knuckle, which is parallel to the plane of symmetry of the wheel. The camber therefore ensures that the weight of the vehicle to which the wheel is subjected moves towards the inside of the handlebar, to reduce wear on the wheel bearings; therefore, providing a negative angle to the wheels of the single seater ensures that, in the event of a given lateral stress, the compression of the suspension of the wheel that bears more weight places it in such a position that the plane of symmetry of the wheel is practically perpendicular to the asphalt, ensuring greater tyre-surface contact.

6.1.5 Caster angle

The higher the caster angle, the heavier the caster will be, the more effort will be required. However, if the angle is reduced, the direction becomes too light and unstable. Therefore, the value of the angle of advance must reach a compromise between the mentioned aspects, in such a way that it favours the "self-guiding" of the car, reason why it is susceptible to the existing differences between the wheels of a same axle.

If front-wheel drive, the caster is usually between 6° and 12°; if rear-wheel drive, the caster is usually between 3° and 5°. Within these recommended values, single seater Formula SAE are usually taken angles of advance between 3° and 6° for the front driving axle and between 4° and 9° for the rear tractor. The forward angle is usually adjusted by varying the lengths of the steering reaction arms (both upper and lower), or by varying the position of the additional washers that are anchored to the trapezoids that make up the suspension parallelogram.

6.1.6 King-pin inclination

The recommendations regarding the starting angle are different for commercial vehicles, which have values between 4° and 12°, that, for competition vehicles, where the inclination is limited to tighter values. In general, the priority for single seaters is not premature wear on the bearings and the stub axle, but rather the fact of reducing the hardness of the steering in the front axle as it is unassisted. Therefore, the value of the inclination of the pivot axle in these cases is usually between 3° and 6°. It should be noted that, in the case of the rear axle, the angle of exit does not revert as much importance as in the front, although its study is key to reducing the values of stresses and tensions in bars. The values of this parameter are usually positive, although it has the disadvantage that, during the braking process, the torque induced on the wheels by the action of the friction force and the weight of the car, makes it destabilise when the steering is opened. If it is negative, the opposite occurs.

6.1.7 Scrub radius

The Scrub Radius is generally set at positive values, but in no case null or close to zero, as this would lead to the generation of high stresses and increased rigidity in the steering system components. Some reference values place it around $15 - 25\ mm$, although registers of up to $40 - 50\ mm$ are permissible.

6.1.8 Toe angle

The convergence angle is usually measured in linear units (usually in mm) or in angular units. The most common convergence values range from ± 1 and $\pm 5\ mm$, depending on whether the configuration is toe-in or toe-out. This is an important aspect for wheel guidance, and it is preferable that it does not change sign with respect to its static value, in order to favour the behaviour of the steering in the case of the front axle.

6.1.9 Anti-features

- ***Anti-squat:*** a certain percentage of anti-squat is recommended at the rear of the car, this being a moderate value, usually in the range of $0 - 50\%$.
- ***Anti-dive:*** a certain percentage of anti-sinking is recommended at the front of the single seater during the braking process, with an admissible value of slightly more than 30%.
- ***Anti-lift:*** it is recommended, as in the case of anti-squat, values in the range of $0 - 50\%$, to avoid excessive pitching in the rear of the car, when the vehicle is in a braking process.

6.2 Suspension's kinematics design

Considering that the preferred suspension type is the double-wishbone, there exist a procedure that allows to design the suspension itself by setting the wanted characteristics. This procedure requires the design in two plans: *front* and *side views*.

6.2.1 Front-view design

For the front view design, different phases are considered:

1. ***Desired camber recovery.*** The camber recovery is a percentage parameter that relates the variation of the wheel-vehicle drop angle with respect to the vehicle roll. That is to say, a camber recovery equal to 100% means that the more the chassis rolls, the more the wheels will always remain perpendicular to

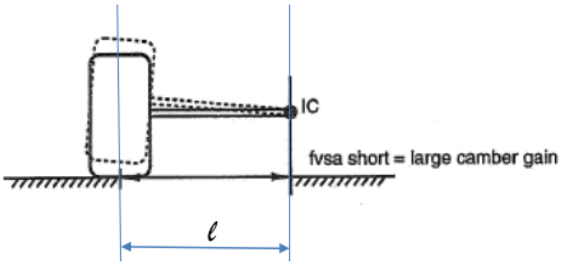

Figure 38. Camber change rate.

the ground. Considering this value, one can look for the extension l of the virtual arm that connects the wheel to the centre of instantaneous rotation, around which the wheel makes its rotation during its displacement.

$$l = \frac{t/2}{1 - \frac{\Delta\gamma}{\phi}}$$

where t is the vehicle track and $\Delta\gamma/\phi$ the camber recovery value.

2. ***Height of the balancing centre.*** It has to be in a point of the plane of symmetry of the vehicle considering that it will affect the evolution of the camber angle and the rigidity of the suspensions as well: the higher it will be, the higher the rigidity of the suspensions, given that the cam of the centrifugal force that acts in the centre of gravity is bigger and the roll will be bigger. At the same time, a low centre of roll would be better by the evolution of the angle of fall, because less would be affected by the displacement of the wheel.
3. ***Central line of the oscillating arms.*** Once the centre of instantaneous rotation of the wheels has been searched for, it is possible to draw the lines passing through this and through the anchorages where the oscillating arms have to stay. Thus, it is necessary to fix the ball joints considering that the lower one should be as much as possible close to the ground, considering all clearances and compliances of the tire, to reduce the forces on the lower arm and balance at best the bending coming from the side forces. Considering the upper ball joint, its position depends mainly on the packaging requests.
4. ***Extension of the oscillating arms.*** Generally, to get a good camber evolution, the upper arm has to be shorter than the lower one. However, by modifying the extensions of the two arms, what is called *camber gain* is controlled: a large camber gain is obtained with a shorter upper swing arm and means that the variation of the falling angle is larger as well, which is good for a track with many curves; a smaller camber gain is obtained with a longer upper arm, which implies a smaller variation of the camber angle, perfect for faster tracks. Why? To always guarantee a good contact surface between wheel and ground. In addition, this camber gain can be modified by changing the position of the anchors, moving the roll centre.
5. ***Tie rod centre line.*** It also has to pass through the centre of instantaneous rotation in order not to obtain the effect of undesired steering (*bump steer*), which effect is explained in Chapter 4.
6. ***Tie rod extension.*** The tie rod is what affects the evolution of the angle of convergence (toe angle) during the displacement of the wheel, considering the

wear of the tire. This angle will be negative by the toe-in, i.e. when the wheels converge in front of the vehicle, and positive by the toe-out, when the wheels converge behind. Any time there is a positive convergence angle, the stiffness of the axle increases: for example, during braking, the angle would have to be positive for the front axle, so that a behaviour of more understeer is present. The typical ride of the convergence angle is positive in bounce and negative in rebound, while what is obtained is greater linear stability with toe-in and better response to turning with toe-out.

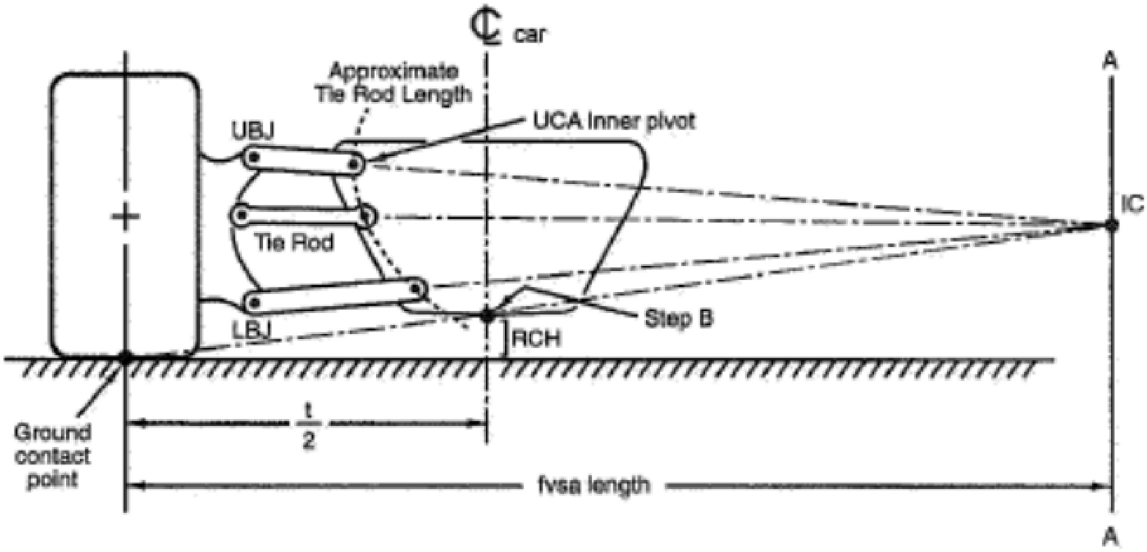

Figure 39. Front-view design scheme.

6.2.2 Side-view design

For the side view design, the main objective is to define the instantaneous rotation centre to obtain the desired values of the anti-features. This is obtained through different angles, with respect to the wheel-floor contact (external action, brakes) and also to the wheel centre (motor axle, braking and traction).

Clearly, the angles have to be a compromise between the different anti-features, since anti-lift and anti-dive (for the front axle) refer to different points, as said before, as for the rear axle. The formulas used by the front axle are:

$$\phi_1 = \tan^{-1}\left[\frac{h_{CG}}{l \cdot K} \cdot (\%\, ANTIDIVE)\right]$$

$$\phi_1' = \tan^{-1}\left[\frac{h_{CG}}{l \cdot K} \cdot (\%\, ANTILIFT)\right]$$

$$\phi_1'' = \tan^{-1}\left[\frac{h_{CG}}{l} \cdot (\%\, ANTILIFT)\right]$$

where:

- h_{CG} is the height of the center of gravity from the ground;
- l is the wheelbase;

- K is the percentage of braking to the front axle;
- ϕ_1 is the angle that has to be positioned on the wheel-floor contact by the anti-dive, considering an external intervention by the braking (brakes);
- ϕ_1' is the angle that has to be positioned in the centre of the wheel by the anti-lift, considering an "internal" intervention (i.e. the effect that the motor has on the braking, if present);
- ϕ_1'' is the angle that has to be positioned in the centre of the wheel as well, considering a motor axle in traction phase.

The same considerations have to be made by the rear axle; instead, here there is the anti-squat and not the anti-dive.

$$\phi_1 = \tan^{-1}\left[\frac{h_{CG}}{l \cdot (1-K)} \cdot (\%\ ANTILIFT)\right]$$

$$\phi_1' = \tan^{-1}\left[\frac{h_{CG}}{l \cdot (1-K)} \cdot (\%\ ANTILIFT)\right]$$

$$\phi_1'' = \tan^{-1}\left[\frac{h_{CG}}{l} \cdot (\%\ ANTISQUAT)\right]$$

In fact, the angles have to be a compromise, because it is clearly impossible to get 100% on all anti-features. Following the recommended values, the anti-squat would have to be between 0 and 50%, the anti-dive greater than 30% (many times in competition it would be at least 80%) and the anti-lift between 0 and 50% as well.

Once you have searched for the optimal angles, such as the front suspension, you can identify the instantaneous rotation centre of the wheel, then draw the lines through that and through the anchors and look for the centre line of the two oscillating arms.

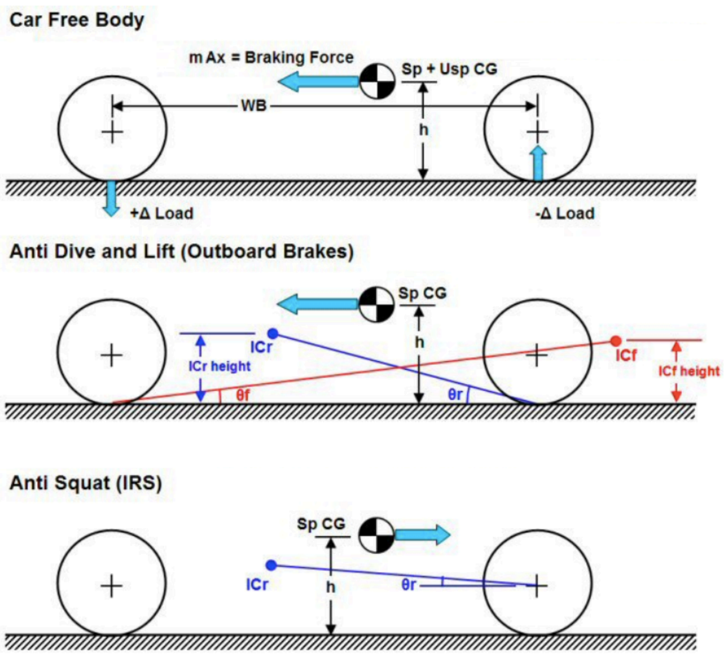
Car Free Body
m Ax = Braking Force
Sp + Usp CG
WB
h
+Δ Load
-Δ Load
Anti Dive and Lift (Outboard Brakes)
Sp CG
ICr
ICr height
θf
h
θr
ICf
ICf height
Anti Squat (IRS)
Sp CG
ICr
h
θr

Figure 40. Anti-feature characteristic angles.

6.3 Suspension's dynamics design

The first step in choosing spring stiffness is to choose your desired ***ride frequencies***, front and rear. A ride frequency is the undamped natural frequency of the body in ride. The higher the frequency, the stiffer the ride. So, this parameter can be viewed as normalized ride stiffness. Based on the application, there are some recommendations to consider:

- $0.5 - 1.5\ Hz$ for passenger cars;
- $1.5 - 2.0\ Hz$ for sedan race cars and moderate downforce formula cars;
- $3.0 - 5.0 +\ Hz$ for high downforce race cars.

Lower frequencies produce a softer suspension with more mechanical grip and the response will be slower in transient (what drivers report as "lack of support"). Higher frequencies create less suspension travel for a given track, allowing lower ride heights, and in turn, lowering the centre of gravity. Ride frequencies front are rear are generally not the same, there are several theories to provide a baseline.

There is one aspect to consider when setting suspension frequency: in the case of hitting an obstacle, having the same ride frequency for both axles, the body will start pitching, since the rear sprung mass oscillates with the same frequency but delayed of a certain time (given by the length of the wheelbase).

So, generally, the rear ride frequency is increased a bit with respect to the front, to let it oscillate faster and synchronize faster with the oscillation of the front, thus entering in phase and minimize pitch.

For a given wheelbase and speed, a frequency split front to rear can be calculated to minimize pitching of the body due to road bumps. A common split is 10 – 20% front to rear.

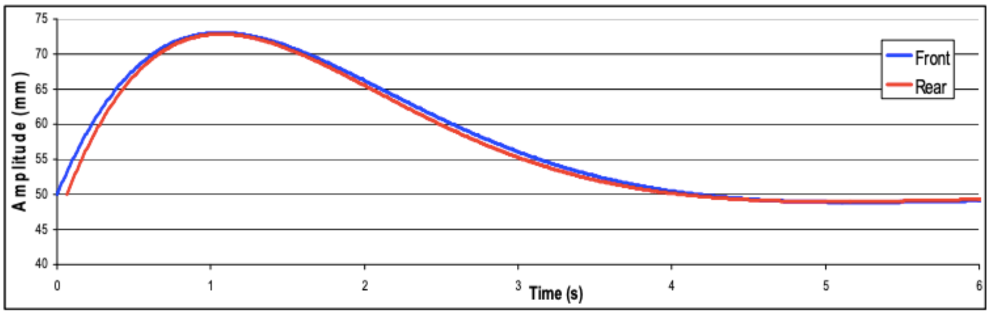

Figure 41. Rear frequency increased by 10%.

The above theory was originally developed for passenger cars, where comfort takes priority over performance, which leads to low damping ratios, and minimum pitching over bumps. Race cars in general run higher damping ratios, and have a much smaller concern for comfort, leading to some race cars using higher front ride frequencies. The higher damping ratios will reduce the amount of oscillation resultant from road bumps, in return reducing the need for a flat ride.

A higher front ride frequency in a race car allows faster transient response at corner entry, less ride height variation on the front (the aerodynamics are usually more pitch sensitive on the front of the car) and allows for better rear wheel traction (for rear wheel drive cars) on corner exit. The ride frequency split should be chosen based on which is more important on the car you are racing, the track surface, the speed, pitch sensitivity, etc.

Once the ride frequencies are chosen, the spring rate needed can be determined from the motion ratio of the suspension, sprung mass supported by each wheel, and the desired ride frequency.

$$f = \frac{1}{2\pi}\sqrt{\frac{K_W}{M}}$$

$$K_s = K_W \cdot MR^2 = 4\pi^2 f^2 m_{sm} \cdot MR^2$$

Similar to choosing ride frequencies for bump travel, a ***roll stiffness*** must be chosen next. The normalized roll stiffness number is the roll gradient, expressed in degrees of body roll per g of lateral acceleration. A lower roll gradient produces less body roll per degree of body roll, resulting in a stiffer vehicle in roll. Typical values are listed below:

- 0.2 – 0.7 deg/g for stiff higher downforce cars;
- 1 – 1.8 deg/g for low downforce sedans.

A stiffer roll gradient will produce a car that is faster responding in transient conditions, but at the expense of mechanical grip over bumps in a corner. Once a roll gradient has been chosen, the roll gradient of the springs should be calculated, the anti-roll bar stiffness is used to increase the roll gradient to the chosen value.

The roll gradient is usually not shared equally by the front and rear: Milliken proposed to use the weight distribution as a solution, but with this procedure a 5% more is added to the front stiffness, that OptimumG guide call it *magic number*.

So, roll stiffness is computed, both for front and rear.

$$\frac{\phi_r}{a_y} = \frac{mgh}{K_{\phi f} + K_{\phi r}}$$

$$K_{\phi f} = \frac{\pi t_f^2 K_{lf} K_{rf}}{180\left(K_{lf} + K_{rf}\right)}$$

$$K_{\phi r} = \frac{\pi t_r^2 K_{lr} K_{rr}}{180(K_{lr} + K_{rr})}$$

Then, it can be possible that vehicle roll stiffness is not sufficient, considering a desired roll gradient. Thus, the way to compensate this lack is to put an anti-roll bar on the front and on the rear. The formulas listed below allow to compute the two stiffness, considering the weight distribution and the *magic number*.

$$K_{\phi,des} = \frac{mgh}{\phi/a_y}$$

$$K_{\phi,arb} = \frac{\pi}{180}\left[\frac{K_{\phi,des}K_T\left(t^2/2\right)}{K_T\cdot\left(t^2/2\right)\frac{\pi}{180} - K_{\phi,des}}\right] - \frac{\pi K_W\cdot\left(t^2/2\right)}{180}$$

$$K_{\phi,farb} = K_{\phi,arb}\frac{N_{mag}}{100}MR_{farb}^2$$

$$K_{\phi,rarb} = K_{\phi,arb}\frac{100 - N_{mag}}{100}MR_{rarb}^2$$

As you can have four different spring rates - ride, single wheel bump, roll, and pitch - in an ideal situation, you will have four different ***damping ratios*** (ζ). The first step is to calculate the desired damping in ride, single wheel bump, roll, and finally pitch. An undamped system will tend to eternally vibrate at its natural frequency. As the damping ratio is increased from zero, the oscillation trails off as the system approaches a steady state value. Eventually, critical damping is reached- the fastest response time without overshoot. Beyond critical damping, the system is slow responding. An important point to understand that will be useful when tuning the shocks on the car is that once any damping is present, the amount of damping does not change the steady state value- it only changes the amount of time to get there and the overshoot.

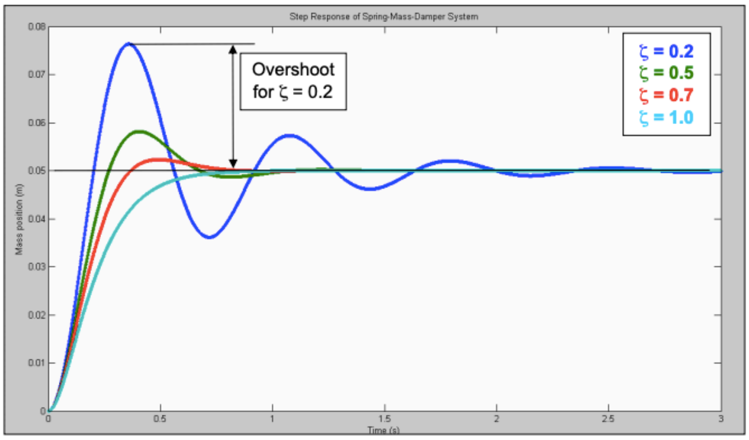

Figure 42. Damping influence on the frequency response.

The first place to start on damping is ride motion. Choosing a damping ratio is a trade-off between response time and overshoot- you want the smallest of each. Passenger vehicles generally use a damping ratio of approximately 0.25 for maximizing ride comfort. In race cars, 0.65 to 0.70 is a good baseline; this provides much better body control than a passenger car (less overshoot), and faster response than critical damping. Some successful teams end up running damping ratios in ride greater than 1, this does not indicate that damping ratios in ride should be large, it shows that there is a compensation for a lack of damping in roll and pitch, as the dampers that control ride motion usually also control the roll and pitch motion.

7. ANALYSIS OF SUSPENSION MODELS

The first analysis of this project is carried out on the last combustion vehicle designed by the team. The project referred to is that of Daniel, one of the students of the team who dedicated himself, in a similar way to this treatise, to the suspension of the single-seater. In fact, the points of the optimal geometry found are reused, which will then be analysed cinematically and dynamically.

Then, an "electric" solution will be proposed for the same characteristics of the vehicle: the push-rod will be raised and the arms will be moved away from each other, as if there were the motor installed in the wheel. This last optimization will be then used as a starting point for the final suspension model for the 2020 electric single seater.

7.1 Petrol vehicle

The first analysis is devoted to the suspension geometries of the last UPM Racing combustion vehicle. As anticipated, their kinematic behaviour will be analysed and compared to a new solution.

7.1.1 Geometries

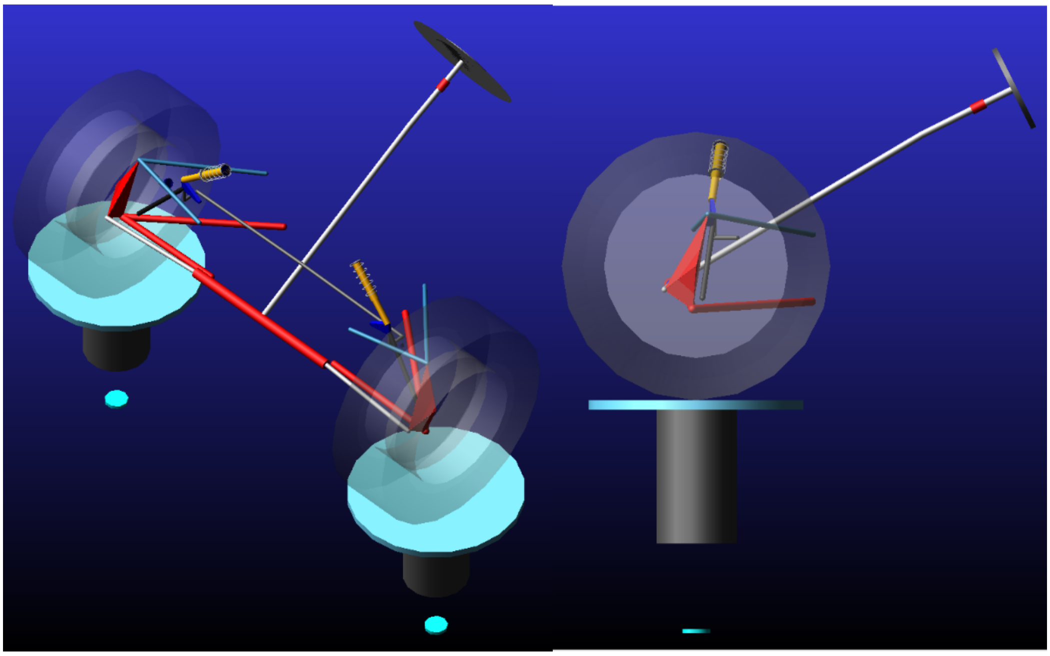

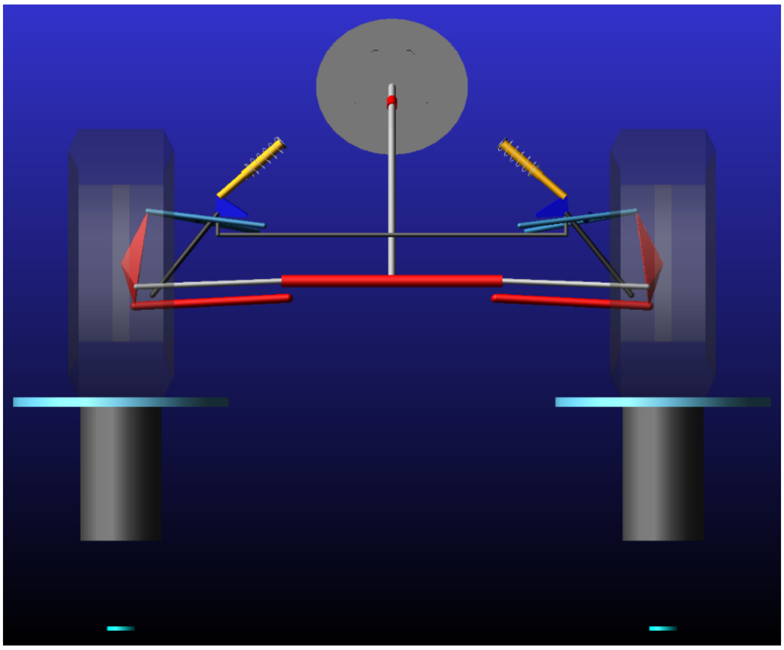

The two geometries are shown: above there is the front suspension, while below the rear one.

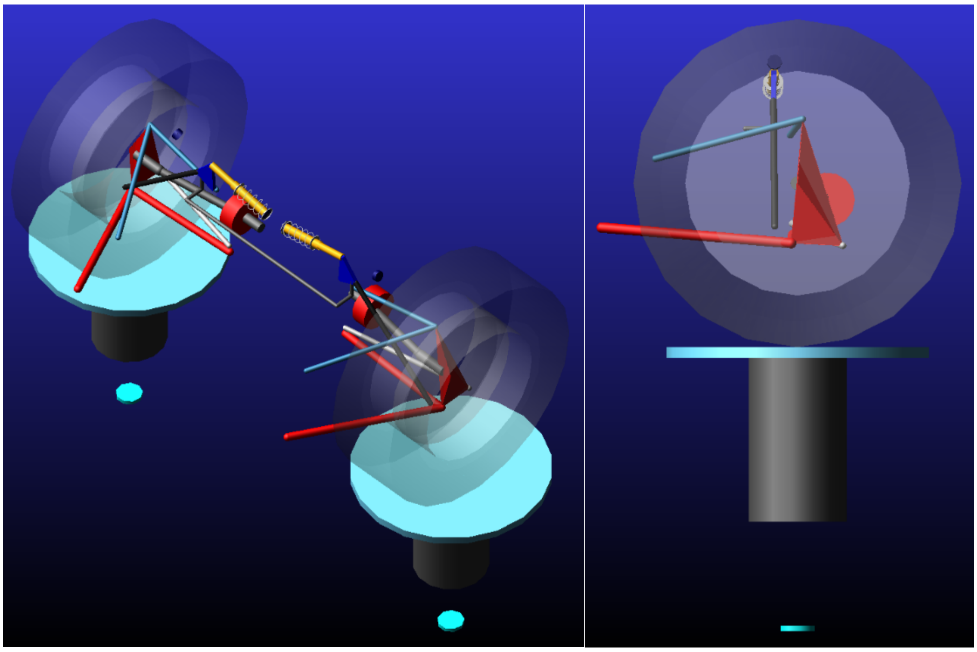

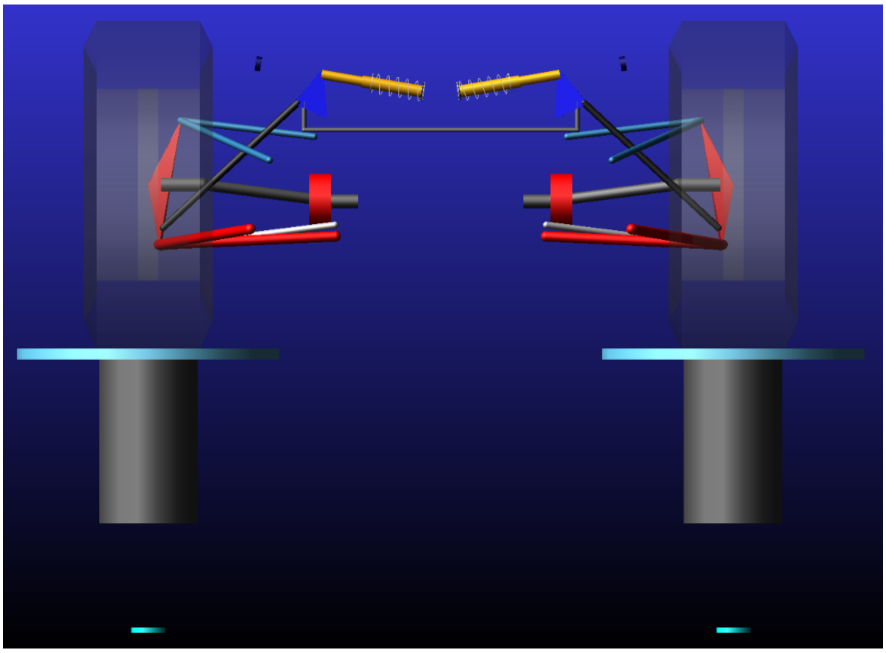

7.1.2 Kinematic analysis

In the following, are shown all the plots relative to the main suspension parameters explained in Chapter 5, distinguishing front and rear suspensions.

7.1.2.1 Front suspension

7.1.2.1.1 Parallel

The parallel wheel travel is a simulation aimed at considering the same amount of displacement for both wheels. As it can be seen, the curves for left and right wheels coincide.

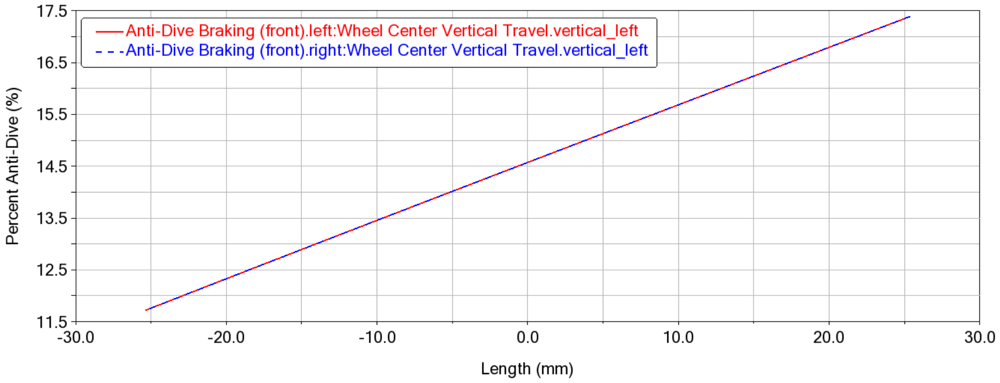

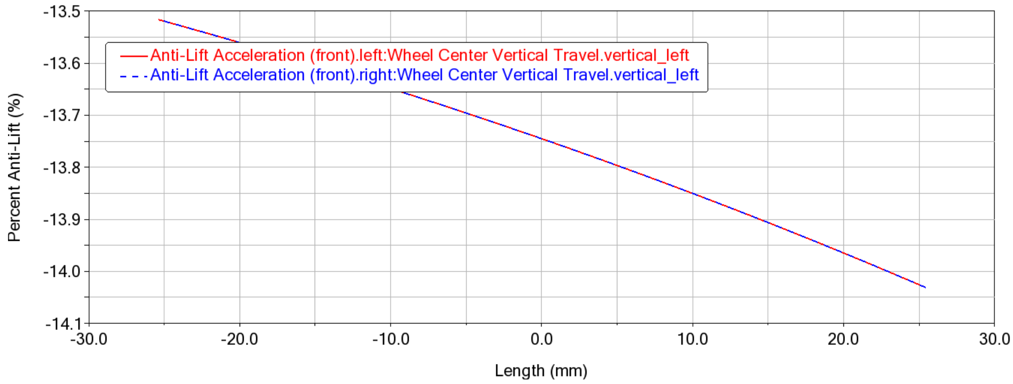
Anti-Lift Acceleration (front).left:Wheel Center Vertical Travel.vertical_left
Anti-Lift Acceleration (front).right:Wheel Center Vertical Travel.vertical_left
Percent Anti-Lift (%)
-13.5
-13.6
-13.7
-13.8
-13.9
-14.0
-14.1
-30.0
-20.0
-10.0
0.0
10.0
20.0
30.0
Length (mm)

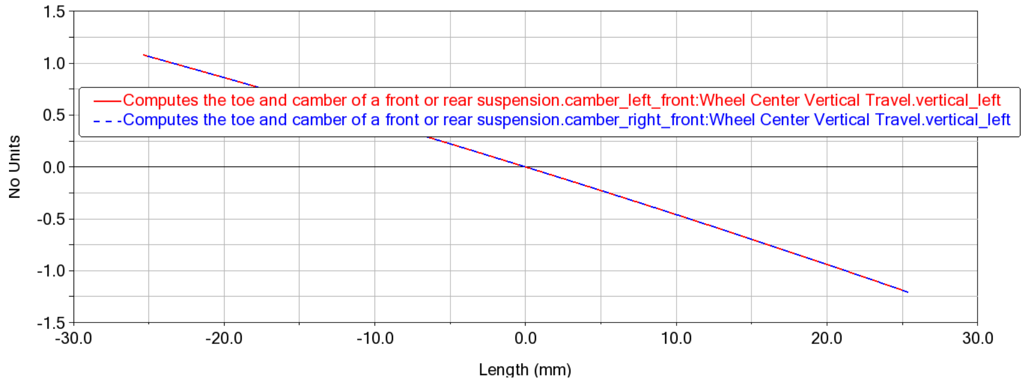
Computes the toe and camber of a front or rear suspension.camber_left_front:Wheel Center Vertical Travel.vertical_left
Computes the toe and camber of a front or rear suspension.camber_right_front:Wheel Center Vertical Travel.vertical_left
No Units
1.5
1.0
0.5
0.0
-0.5
-1.0
-1.5
-30.0
-20.0
-10.0
0.0
10.0
20.0
30.0
Length (mm)

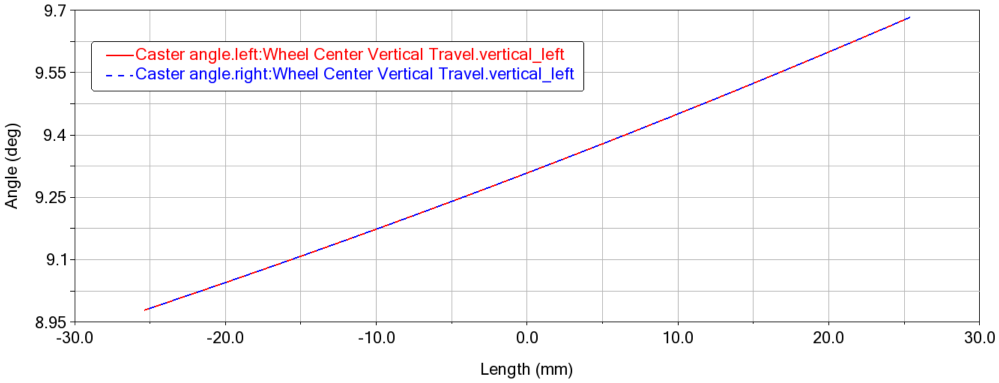
Caster angle.left:Wheel Center Vertical Travel.vertical_left
Caster angle.right:Wheel Center Vertical Travel.vertical_left
Angle (deg)
9.7
9.55
9.4
9.25
9.1
8.95
-30.0
-20.0
-10.0
0.0
10.0
20.0
30.0
Length (mm)

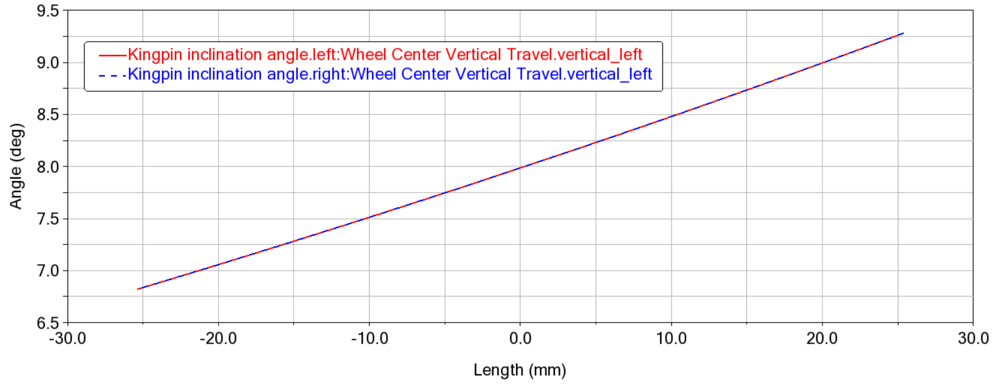
Kingpin inclination angle.left:Wheel Center Vertical Travel.vertical_left
Kingpin inclination angle.right:Wheel Center Vertical Travel.vertical_left
Angle (deg)
9.5
9.0
8.5
8.0
7.5
7.0
6.5
-30.0
-20.0
-10.0
0.0
10.0
20.0
30.0
Length (mm)

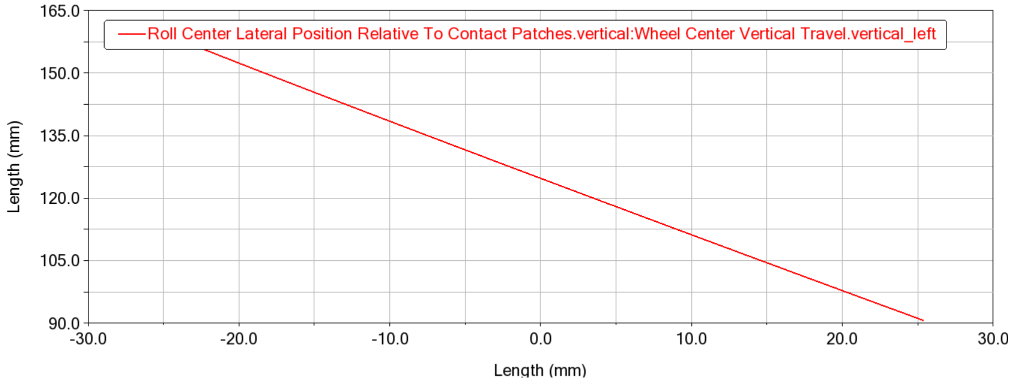
Roll Center Lateral Position Relative To Contact Patches.vertical:Wheel Center Vertical Travel.vertical_left
Length (mm)
165.0
150.0
135.0
120.0
105.0
90.0
-30.0
-20.0
-10.0
0.0
10.0
20.0
30.0
Length (mm)

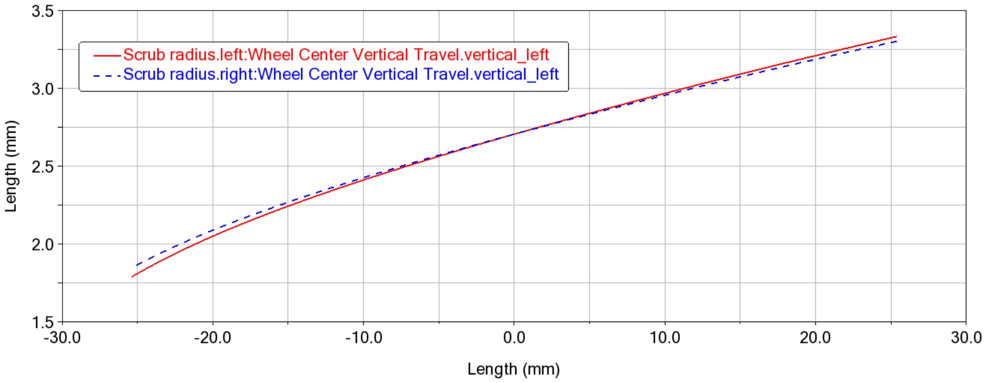
Scrub radius.left:Wheel Center Vertical Travel.vertical_left
Scrub radius.right:Wheel Center Vertical Travel.vertical_left
Length (mm)
3.5
3.0
2.5
2.0
1.5
-30.0
-20.0
-10.0
0.0
10.0
20.0
30.0
Length (mm)

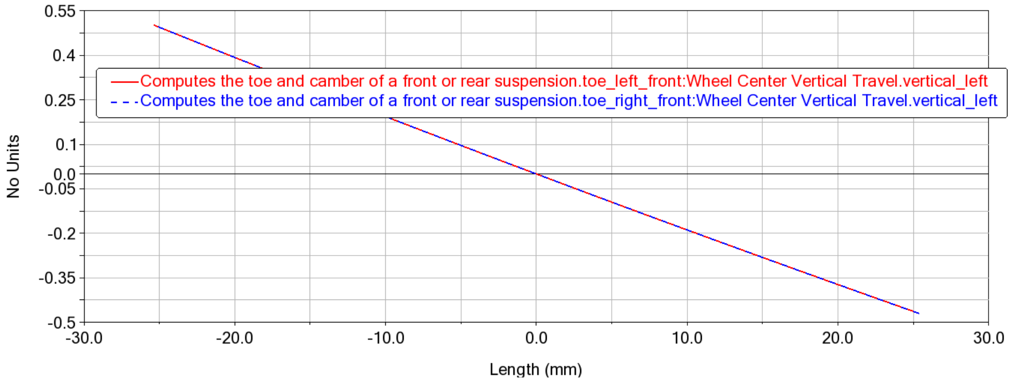
Computes the toe and camber of a front or rear suspension.toe_left_front:Wheel Center Vertical Travel.vertical_left
Computes the toe and camber of a front or rear suspension.toe_right_front:Wheel Center Vertical Travel.vertical_left
No Units
0.55
0.4
0.25
0.1
0.0
-0.05
-0.2
-0.35
-0.5
-30.0
-20.0
-10.0
0.0
10.0
20.0
30.0
Length (mm)

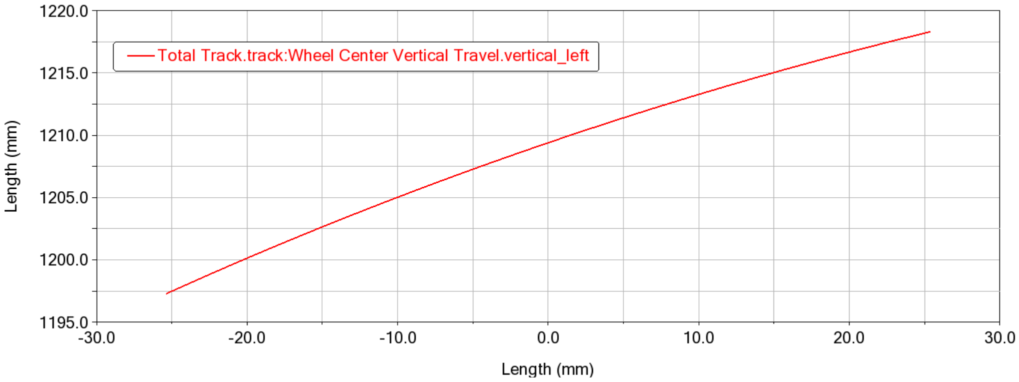
Total Track.track:Wheel Center Vertical Travel.vertical_left
Length (mm)
1220.0
1215.0
1210.0
1205.0
1200.0
1195.0
-30.0
-20.0
-10.0
0.0
10.0
20.0
30.0
Length (mm)

7.1.2.1.2 Opposite

On the contrary, this simulation studies the effect of an opposite wheel travel: the wheels run the same path but in an opposite way, simulating cornering conditions. As a matter of fact, the curves of each plot are symmetric for left and rear.

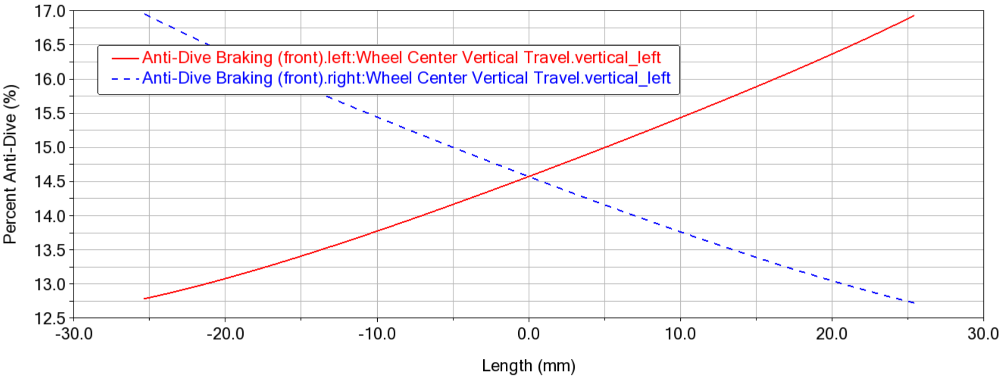

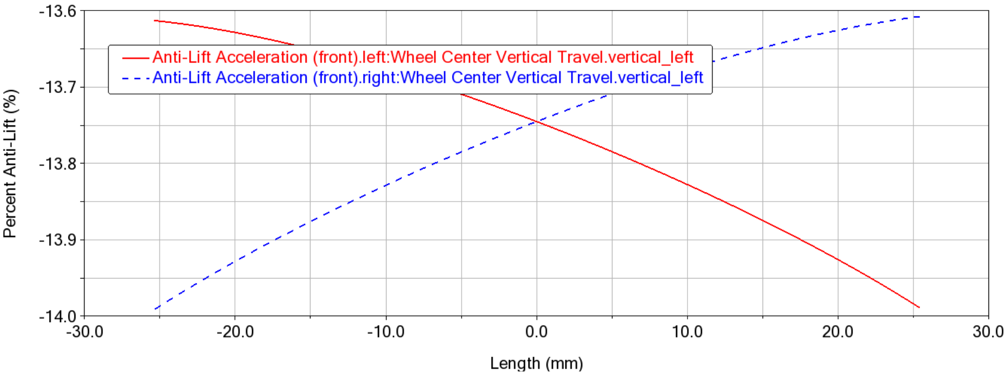

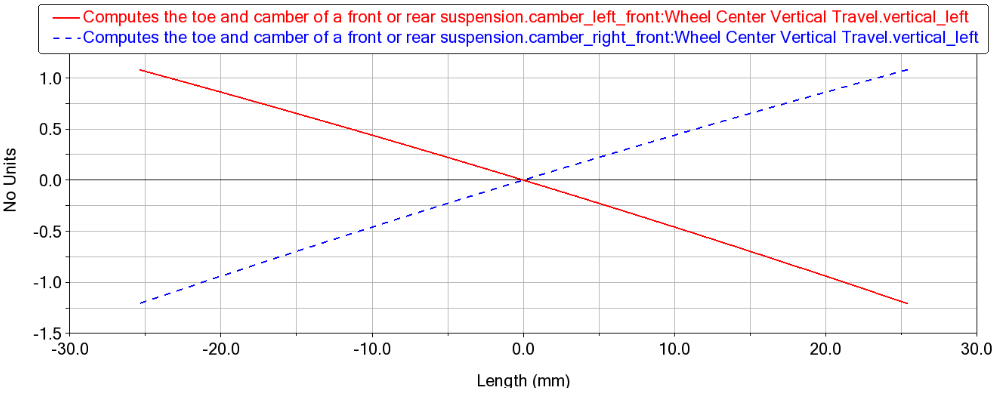

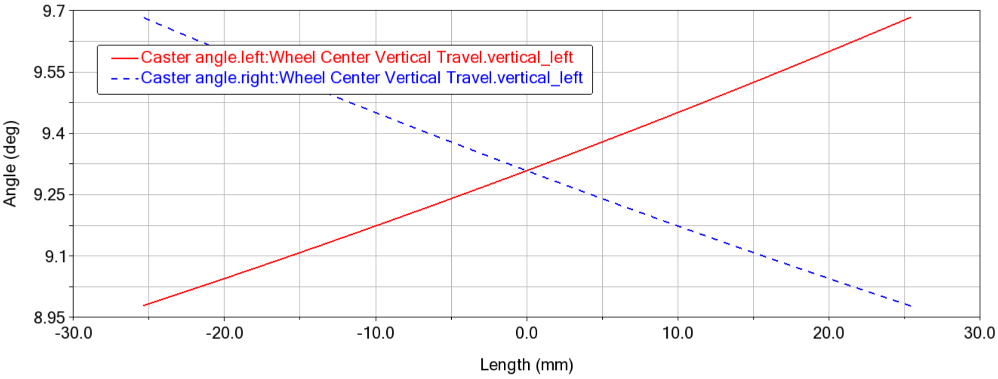

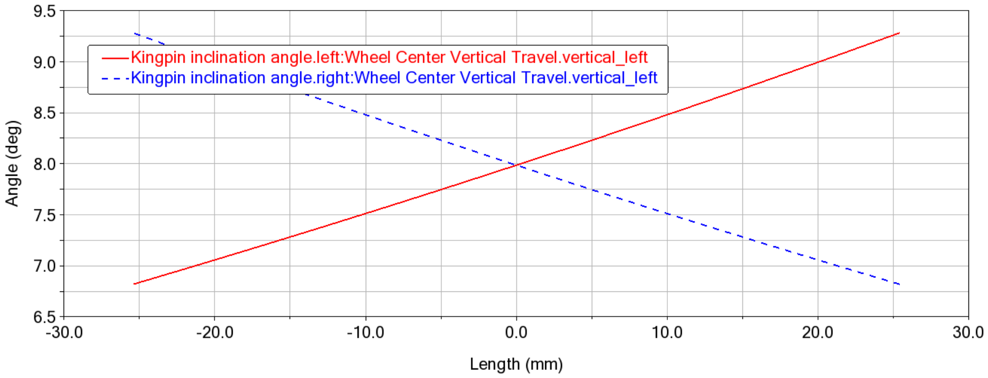
Kingpin inclination angle.left:Wheel Center Vertical Travel.vertical_left
Kingpin inclination angle.right:Wheel Center Vertical Travel.vertical_left
Angle (deg)
9.5
9.0
8.5
8.0
7.5
7.0
6.5
-30.0
-20.0
-10.0
0.0
10.0
20.0
30.0
Length (mm)

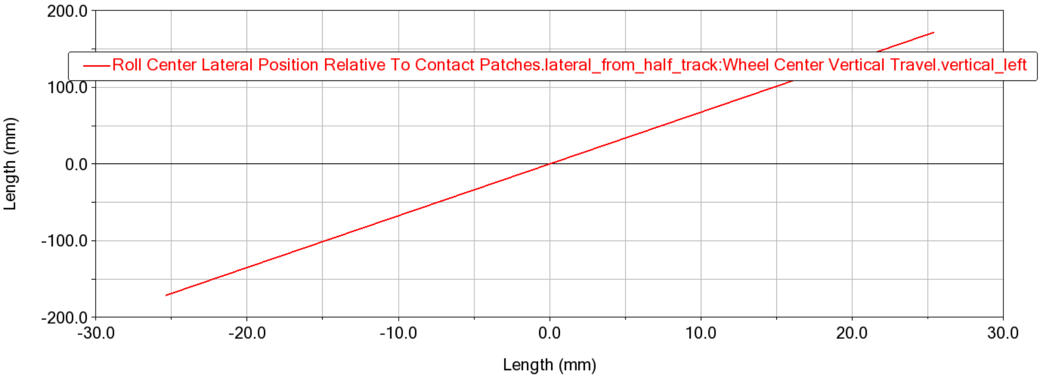
Roll Center Lateral Position Relative To Contact Patches.lateral_from_half_track:Wheel Center Vertical Travel.vertical_left
Length (mm)
200.0
100.0
0.0
-100.0
-200.0
-30.0
-20.0
-10.0
0.0
10.0
20.0
30.0
Length (mm)

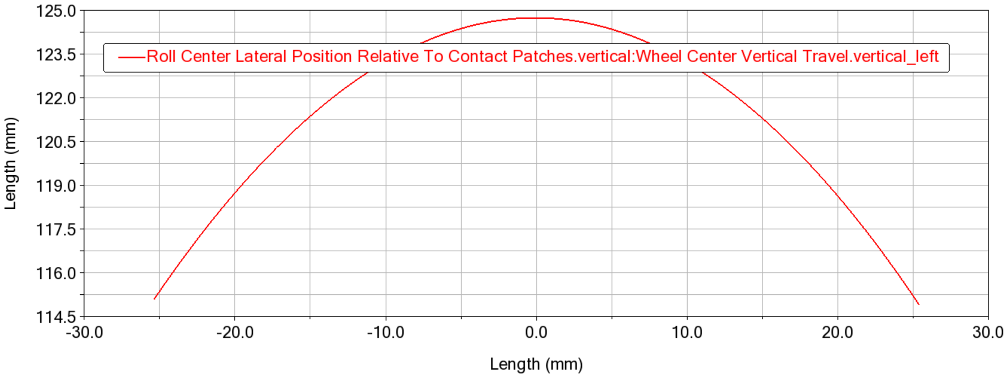
Roll Center Lateral Position Relative To Contact Patches.vertical:Wheel Center Vertical Travel.vertical_left
Length (mm)
125.0
123.5
122.0
120.5
119.0
117.5
116.0
114.5
-30.0
-20.0
-10.0
0.0
10.0
20.0
30.0
Length (mm)

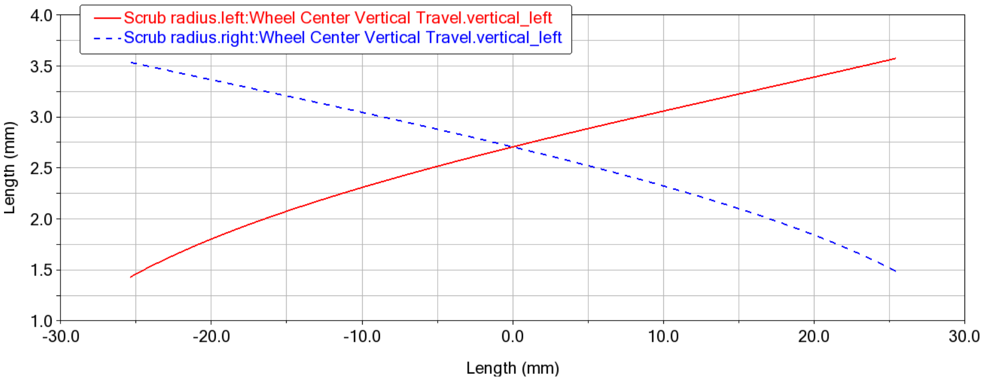
Scrub radius.left:Wheel Center Vertical Travel.vertical_left
Scrub radius.right:Wheel Center Vertical Travel.vertical_left
Length (mm)
4.0
3.5
3.0
2.5
2.0
1.5
1.0
-30.0
-20.0
-10.0
0.0
10.0
20.0
30.0
Length (mm)

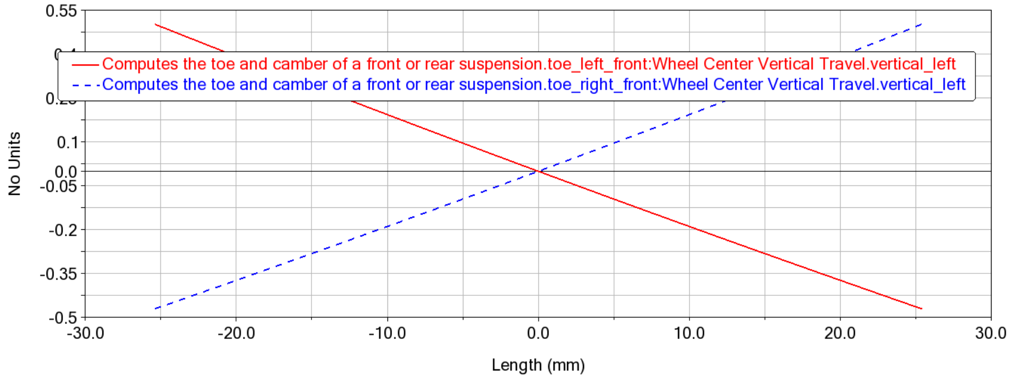

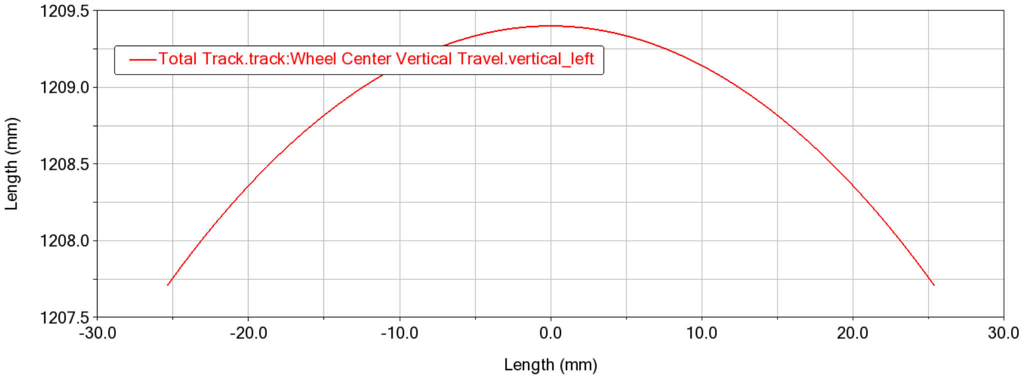

7.1.2.2 *Rear suspension*

7.1.2.2.1 Parallel

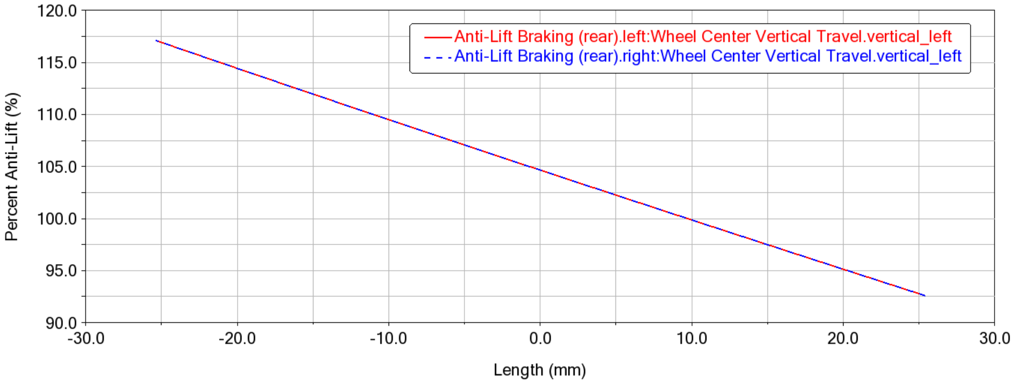

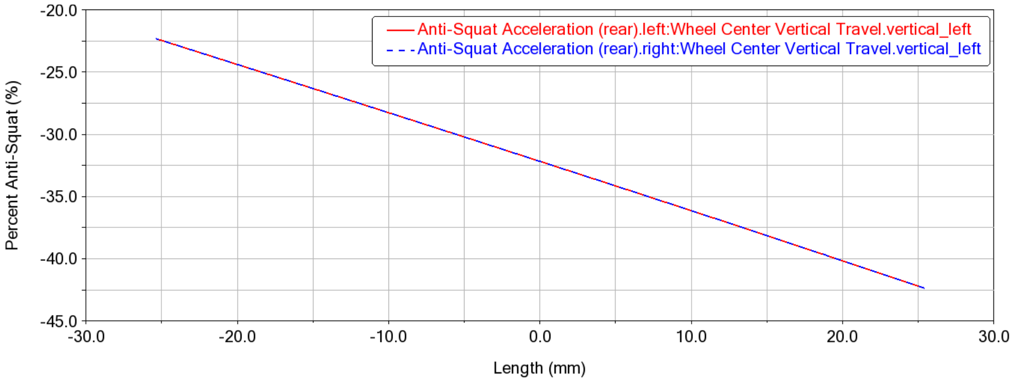

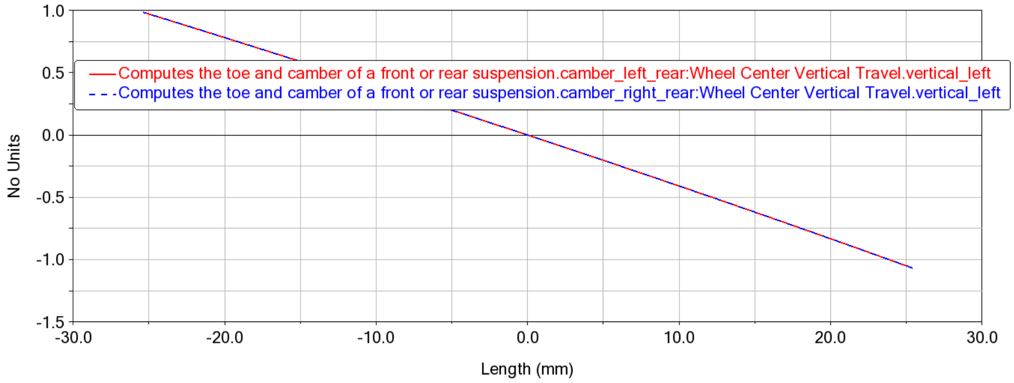
Computes the toe and camber of a front or rear suspension.camber_left_rear:Wheel Center Vertical Travel.vertical_left
Computes the toe and camber of a front or rear suspension.camber_right_rear:Wheel Center Vertical Travel.vertical_left
No Units
1.0
0.5
0.0
-0.5
-1.0
-1.5
-30.0
-20.0
-10.0
0.0
10.0
20.0
30.0
Length (mm)

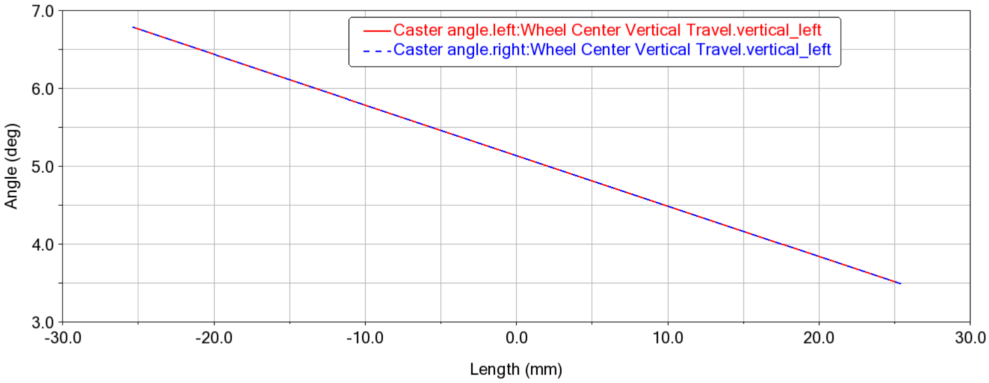
Caster angle.left:Wheel Center Vertical Travel.vertical_left
Caster angle.right:Wheel Center Vertical Travel.vertical_left
Angle (deg)
7.0
6.0
5.0
4.0
3.0
-30.0
-20.0
-10.0
0.0
10.0
20.0
30.0
Length (mm)

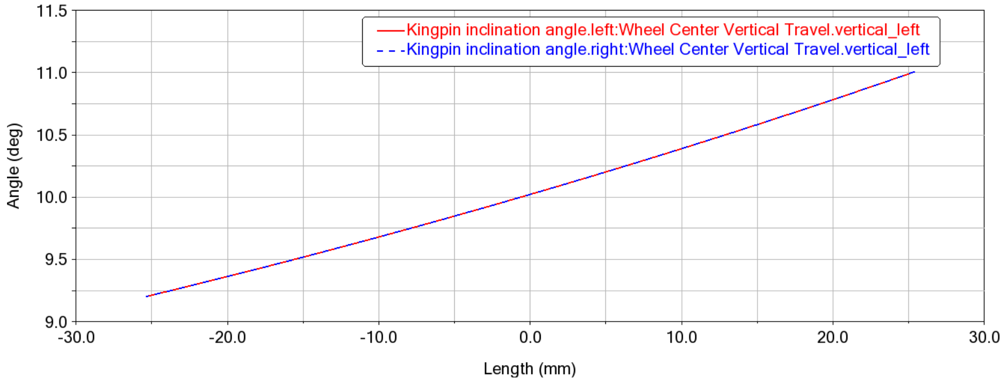
Kingpin inclination angle.left:Wheel Center Vertical Travel.vertical_left
Kingpin inclination angle.right:Wheel Center Vertical Travel.vertical_left
Angle (deg)
11.5
11.0
10.5
10.0
9.5
9.0
-30.0
-20.0
-10.0
0.0
10.0
20.0
30.0
Length (mm)

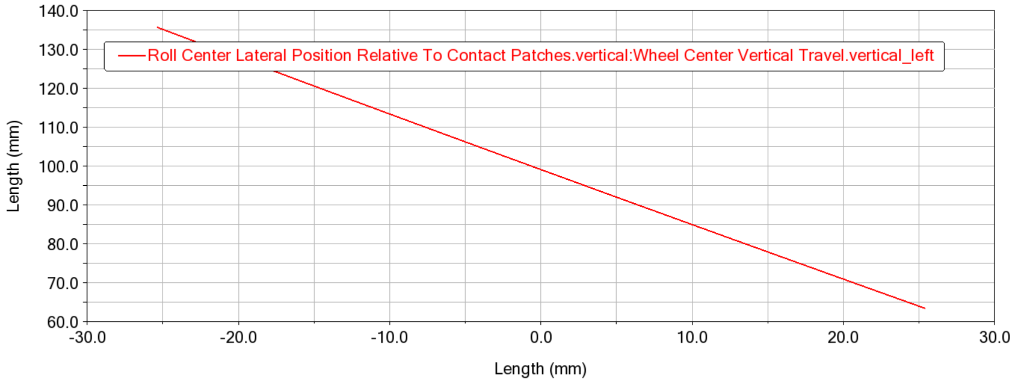
Roll Center Lateral Position Relative To Contact Patches.vertical:Wheel Center Vertical Travel.vertical_left
Length (mm)
140.0
130.0
120.0
110.0
100.0
90.0
80.0
70.0
60.0
-30.0
-20.0
-10.0
0.0
10.0
20.0
30.0
Length (mm)

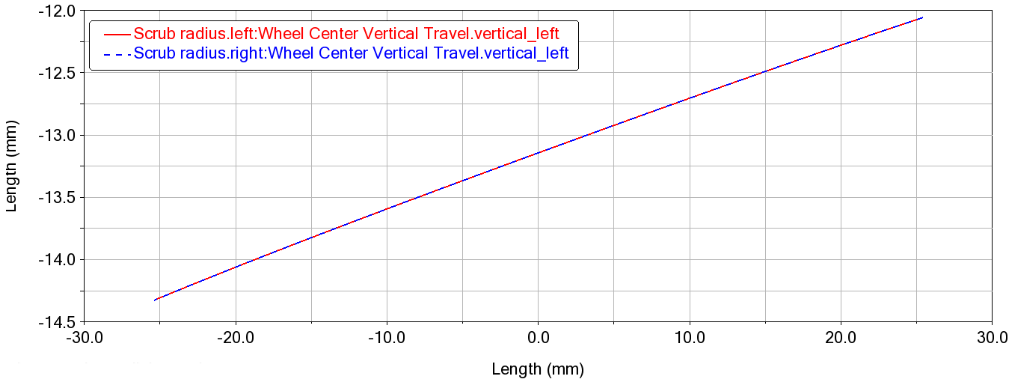

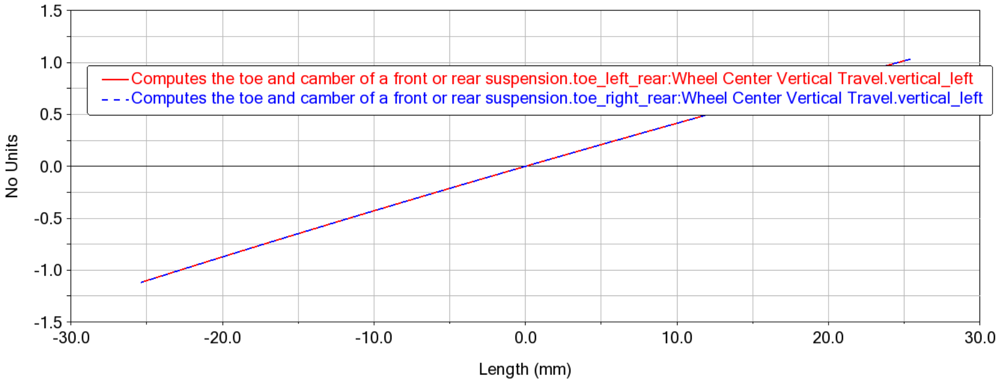

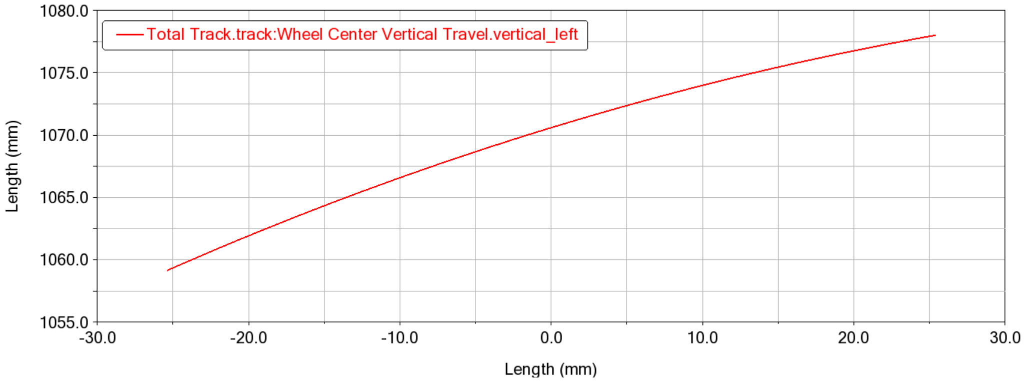

7.1.2.2.2 Opposite

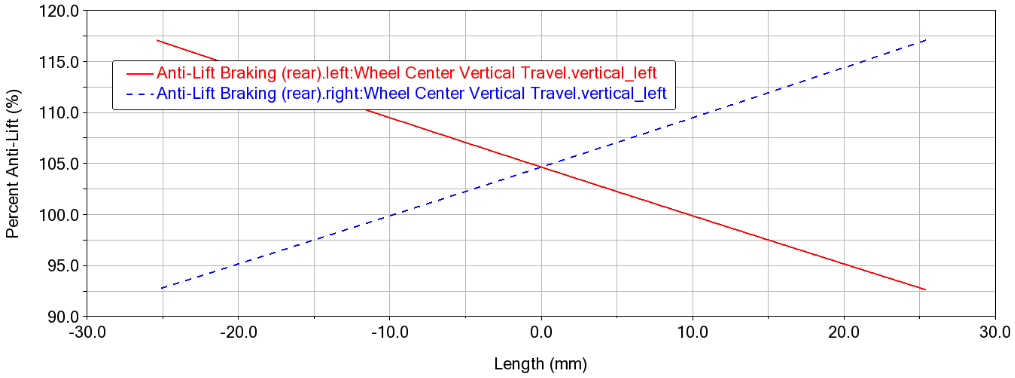

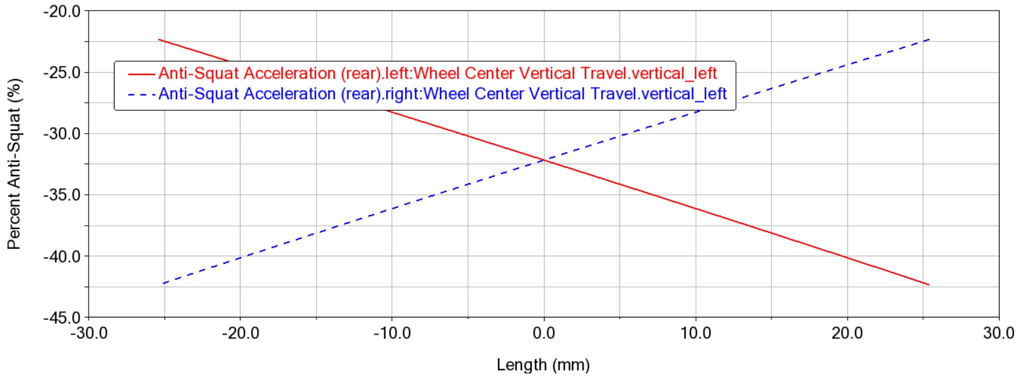

Anti-Squat Acceleration (rear).left:Wheel Center Vertical Travel.vertical_left
Anti-Squat Acceleration (rear).right:Wheel Center Vertical Travel.vertical_left
Percent Anti-Squat (%)
-20.0
-25.0
-30.0
-35.0
-40.0
-45.0
-30.0
-20.0
-10.0
0.0
10.0
20.0
30.0
Length (mm)

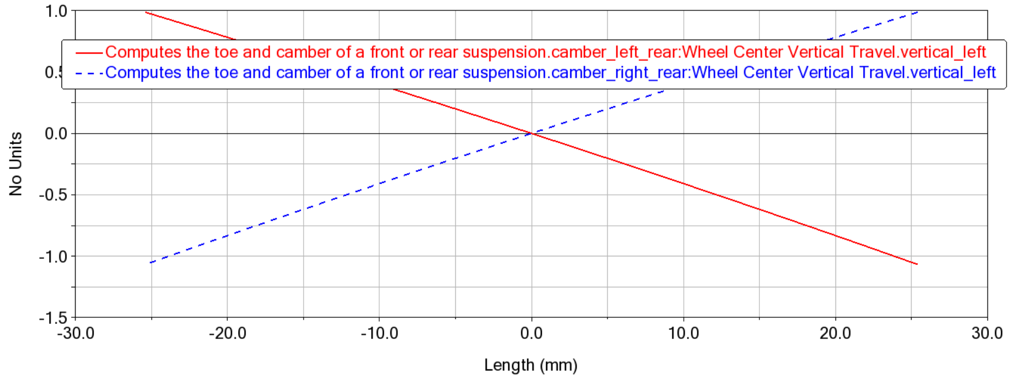

Computes the toe and camber of a front or rear suspension.camber_left_rear:Wheel Center Vertical Travel.vertical_left
Computes the toe and camber of a front or rear suspension.camber_right_rear:Wheel Center Vertical Travel.vertical_left
No Units
1.0
0.5
0.0
-0.5
-1.0
-1.5
-30.0
-20.0
-10.0
0.0
10.0
20.0
30.0
Length (mm)

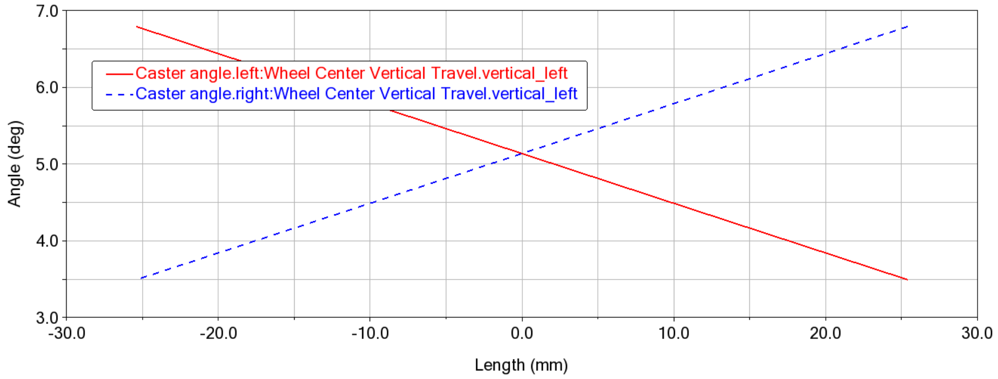

Caster angle.left:Wheel Center Vertical Travel.vertical_left
Caster angle.right:Wheel Center Vertical Travel.vertical_left
Angle (deg)
7.0
6.0
5.0
4.0
3.0
-30.0
-20.0
-10.0
0.0
10.0
20.0
30.0
Length (mm)

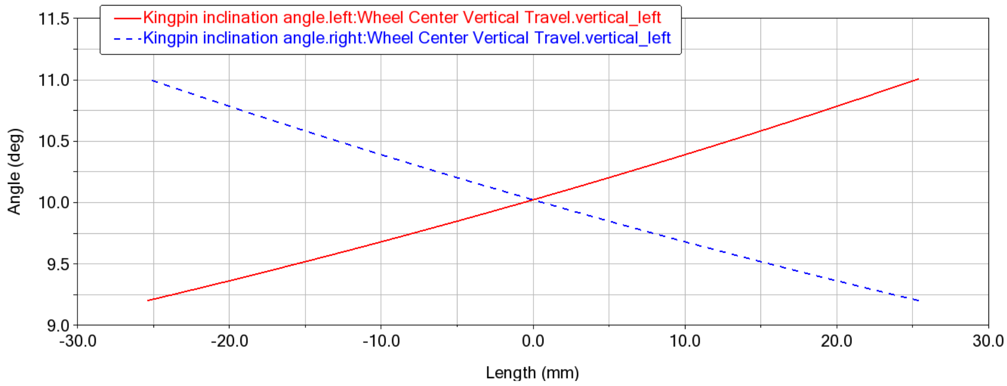

Kingpin inclination angle.left:Wheel Center Vertical Travel.vertical_left
Kingpin inclination angle.right:Wheel Center Vertical Travel.vertical_left
Angle (deg)
11.5
11.0
10.5
10.0
9.5
9.0
-30.0
-20.0
-10.0
0.0
10.0
20.0
30.0
Length (mm)

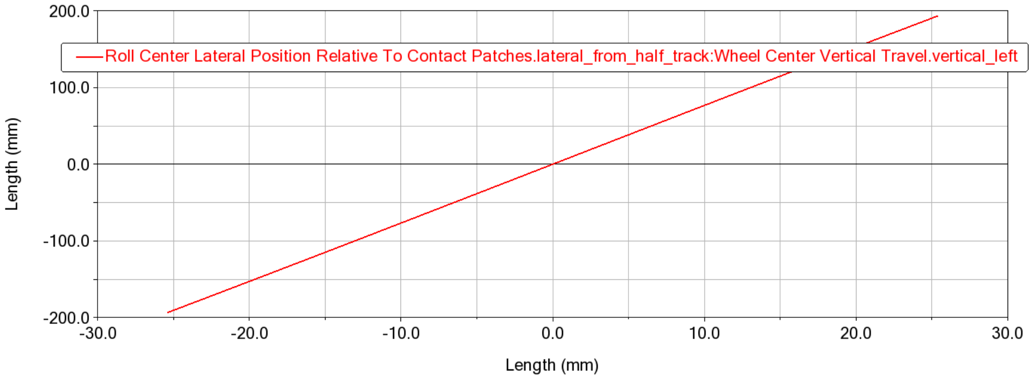
Roll Center Lateral Position Relative To Contact Patches.lateral_from_half_track:Wheel Center Vertical Travel.vertical_left
Length (mm)
200.0
100.0
0.0
-100.0
-200.0
-30.0
-20.0
-10.0
0.0
10.0
20.0
30.0
Length (mm)

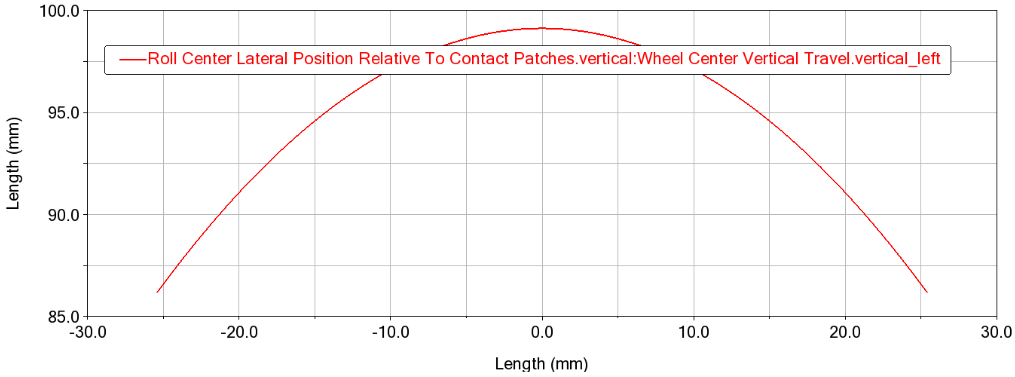
Roll Center Lateral Position Relative To Contact Patches.vertical:Wheel Center Vertical Travel.vertical_left
Length (mm)
100.0
95.0
90.0
85.0
-30.0
-20.0
-10.0
0.0
10.0
20.0
30.0
Length (mm)

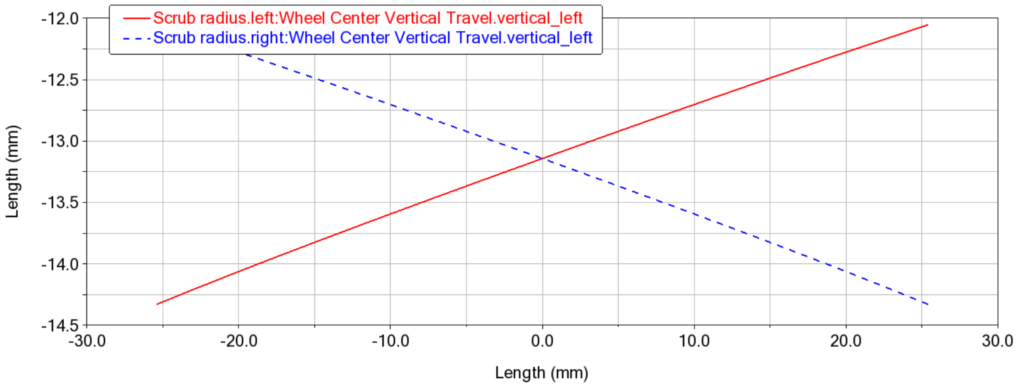
Scrub radius.left:Wheel Center Vertical Travel.vertical_left
Scrub radius.right:Wheel Center Vertical Travel.vertical_left
Length (mm)
-12.0
-12.5
-13.0
-13.5
-14.0
-14.5
-30.0
-20.0
-10.0
0.0
10.0
20.0
30.0
Length (mm)

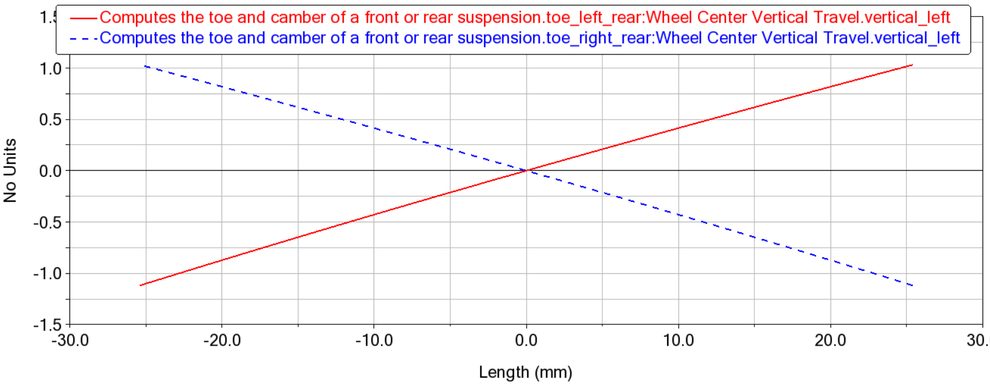
Computes the toe and camber of a front or rear suspension.toe_left_rear:Wheel Center Vertical Travel.vertical_left
Computes the toe and camber of a front or rear suspension.toe_right_rear:Wheel Center Vertical Travel.vertical_left
No Units
1.
1.0
0.5
0.0
-0.5
-1.0
-1.5
-30.0
-20.0
-10.0
0.0
10.0
20.0
30.0
Length (mm)

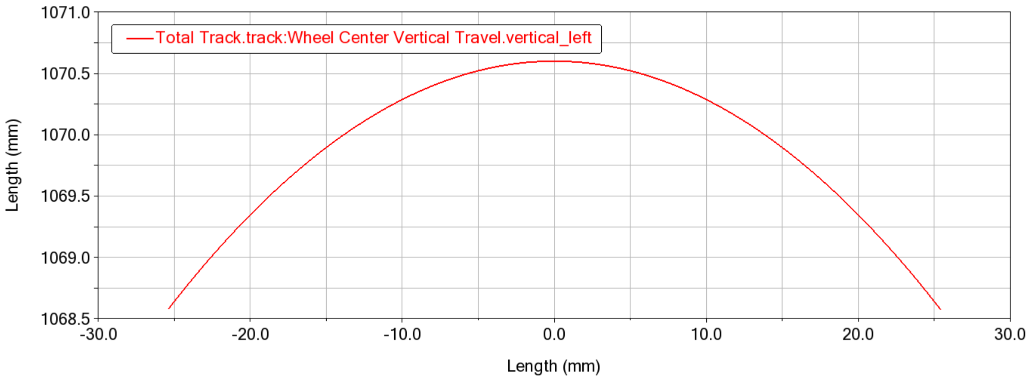

7.1.3 Definition of improving points

Considering the front suspension, one of the first things to improve is the height of the roll centre: a value of more than $120\ mm$ for the front is excessive: an acceptable value is around $50 - 70\ mm$. Also note that this value is higher than the rear suspension.

For this reason, the range of variation of the camber is very wide (about 2°): it would be worth reducing it to improve the contact of the tire on the ground.

Speaking of the anti-dive feature, this is within the recommended range, but can be increased slightly. What is not really correct is that the anti-lift characteristic takes on negative values: this effect increases the lifting of the wheel when accelerating, thus creating a pro-lift effect.

The caster value, on the other hand, can be considered good, although it could be reduced to reduce the pilot's difficulty in manoeuvring the single seater. Another effect that affects the control of the vehicle is given by the scrub radius, which for the front suspension should be negative, to naturally balance the undesired steering to the locking of one of the wheels. In this case, the value is slightly positive, which means a greater need for control and skill on the part of the driver.

Finally, the range of variation of the toe angle is very large and should be reduced. However, it should be noted that, also looking at the variation on the rear suspension, the variation is of the "stable" type: in case of braking (curve entrance), the vehicle tends to be more understeer.

The other parameters, on the other hand, have acceptable values, even the lateral displacement of the roll centre in case of opposite wheel travel.

Focusing on the rear suspension, however, we can say that the vertical position of the roll centre is not bad, but could be lowered slightly, to improve the other features. Its lateral displacement is similar to the front suspension.

The camber angle, for example, again has a large range of variation, as does the toe angle.

In this case, the anti-features are wrong, as the anti-lift value is completely out of range and in the same way, the anti-squat is negative, creating a pro-squat effect.

Considering the radius scrub, for the same reasoning described above, it should be positive.

A caster angle of this kind is fine to maintain a certain value of directional stability, being the wheels with traction.

The other values are almost good.

From these considerations, the new geometry is developed, aimed at improving the characteristics, keeping in mind the space needed for an in-wheel electric motor.

7.2 Electric vehicle

As said at the beginning of this essay, a solution is proposed as if the previous vehicle was electric, that means, it requires space in the centre of the wheel to host the electric motor. Actually, this is not a problem, due to the fact that the rim is large enough. In the final solution, the considered wheel is more similar to the one that will be used in the competition, thus the geometries that will be analysed now should be modified.

This proposed solution may be seen as a first idea of the final model.

7.2.1 Geometry

The first geometry that is shown in the front suspension.

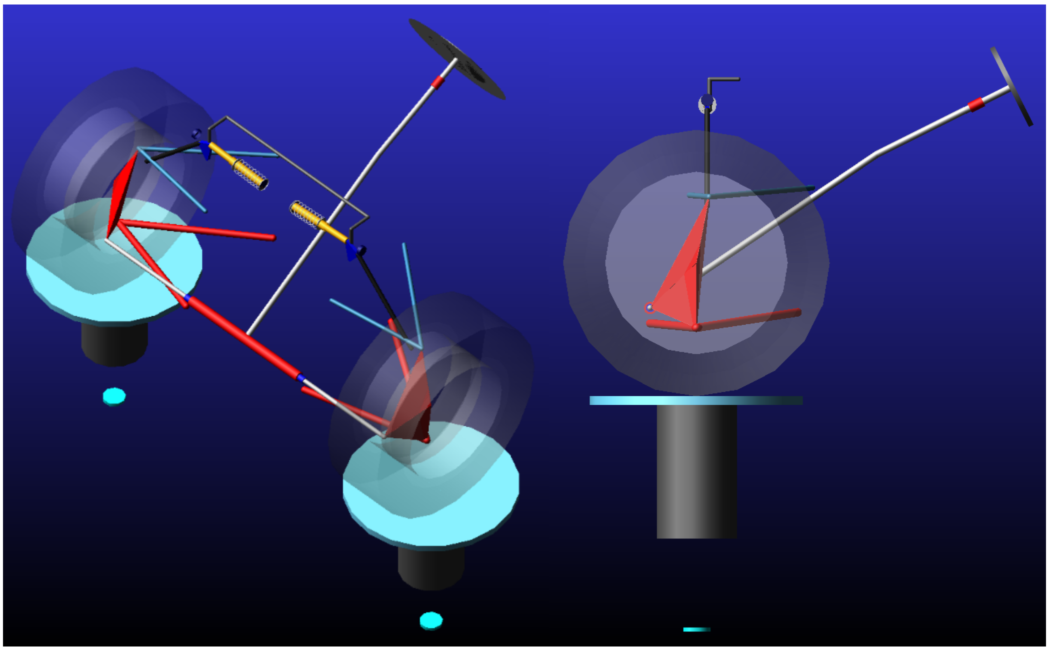

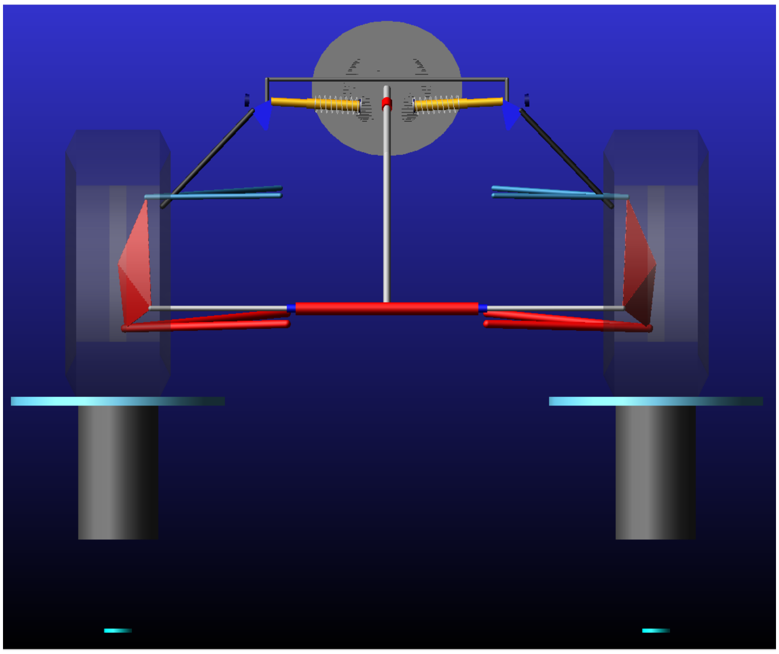

Then, the rear suspension is shown as well.

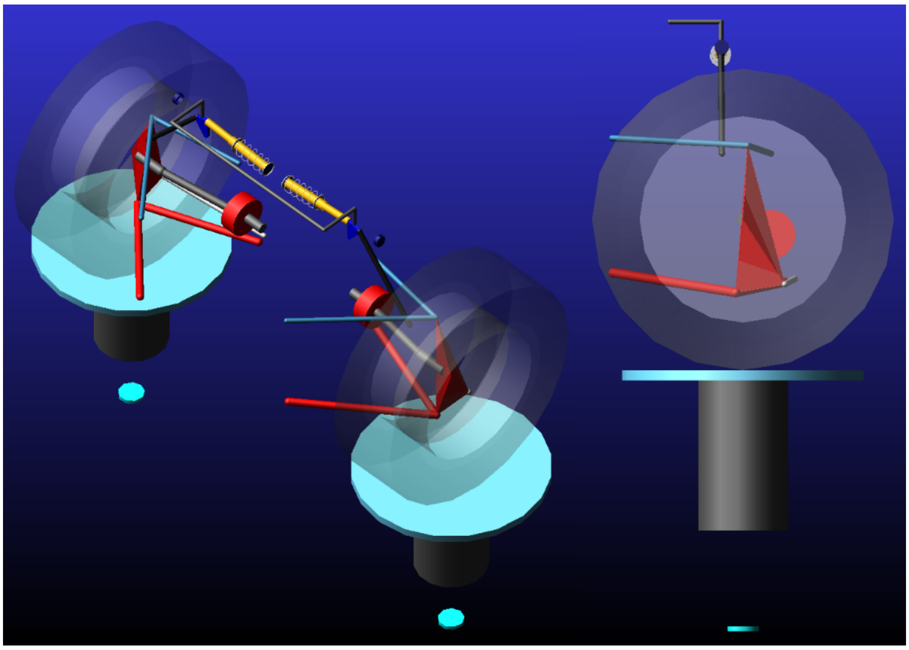

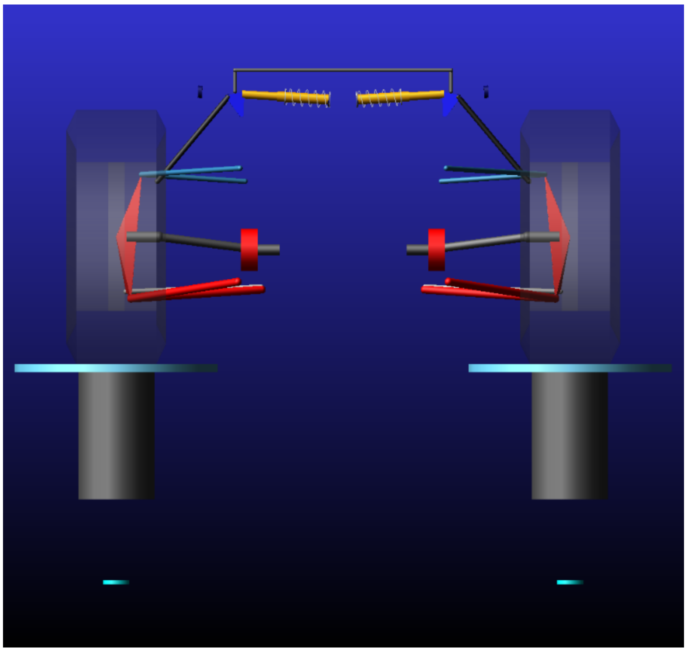

7.2.2 Kinematic analysis

As in the previous case, the kinematic analysis is performed to evaluate differences with the previous model.

7.2.2.1 Front suspension

7.2.2.1.1 Parallel

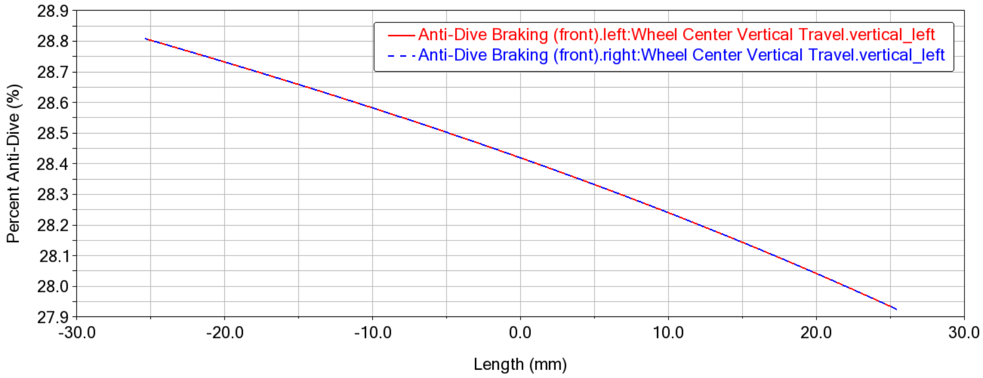

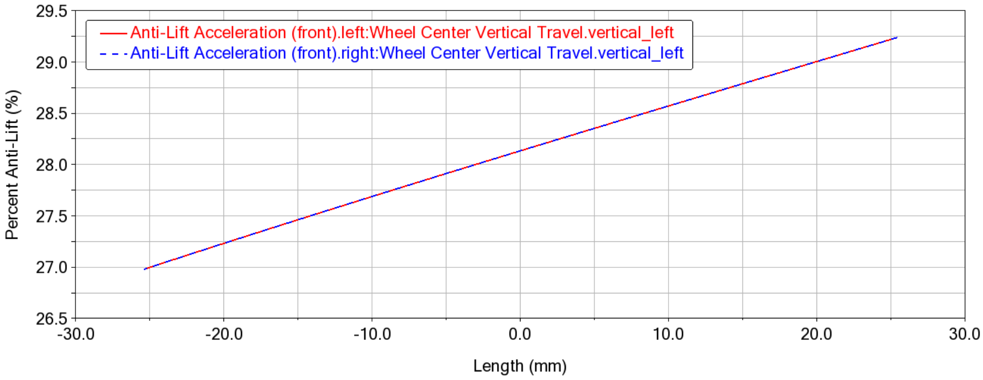

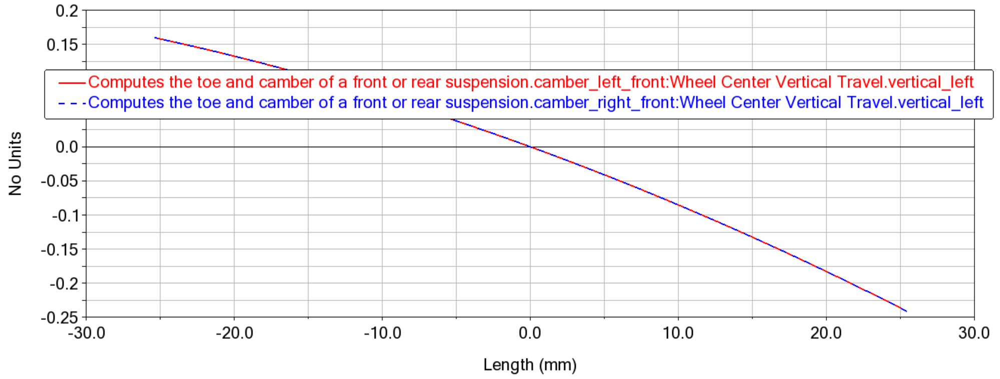
Computes the toe and camber of a front or rear suspension.camber_left_front:Wheel Center Vertical Travel.vertical_left
Computes the toe and camber of a front or rear suspension.camber_right_front:Wheel Center Vertical Travel.vertical_left
No Units
0.2
0.15
0.0
-0.05
-0.1
-0.15
-0.2
-0.25
-30.0
-20.0
-10.0
0.0
10.0
20.0
30.0
Length (mm)

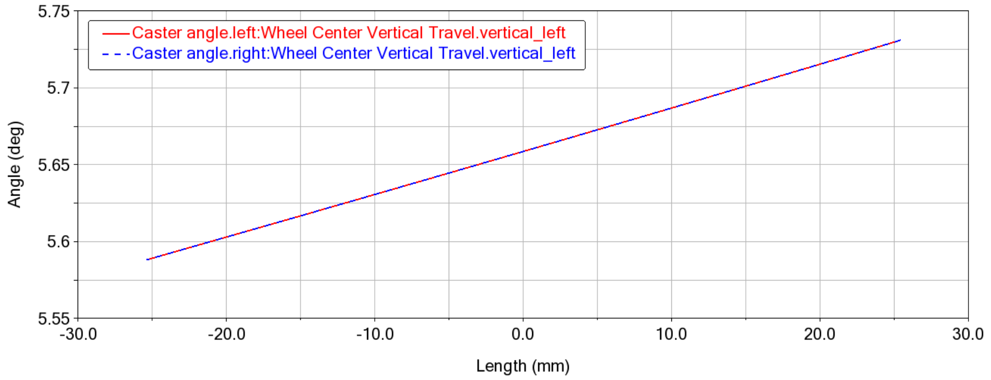
Caster angle.left:Wheel Center Vertical Travel.vertical_left
Caster angle.right:Wheel Center Vertical Travel.vertical_left
Angle (deg)
5.75
5.7
5.65
5.6
5.55
-30.0
-20.0
-10.0
0.0
10.0
20.0
30.0
Length (mm)

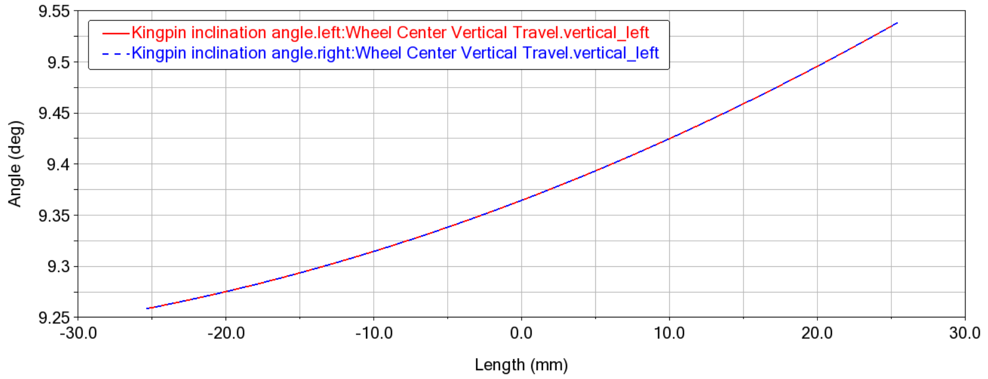
Kingpin inclination angle.left:Wheel Center Vertical Travel.vertical_left
Kingpin inclination angle.right:Wheel Center Vertical Travel.vertical_left
Angle (deg)
9.55
9.5
9.45
9.4
9.35
9.3
9.25
-30.0
-20.0
-10.0
0.0
10.0
20.0
30.0
Length (mm)

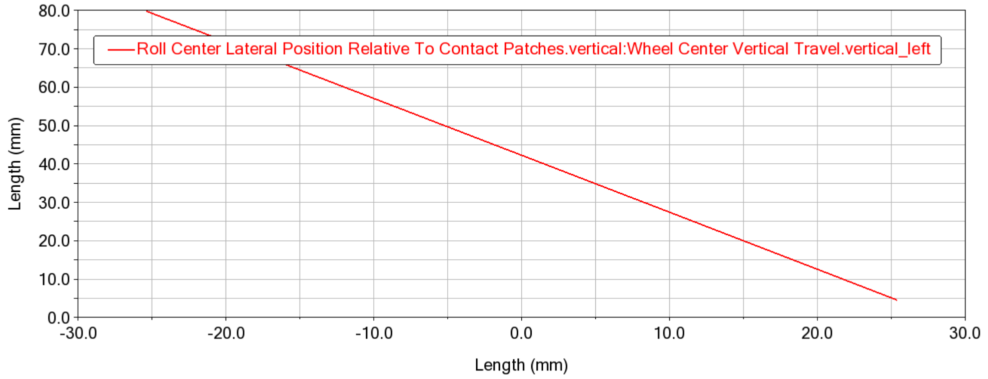
Roll Center Lateral Position Relative To Contact Patches.vertical:Wheel Center Vertical Travel.vertical_left
Length (mm)
80.0
70.0
60.0
50.0
40.0
30.0
20.0
10.0
0.0
-30.0
-20.0
-10.0
0.0
10.0
20.0
30.0
Length (mm)

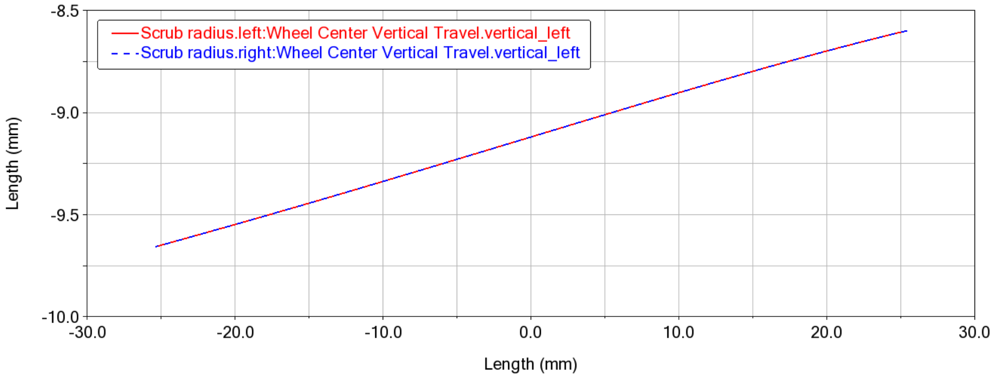

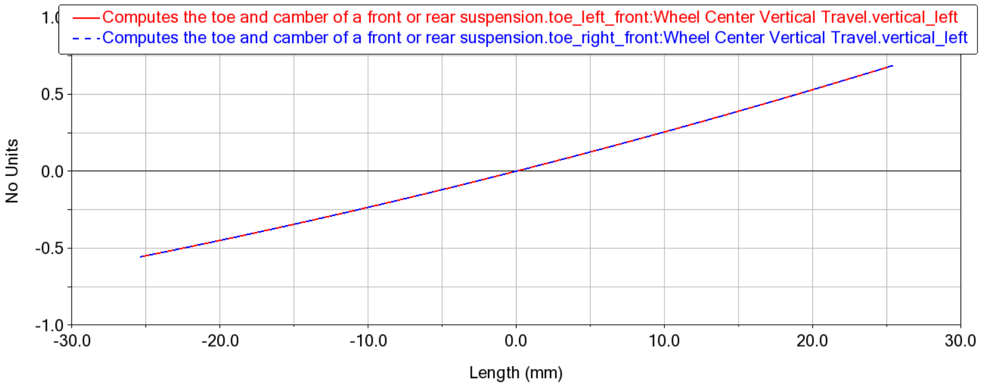

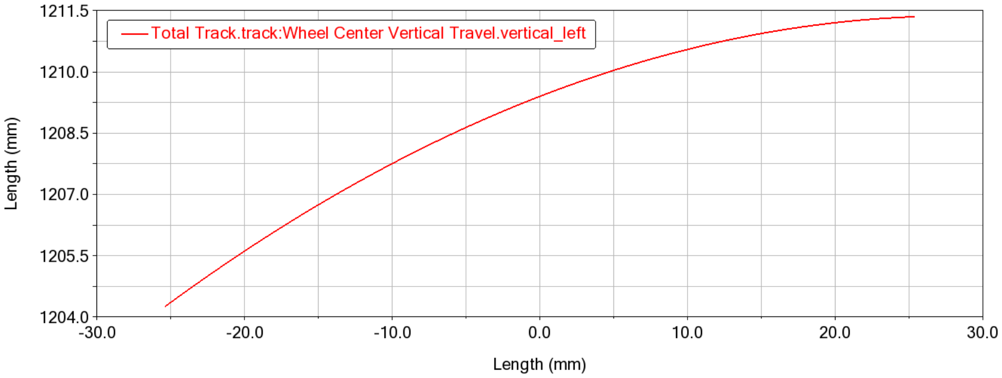

7.2.2.1.2 Opposite

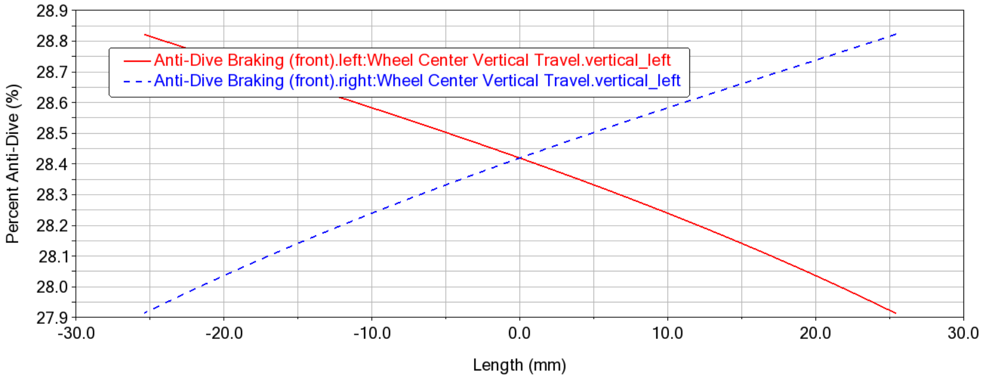

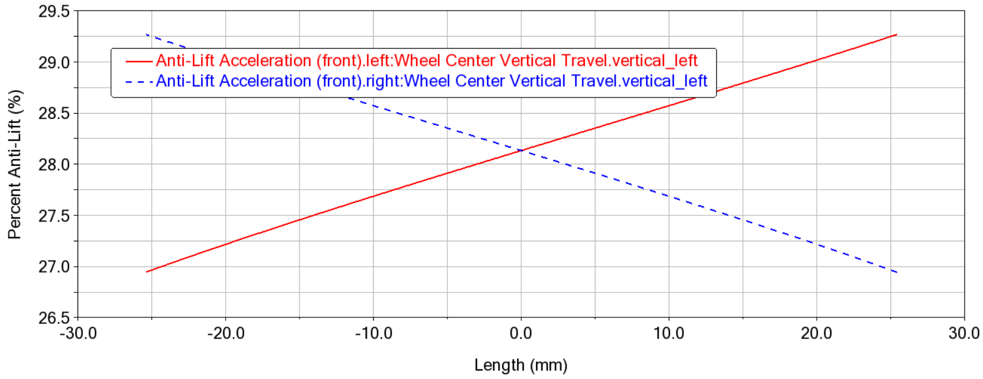
Anti-Lift Acceleration (front).left:Wheel Center Vertical Travel.vertical_left
Anti-Lift Acceleration (front).right:Wheel Center Vertical Travel.vertical_left
Percent Anti-Lift (%)
29.5
29.0
28.5
28.0
27.5
27.0
26.5
-30.0
-20.0
-10.0
0.0
10.0
20.0
30.0
Length (mm)

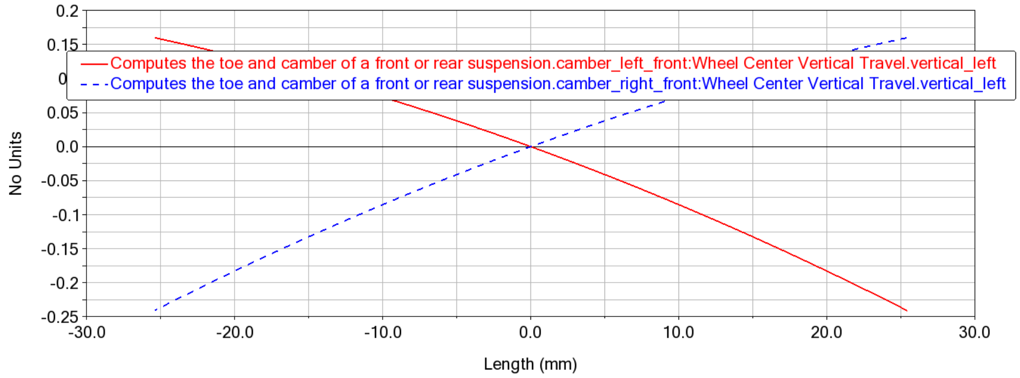
Computes the toe and camber of a front or rear suspension.camber_left_front:Wheel Center Vertical Travel.vertical_left
Computes the toe and camber of a front or rear suspension.camber_right_front:Wheel Center Vertical Travel.vertical_left
No Units
0.2
0.15
0
0.05
0.0
-0.05
-0.1
-0.15
-0.2
-0.25
-30.0
-20.0
-10.0
0.0
10.0
20.0
30.0
Length (mm)

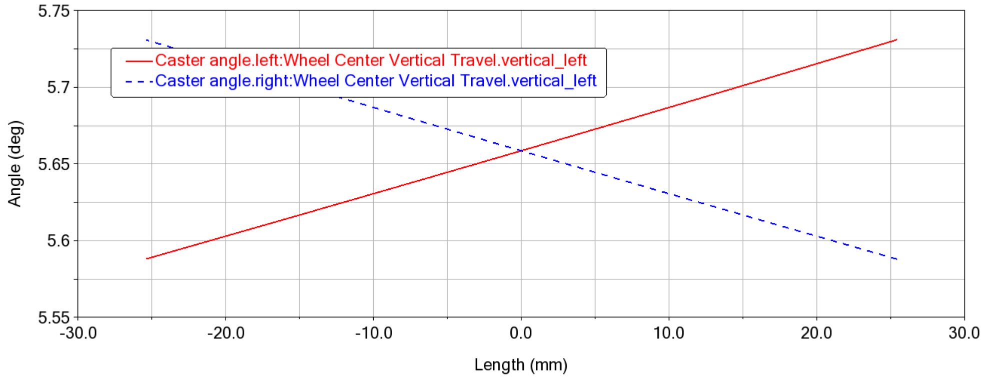
Caster angle.left:Wheel Center Vertical Travel.vertical_left
Caster angle.right:Wheel Center Vertical Travel.vertical_left
Angle (deg)
5.75
5.7
5.65
5.6
5.55
-30.0
-20.0
-10.0
0.0
10.0
20.0
30.0
Length (mm)

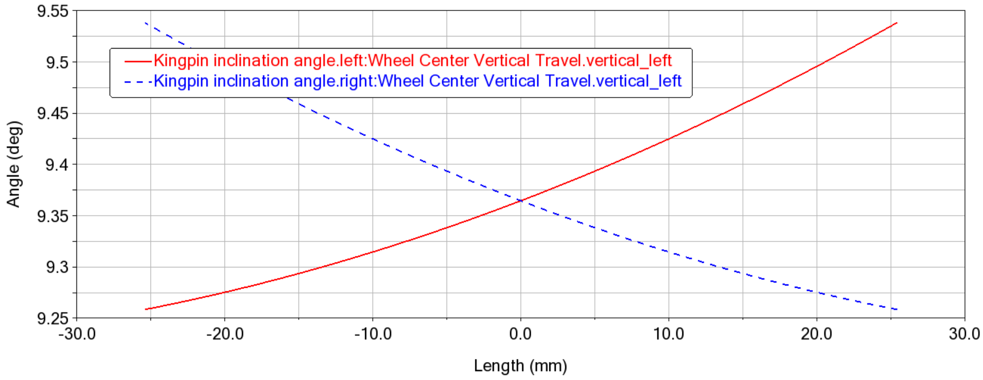
Kingpin inclination angle.left:Wheel Center Vertical Travel.vertical_left
Kingpin inclination angle.right:Wheel Center Vertical Travel.vertical_left
Angle (deg)
9.55
9.5
9.45
9.4
9.35
9.3
9.25
-30.0
-20.0
-10.0
0.0
10.0
20.0
30.0
Length (mm)

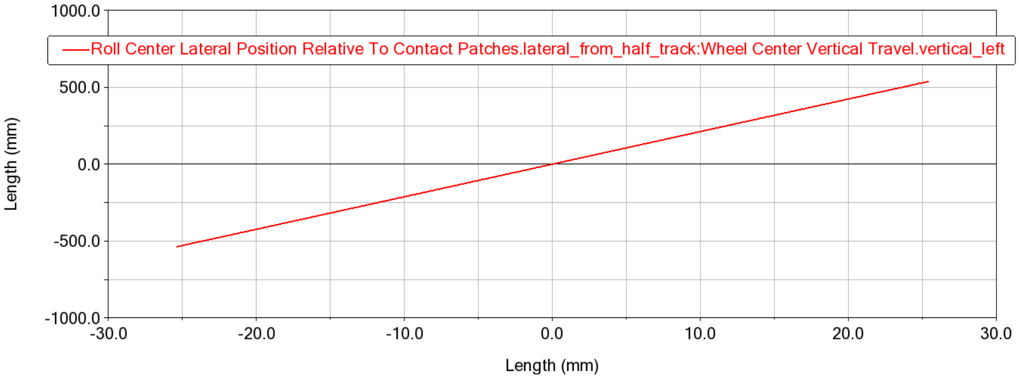
Roll Center Lateral Position Relative To Contact Patches.lateral_from_half_track:Wheel Center Vertical Travel.vertical_left
Length (mm)
1000.0
500.0
0.0
-500.0
-1000.0
-30.0
-20.0
-10.0
0.0
10.0
20.0
30.0
Length (mm)

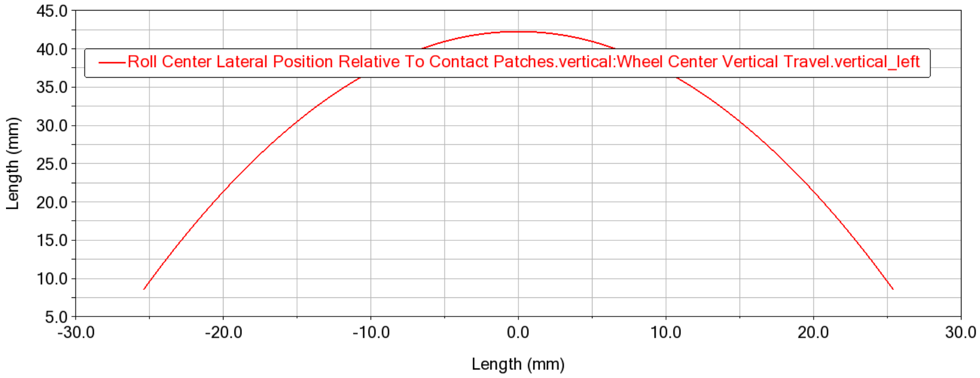
Roll Center Lateral Position Relative To Contact Patches.vertical:Wheel Center Vertical Travel.vertical_left
Length (mm)
45.0
40.0
35.0
30.0
25.0
20.0
15.0
10.0
5.0
-30.0
-20.0
-10.0
0.0
10.0
20.0
30.0
Length (mm)

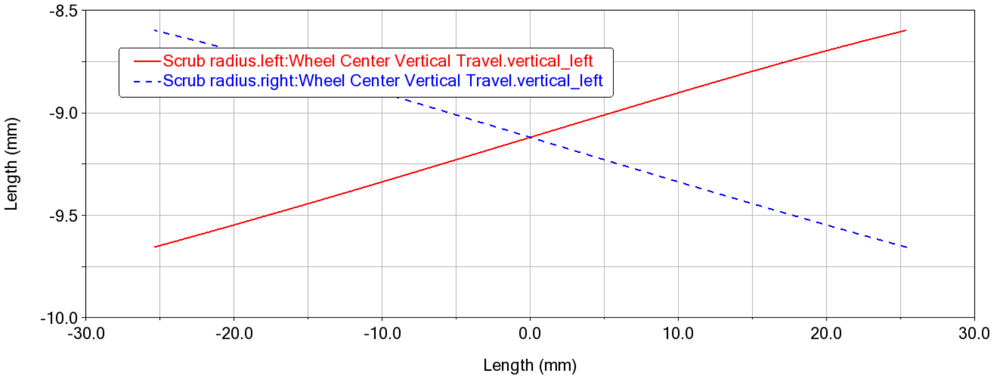
Scrub radius.left:Wheel Center Vertical Travel.vertical_left
Scrub radius.right:Wheel Center Vertical Travel.vertical_left
Length (mm)
-8.5
-9.0
-9.5
-10.0
-30.0
-20.0
-10.0
0.0
10.0
20.0
30.0
Length (mm)

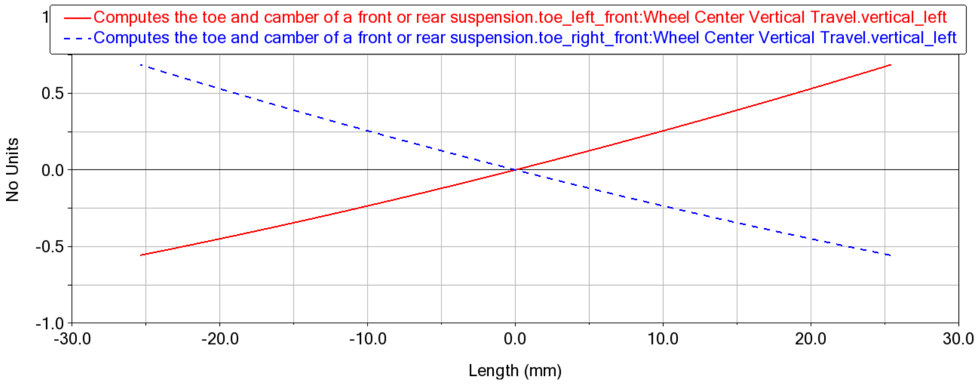
Computes the toe and camber of a front or rear suspension.toe_left_front:Wheel Center Vertical Travel.vertical_left
Computes the toe and camber of a front or rear suspension.toe_right_front:Wheel Center Vertical Travel.vertical_left
No Units
1
0.5
0.0
-0.5
-1.0
-30.0
-20.0
-10.0
0.0
10.0
20.0
30.0
Length (mm)

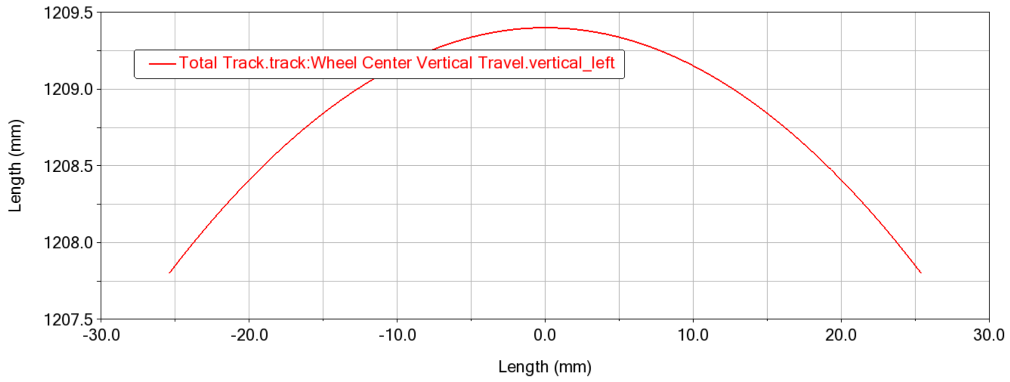

7.2.2.2 *Rear suspension*

7.2.2.2.1 Parallel

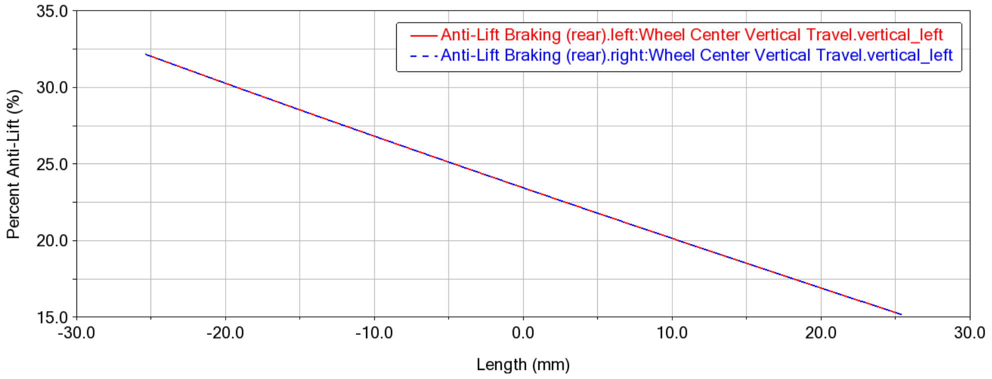

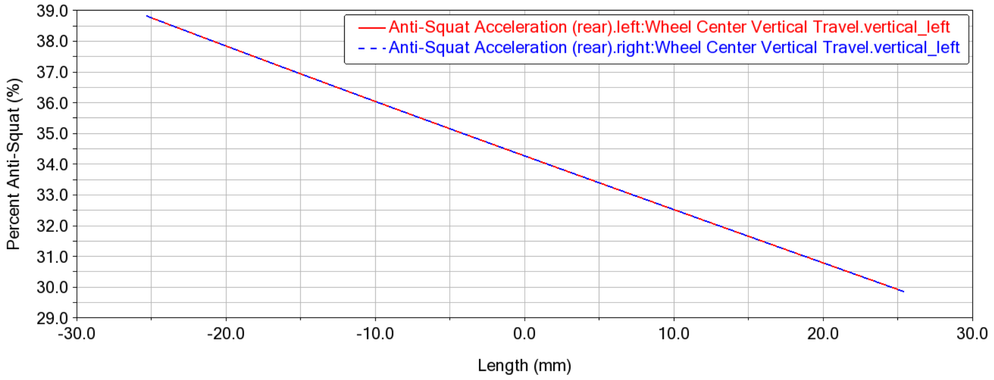

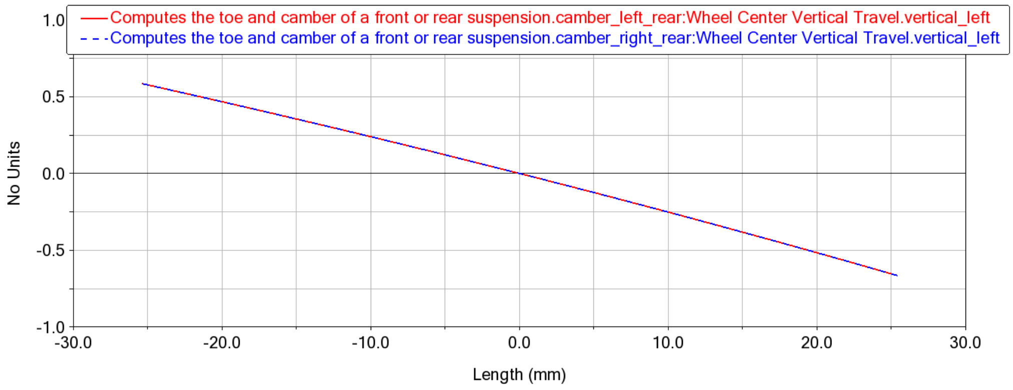

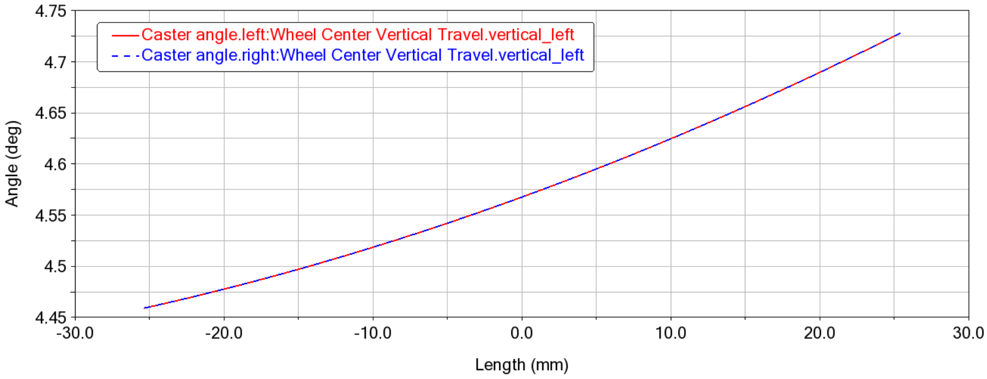
Caster angle.left:Wheel Center Vertical Travel.vertical_left
Caster angle.right:Wheel Center Vertical Travel.vertical_left
Angle (deg)
4.75
4.7
4.65
4.6
4.55
4.5
4.45
-30.0
-20.0
-10.0
0.0
10.0
20.0
30.0
Length (mm)

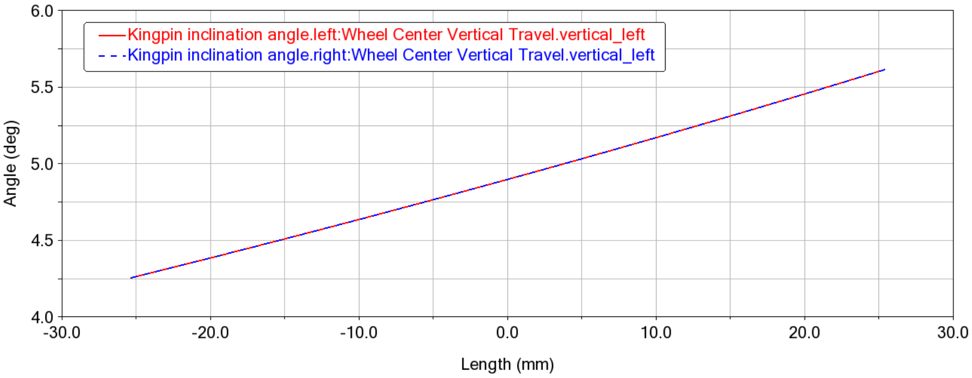
Kingpin inclination angle.left:Wheel Center Vertical Travel.vertical_left
Kingpin inclination angle.right:Wheel Center Vertical Travel.vertical_left
Angle (deg)
6.0
5.5
5.0
4.5
4.0
-30.0
-20.0
-10.0
0.0
10.0
20.0
30.0
Length (mm)

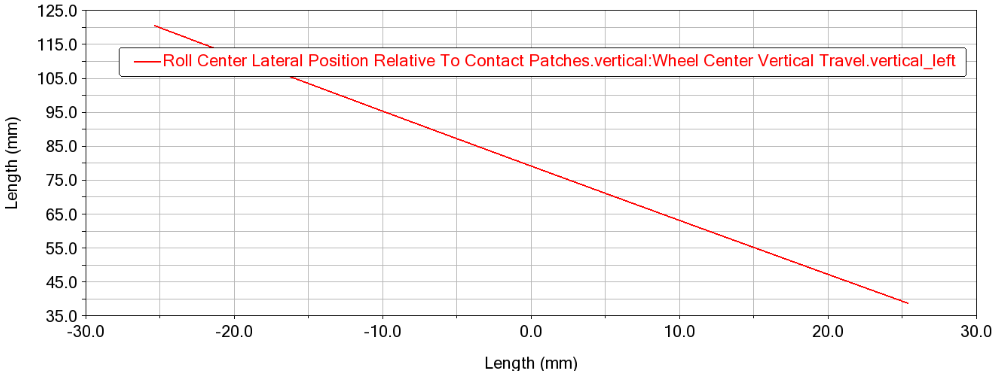
Roll Center Lateral Position Relative To Contact Patches.vertical:Wheel Center Vertical Travel.vertical_left
Length (mm)
125.0
115.0
105.0
95.0
85.0
75.0
65.0
55.0
45.0
35.0
-30.0
-20.0
-10.0
0.0
10.0
20.0
30.0
Length (mm)

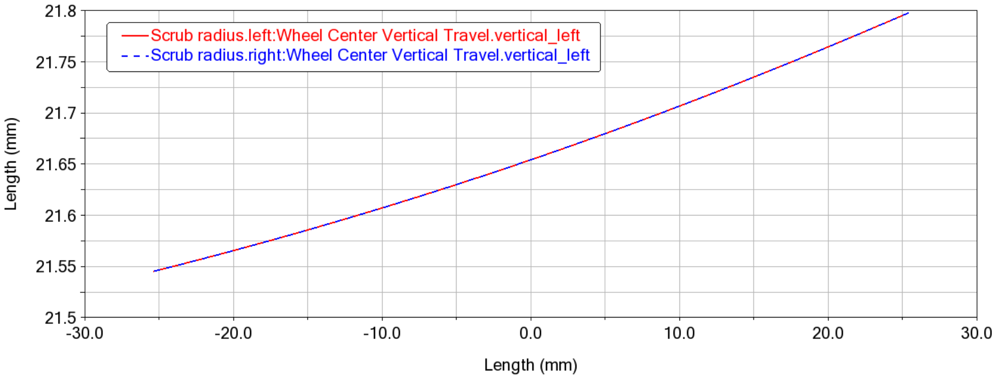
Scrub radius.left:Wheel Center Vertical Travel.vertical_left
Scrub radius.right:Wheel Center Vertical Travel.vertical_left
Length (mm)
21.8
21.75
21.7
21.65
21.6
21.55
21.5
-30.0
-20.0
-10.0
0.0
10.0
20.0
30.0
Length (mm)

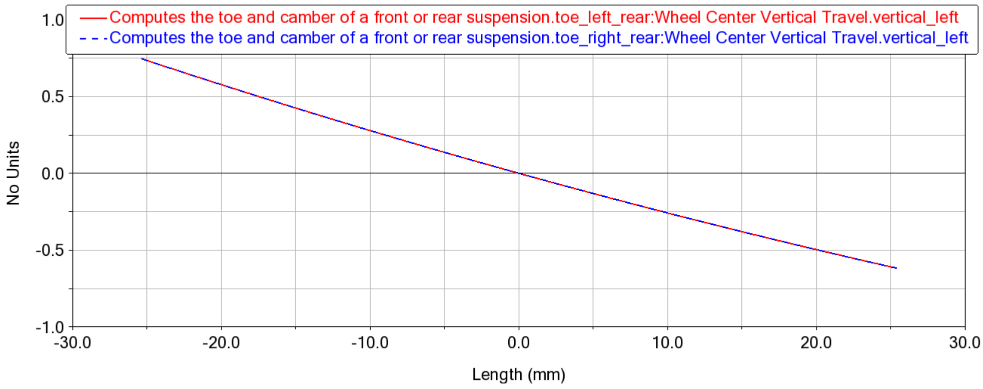

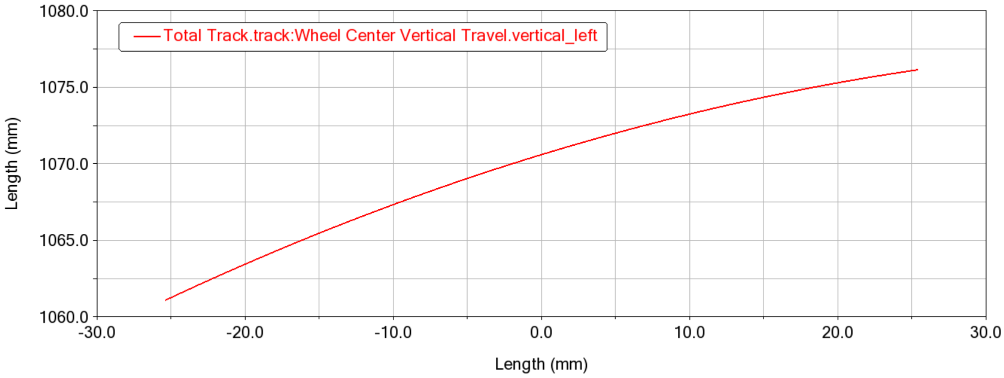

7.2.2.2.2 Opposite

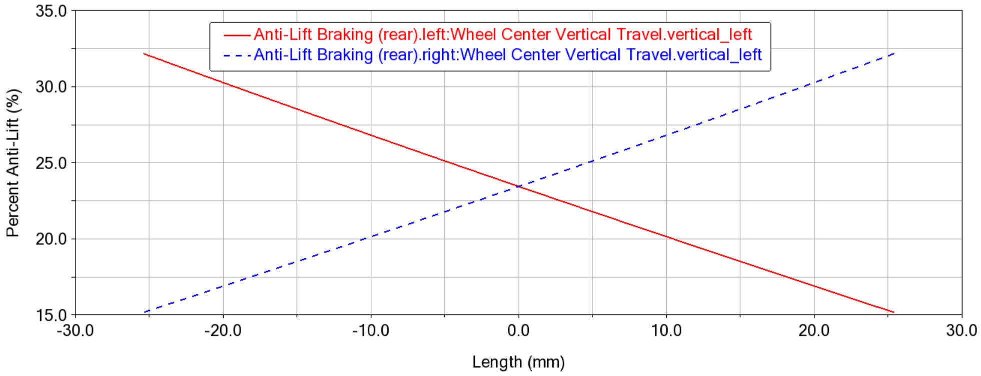

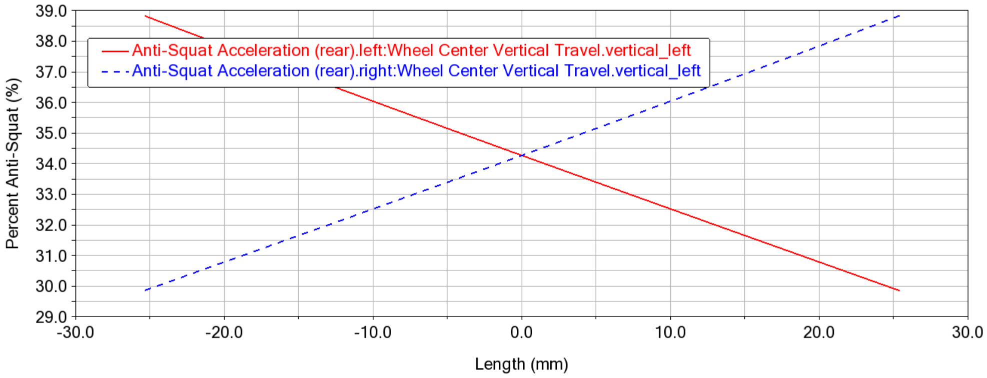

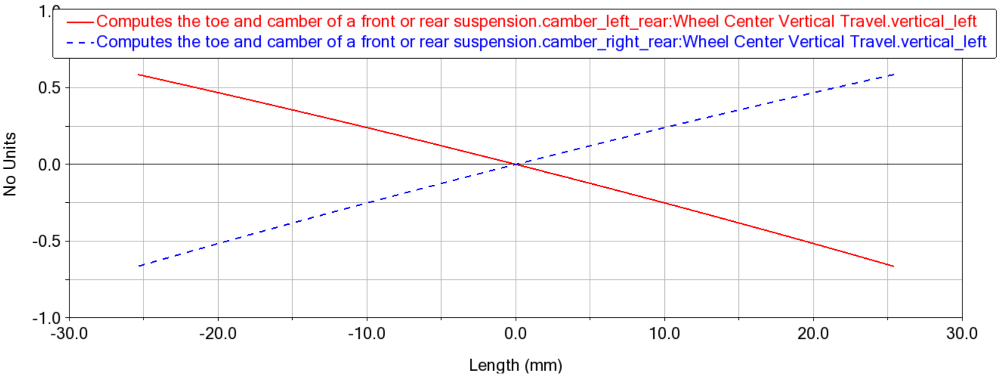
Computes the toe and camber of a front or rear suspension.camber_left_rear:Wheel Center Vertical Travel.vertical_left
Computes the toe and camber of a front or rear suspension.camber_right_rear:Wheel Center Vertical Travel.vertical_left
No Units
1.0
0.5
0.0
-0.5
-1.0
-30.0
-20.0
-10.0
0.0
10.0
20.0
30.0
Length (mm)

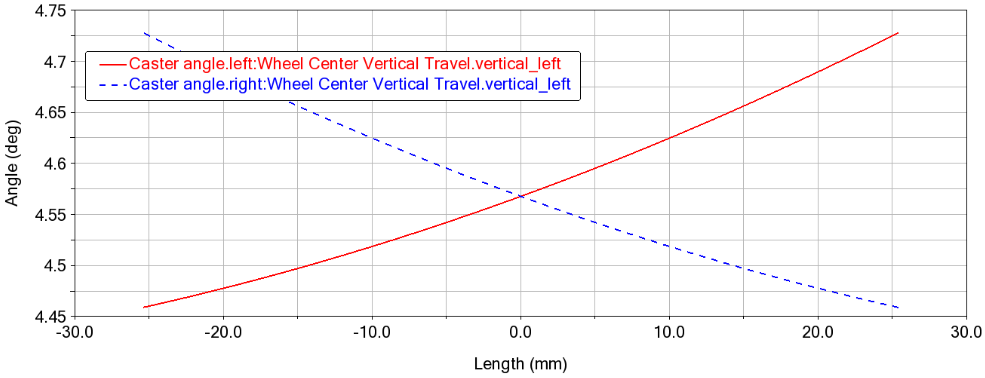
Caster angle.left:Wheel Center Vertical Travel.vertical_left
Caster angle.right:Wheel Center Vertical Travel.vertical_left
Angle (deg)
4.75
4.7
4.65
4.6
4.55
4.5
4.45
-30.0
-20.0
-10.0
0.0
10.0
20.0
30.0
Length (mm)

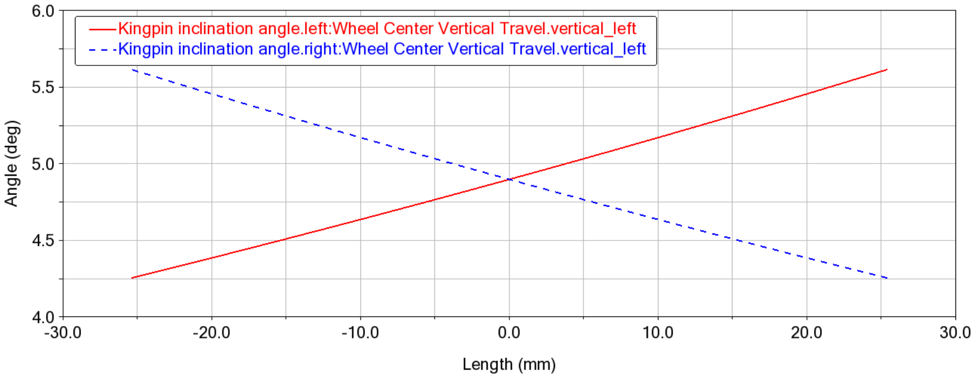
Kingpin inclination angle.left:Wheel Center Vertical Travel.vertical_left
Kingpin inclination angle.right:Wheel Center Vertical Travel.vertical_left
Angle (deg)
6.0
5.5
5.0
4.5
4.0
-30.0
-20.0
-10.0
0.0
10.0
20.0
30.0
Length (mm)

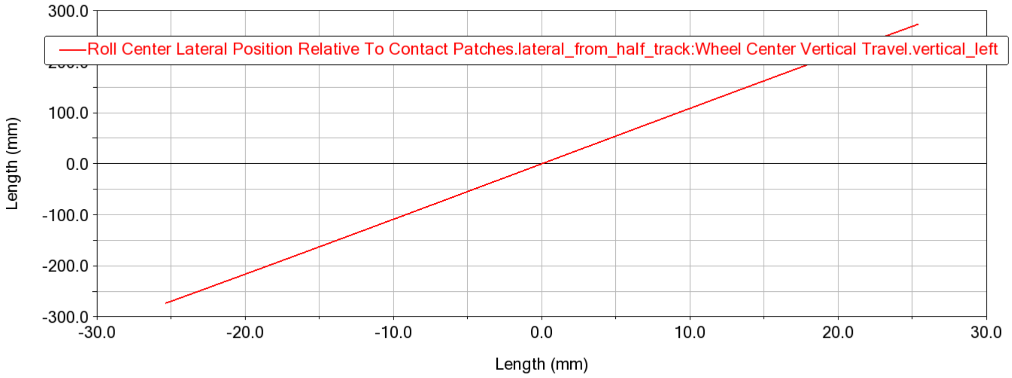
Roll Center Lateral Position Relative To Contact Patches.lateral_from_half_track:Wheel Center Vertical Travel.vertical_left
Length (mm)
300.0
100.0
0.0
-100.0
-200.0
-300.0
-30.0
-20.0
-10.0
0.0
10.0
20.0
30.0
Length (mm)

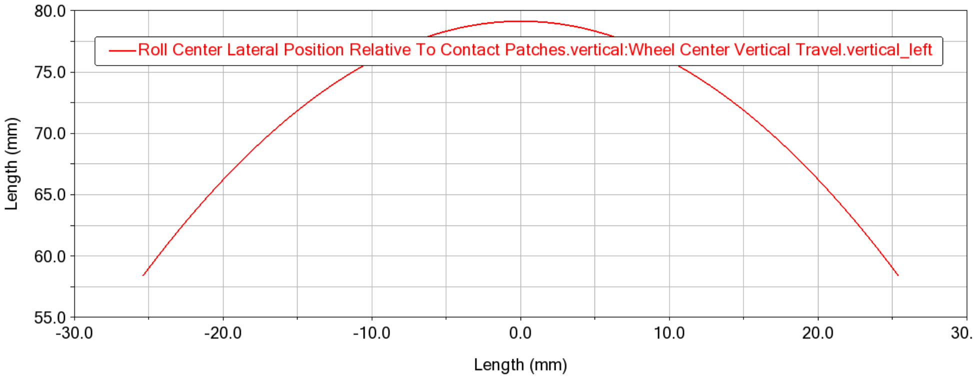

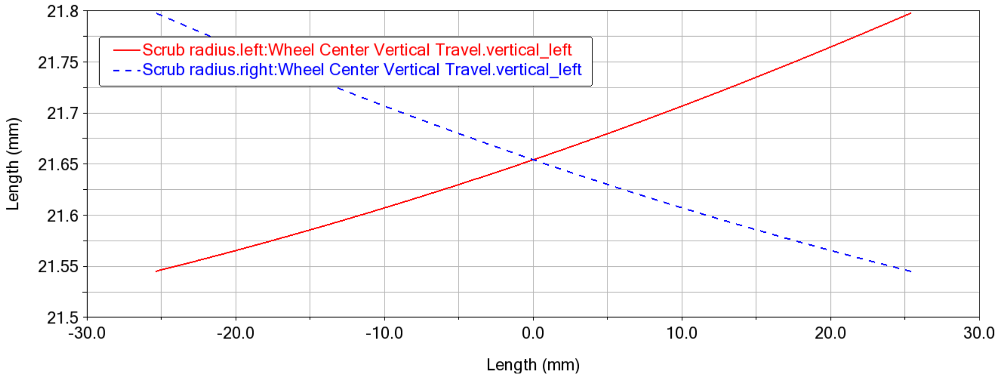

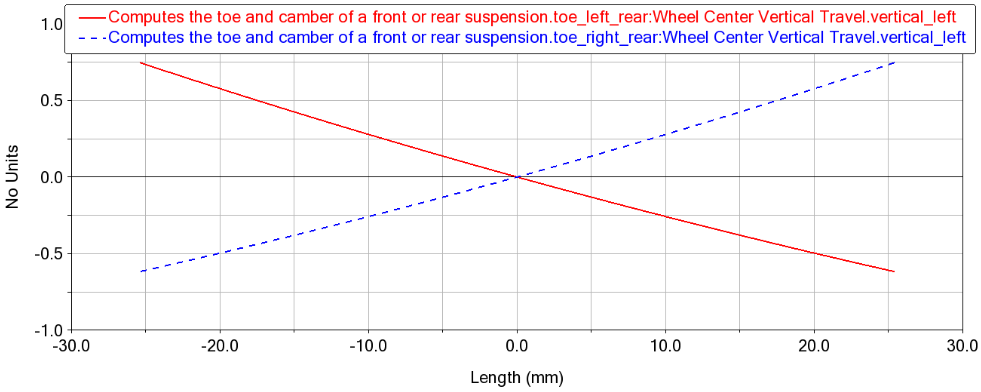

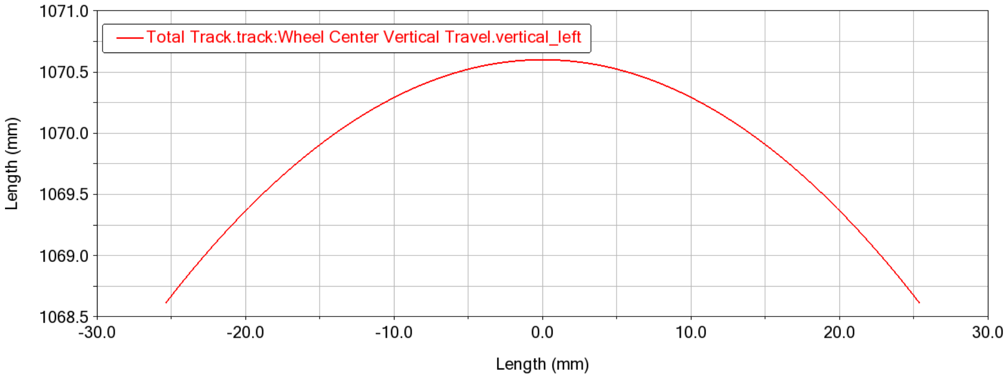

7.2.3 Comments

From the previous kinematic analysis, you can see that most of the suspension parameters have improved, while others, objectively, have not.

Surely, the roll centre, the main parameter of the two suspensions, has been positioned more correctly than before, resulting in a rolling axis that is tilted forward. As a result, the evolution of the camber angle is reduced by half, while the same gain was not achieved for the toe angle.

The anti-features, for both suspensions, now have more reasonable values, within the range and especially moderate.

The radius scrub has been modified to obtain the effect explained in the previous paragraph, that is to balance naturally an unwanted steering due to a blockage or a loss of grip: the value is negative for the front suspension and positive for the rear.

The front caster has been decreased to slightly increase the manoeuvrability and in the same way it has decreased at the rear, also decreasing the longitudinal stability of the axle.

What has unfortunately worsened considerably is the lateral displacement of the roll centre, in the case of opposite wheel travel. This effect will be reduced with the next geometry modification.

The differences between the two models is shown in the following paragraph.

7.3 Comparison

The two models are now compared by putting only the left characteristics, to keep clean the plots, and notice, effectively, the improvements.

7.3.1 Front suspension

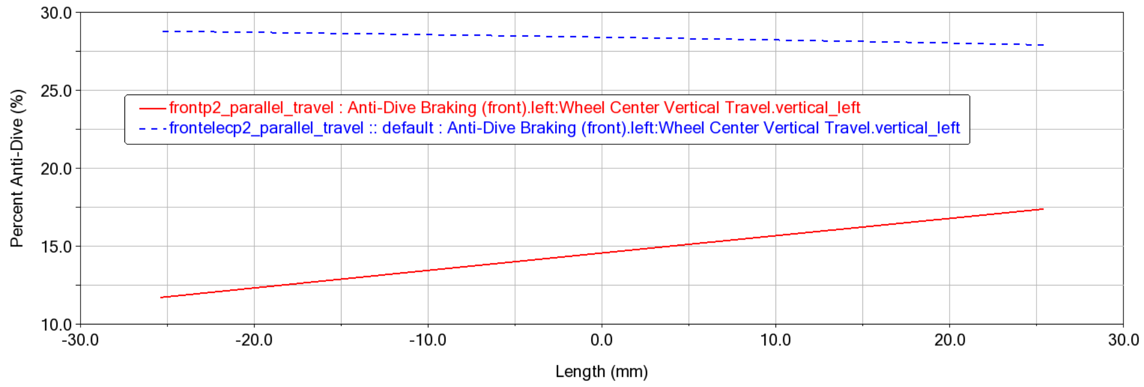

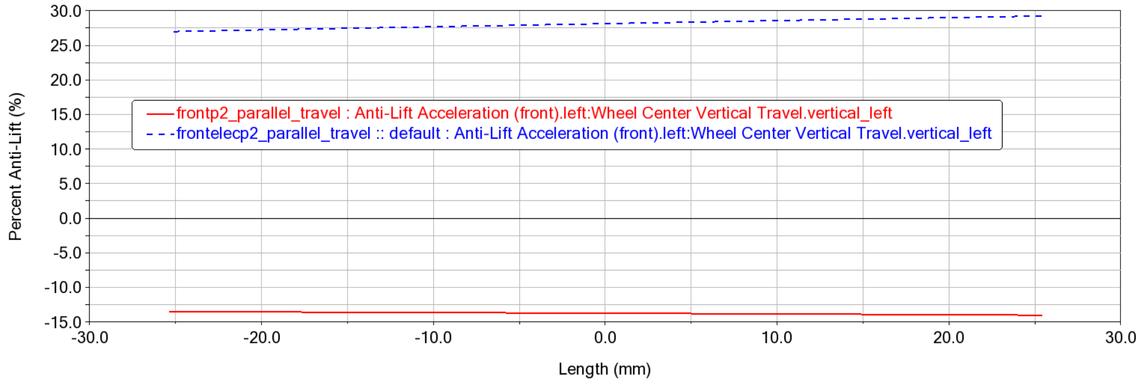

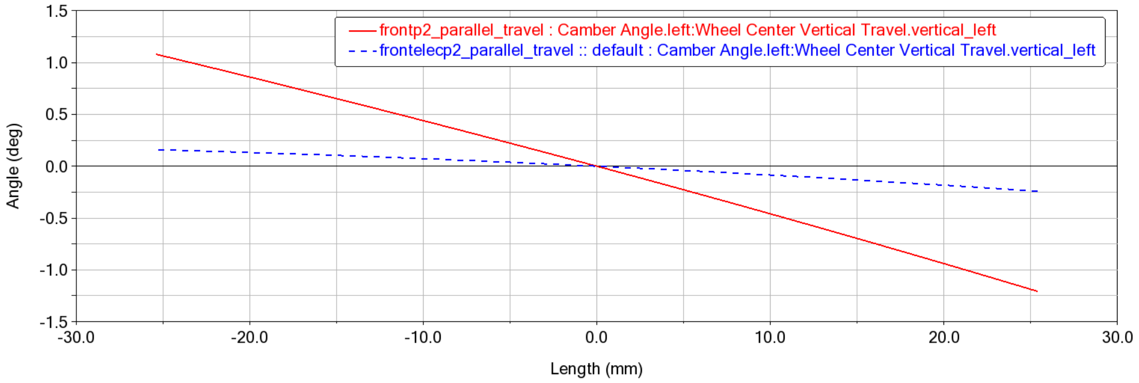
frontp2_parallel_travel : Camber Angle.left:Wheel Center Vertical Travel.vertical_left
frontelecp2_parallel_travel :: default : Camber Angle.left:Wheel Center Vertical Travel.vertical_left
Angle (deg)
1.5
1.0
0.5
0.0
-0.5
-1.0
-1.5
-30.0
-20.0
-10.0
0.0
10.0
20.0
30.0
Length (mm)

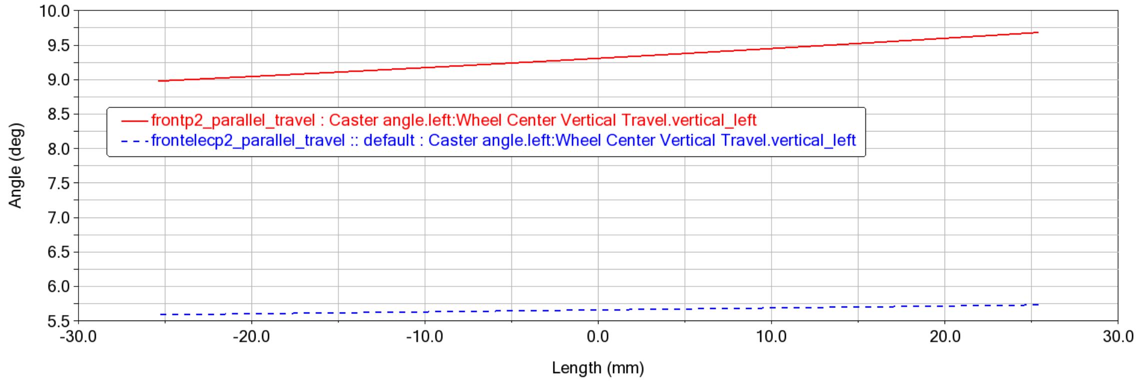
frontp2_parallel_travel : Caster angle.left:Wheel Center Vertical Travel.vertical_left
frontelecp2_parallel_travel :: default : Caster angle.left:Wheel Center Vertical Travel.vertical_left
Angle (deg)
10.0
9.5
9.0
8.5
8.0
7.5
7.0
6.5
6.0
5.5
-30.0
-20.0
-10.0
0.0
10.0
20.0
30.0
Length (mm)

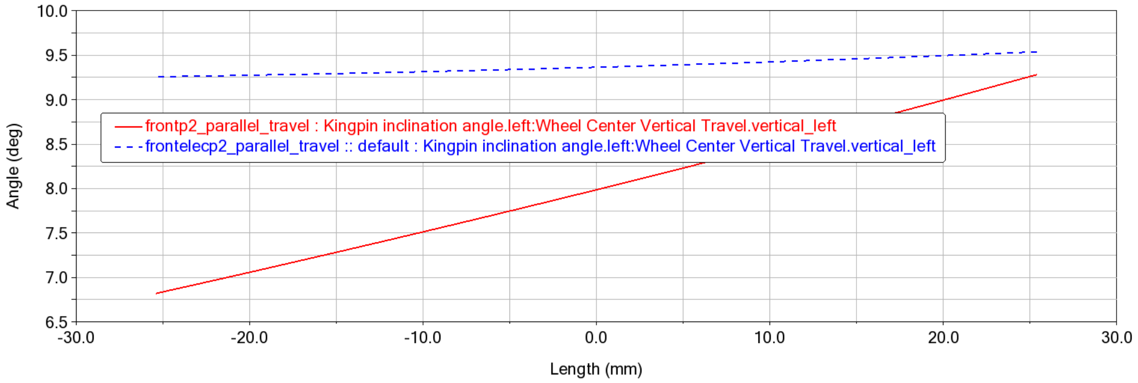
frontp2_parallel_travel : Kingpin inclination angle.left:Wheel Center Vertical Travel.vertical_left
frontelecp2_parallel_travel :: default : Kingpin inclination angle.left:Wheel Center Vertical Travel.vertical_left
Angle (deg)
10.0
9.5
9.0
8.5
8.0
7.5
7.0
6.5
-30.0
-20.0
-10.0
0.0
10.0
20.0
30.0
Length (mm)

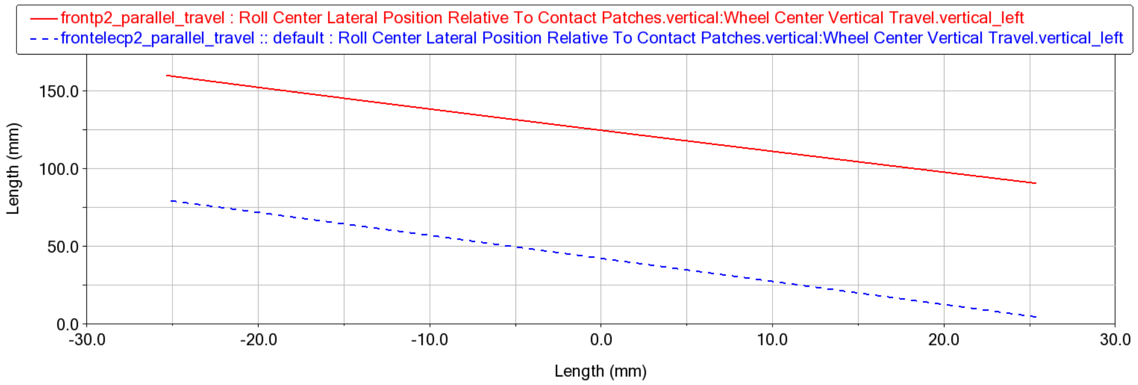
frontp2_parallel_travel : Roll Center Lateral Position Relative To Contact Patches.vertical:Wheel Center Vertical Travel.vertical_left
frontelecp2_parallel_travel :: default : Roll Center Lateral Position Relative To Contact Patches.vertical:Wheel Center Vertical Travel.vertical_left
Length (mm)
150.0
100.0
50.0
0.0
-30.0
-20.0
-10.0
0.0
10.0
20.0
30.0
Length (mm)

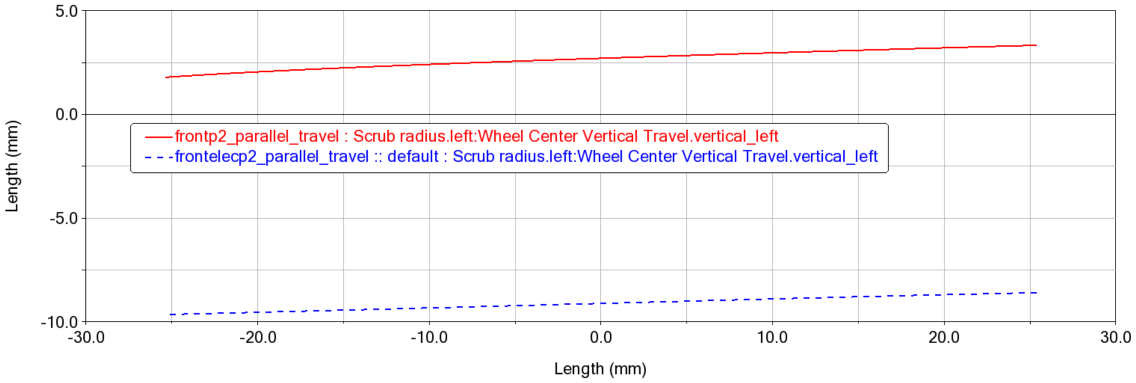

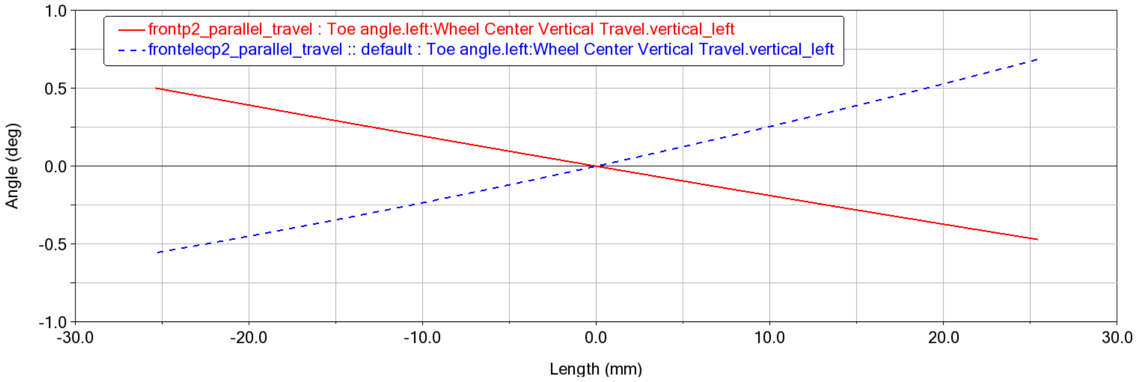

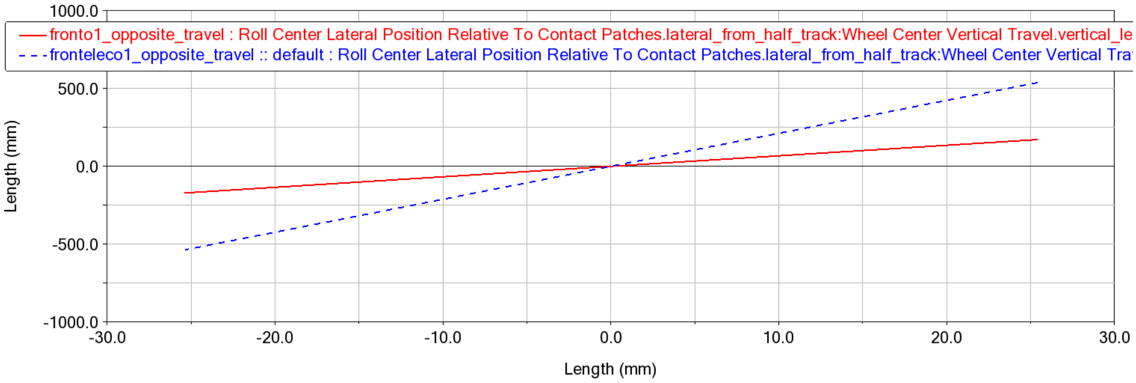

7.3.2 Rear suspension

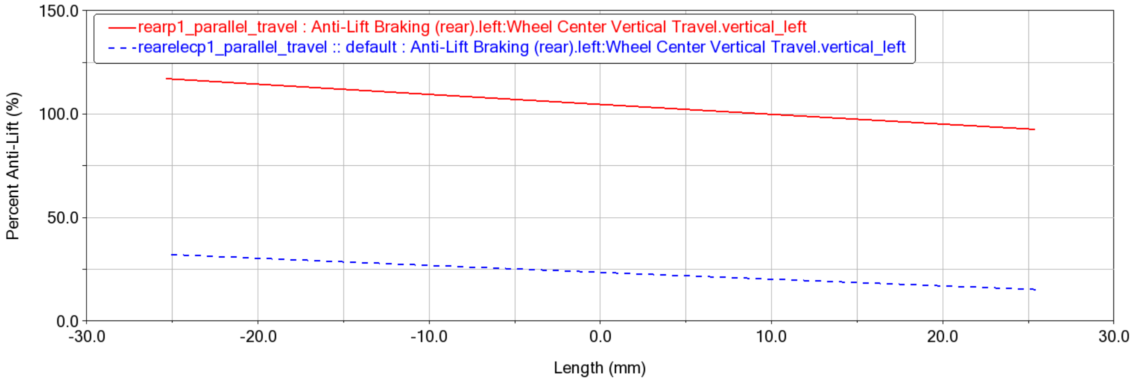

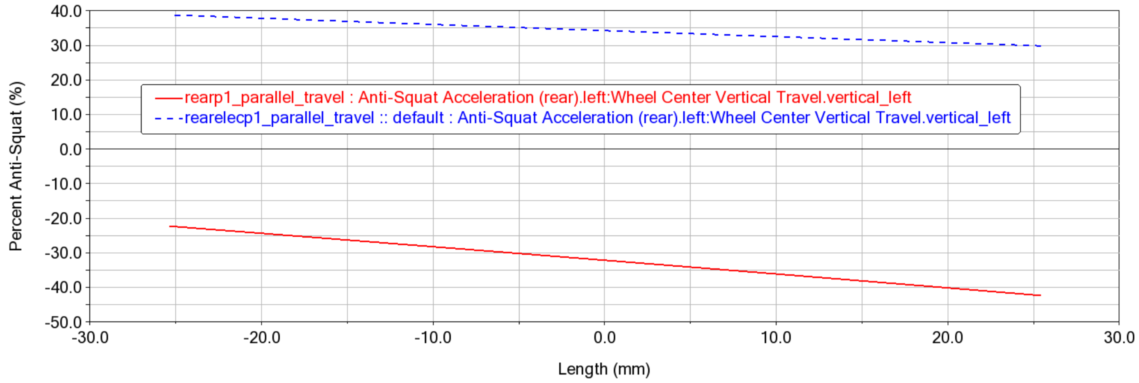
rearp1_parallel_travel : Anti-Squat Acceleration (rear).left:Wheel Center Vertical Travel.vertical_left
rearelecp1_parallel_travel :: default : Anti-Squat Acceleration (rear).left:Wheel Center Vertical Travel.vertical_left
Percent Anti-Squat (%)
40.0
30.0
20.0
10.0
0.0
-10.0
-20.0
-30.0
-40.0
-50.0
-30.0
-20.0
-10.0
0.0
10.0
20.0
30.0
Length (mm)

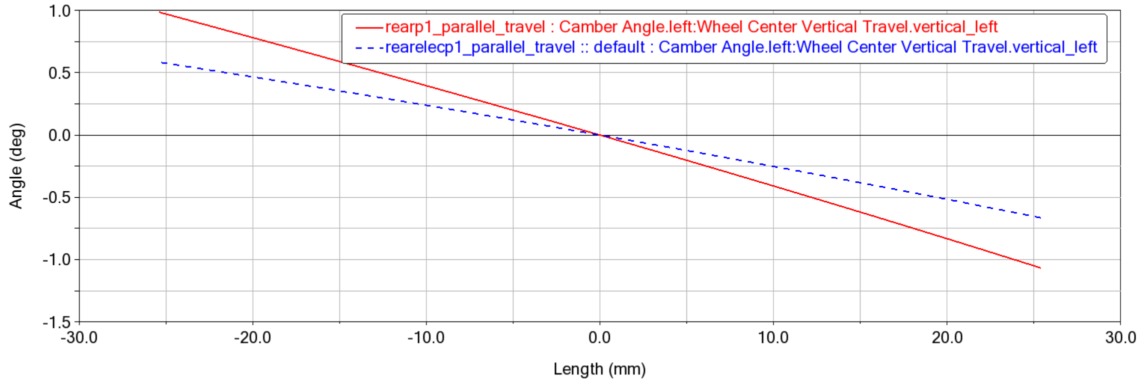
rearp1_parallel_travel : Camber Angle.left:Wheel Center Vertical Travel.vertical_left
rearelecp1_parallel_travel :: default : Camber Angle.left:Wheel Center Vertical Travel.vertical_left
Angle (deg)
1.0
0.5
0.0
-0.5
-1.0
-1.5
-30.0
-20.0
-10.0
0.0
10.0
20.0
30.0
Length (mm)

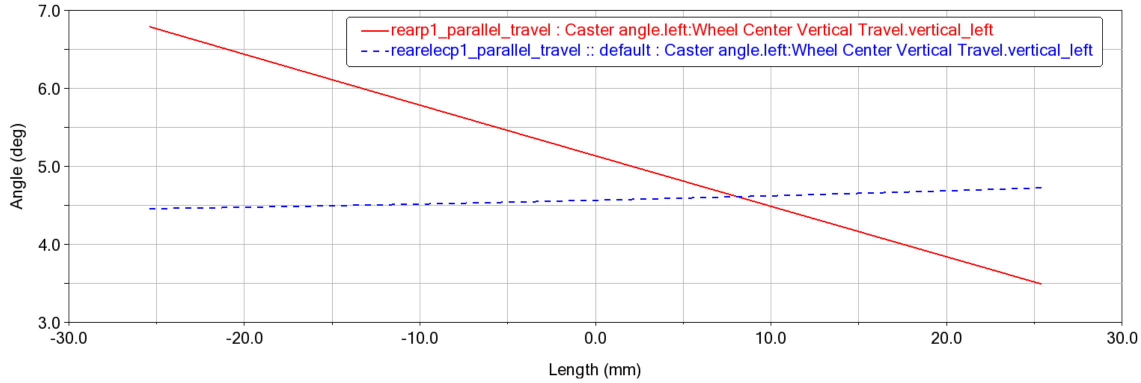
rearp1_parallel_travel : Caster angle.left:Wheel Center Vertical Travel.vertical_left
rearelecp1_parallel_travel :: default : Caster angle.left:Wheel Center Vertical Travel.vertical_left
Angle (deg)
7.0
6.0
5.0
4.0
3.0
-30.0
-20.0
-10.0
0.0
10.0
20.0
30.0
Length (mm)

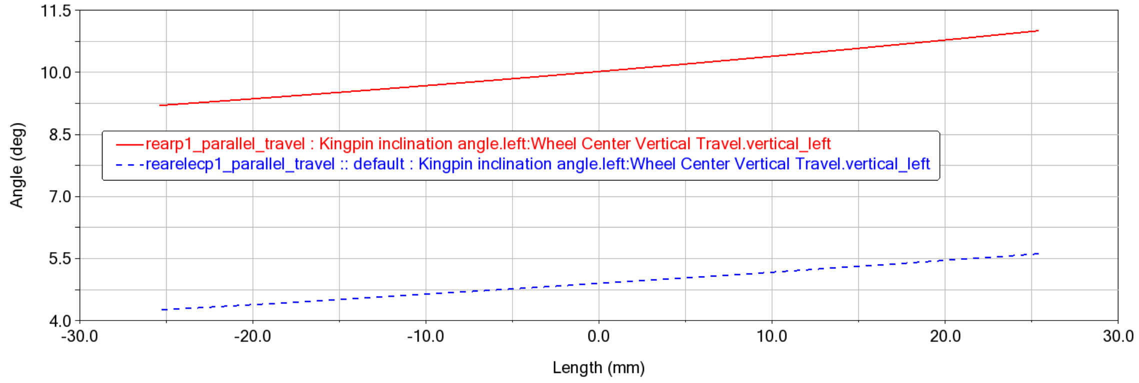
rearp1_parallel_travel : Kingpin inclination angle.left:Wheel Center Vertical Travel.vertical_left
rearelecp1_parallel_travel :: default : Kingpin inclination angle.left:Wheel Center Vertical Travel.vertical_left
Angle (deg)
11.5
10.0
8.5
7.0
5.5
4.0
-30.0
-20.0
-10.0
0.0
10.0
20.0
30.0
Length (mm)

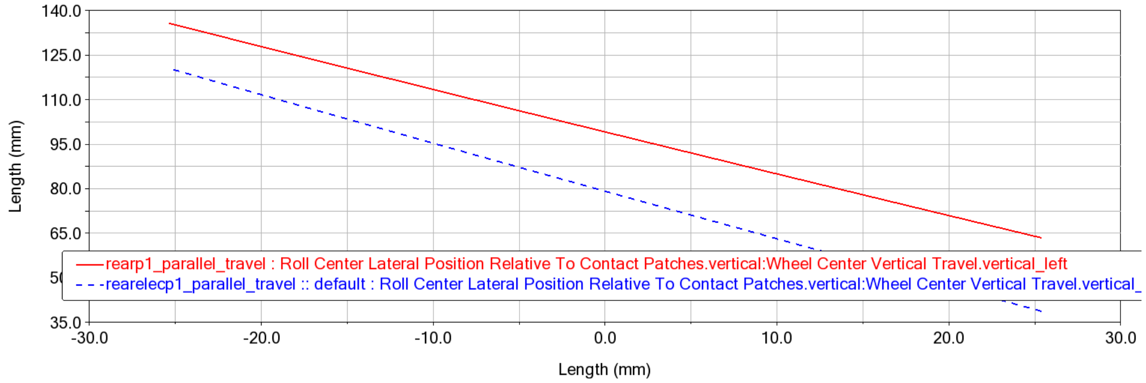
140.0
125.0
110.0
95.0
80.0
65.0
35.0
Length (mm)
-30.0
-20.0
-10.0
0.0
10.0
20.0
30.0
Length (mm)
——rearp1_parallel_travel : Roll Center Lateral Position Relative To Contact Patches.vertical:Wheel Center Vertical Travel.vertical_left
- - -rearelecp1_parallel_travel :: default : Roll Center Lateral Position Relative To Contact Patches.vertical:Wheel Center Vertical Travel.vertical_

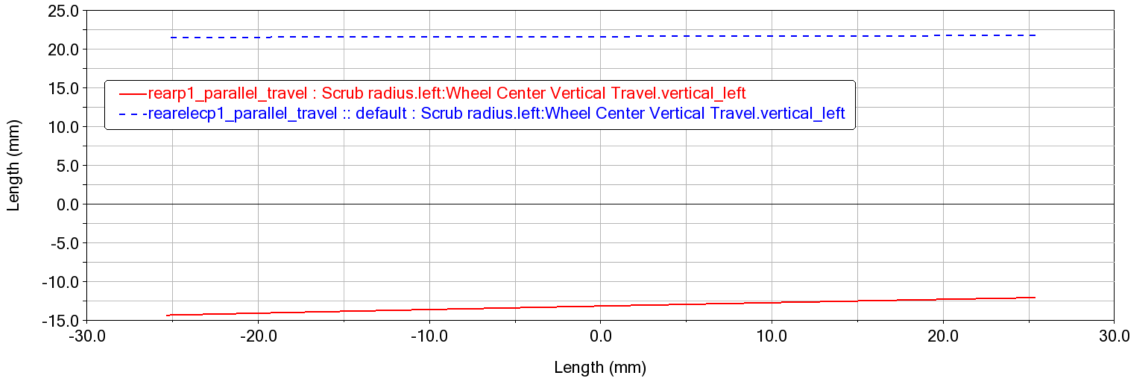
25.0
20.0
15.0
10.0
5.0
0.0
-5.0
-10.0
-15.0
Length (mm)
-30.0
-20.0
-10.0
0.0
10.0
20.0
30.0
Length (mm)
——rearp1_parallel_travel : Scrub radius.left:Wheel Center Vertical Travel.vertical_left
- - -rearelecp1_parallel_travel :: default : Scrub radius.left:Wheel Center Vertical Travel.vertical_left

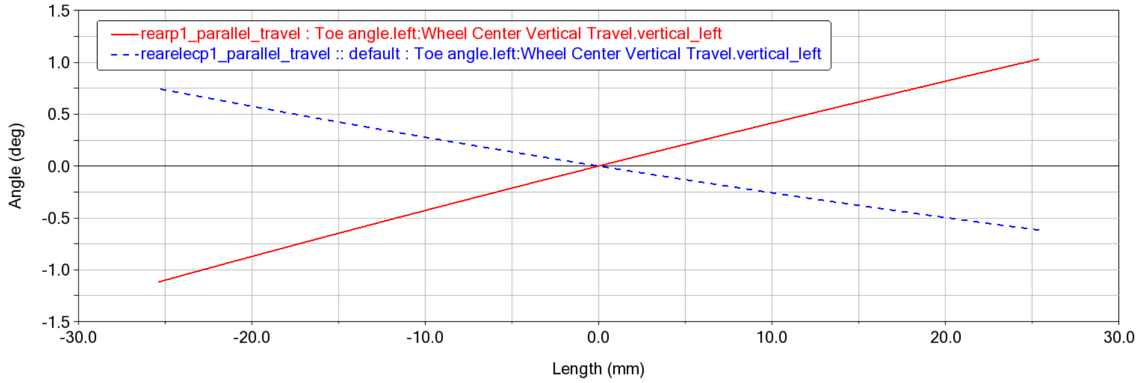
1.5
1.0
0.5
0.0
-0.5
-1.0
-1.5
Angle (deg)
-30.0
-20.0
-10.0
0.0
10.0
20.0
30.0
Length (mm)
——rearp1_parallel_travel : Toe angle.left:Wheel Center Vertical Travel.vertical_left
- - -rearelecp1_parallel_travel :: default : Toe angle.left:Wheel Center Vertical Travel.vertical_left

8. FINAL SUSPENSION MODEL FOR THE 2020 UPM RACING ELECTRIC VEHICLE

8.1 Requirements for the electric vehicle

For the final model, several requirements have to be considered, some used before and some used only now to get as close as possible to the real characteristics of the vehicle.

8.1.1 Electric engine

An important factor to be considered for the design of the suspension is the *electric motor*.

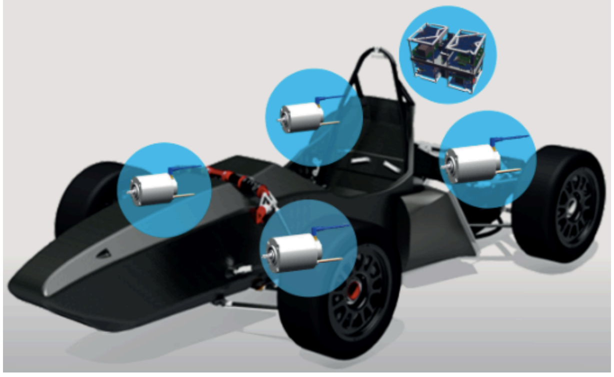

Figure 43. Representation of the four in-wheel electric motors.

The electric motor is an *AMK E1208* synchronous coupled to the knuckle of each wheel, being the same for both axles. It reaches a maximum of 18000 rpm, being at 13500 rpm the point where the maximum torque is reached. This peak torque is delivered by the motor during 1 second, reaching the value of 21 Nm. Also, it offers a maximum nominal torque in continuous regime of 13.8 Nm and a maximum power of 12.3 KW in this same regime. The maximum peak power is 29 KW.

The anchor points of the arms, due to the presence of the electric engine, must be placed close to the circumference of the rim, avoiding, in any case, interference during movement and, above all, the push-rod must be set differently. Its anchorage point to the wheel must be moved from below (most convenient choice) to above. Logically, shock absorbers are also raised and commonly placed horizontally above the bodywork, in front of the rider: this avoids excessive inclinations of the push-rod that would lead to excessive stresses.

Likewise, the dimensioning of the inner diameter of the knuckle requires, in its internal face, to house an available diameter, not only for the engine itself, but for the surrounding forced air-cooling system. The diameter to be considered is 96 mm plus approximately 2 cm more for the cooling.

In addition to influencing the geometric design of the suspension, it also influences the adhesion and forces acting on the vehicle, that will be computed later.

8.1.2 Rear track

Another important aspect to consider is the space to be reserved for *batteries*, that feed the electric motors. These batteries deliver a voltage of 579.6 V at full capacity and are made up of rechargeable lithium and polymer batteries with a potential of 3.7 V and a capacity of 7000 mAh. The charging efficiency is 94.2%.

For reasons of space, the batteries will be placed at the rear, behind the pilot. The space required, therefore, requires the rear track to be increased to 1200 mm, 30 cm more than the old model.

8.1.3 Wheelbase

The wheelbase is extended by 30 mm (up to 1580 mm) with respect to the front design, which results in a general shifting of the components.

8.1.4 Tire characteristic

To bring the model even closer to reality, the tyre's characteristics are modified to achieve the performance of the *Hoosier 6.0/18.0 – 10 LCO* that the team decided to use. To do this, you need to modify the file *tires.tir*, putting the correct size of the wheel and changing the coefficients for the model of Pacejka.

For the first one, the dimensions are 457.2 mm diameter, 152.4 mm width and 0.47 aspect ratio, according to the Hoosier catalogue.

In the second case, the work done by a student of the team was used for his thesis: the values for which the curves of the model approached the real characteristic curves of the tyre were sought, using the test bench available at INSIA.

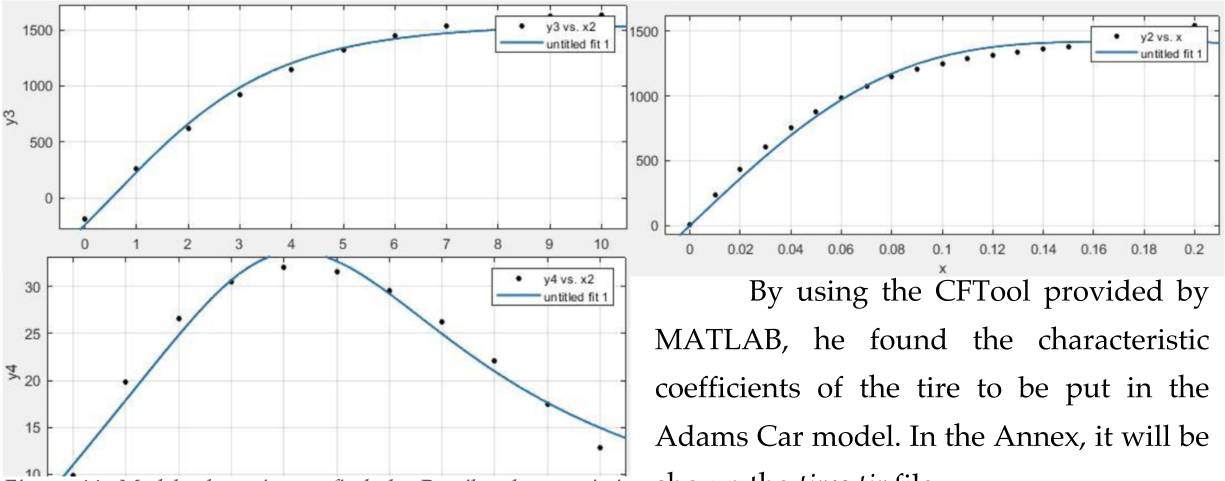

Figure 44. Model adaptation to find the Pacejka characteristic coefficents.

By using the CFTool provided by MATLAB, he found the characteristic coefficients of the tire to be put in the Adams Car model. In the Annex, it will be shown the *tires.tir* file.

Unlike the previous wheel, the current one has a smaller rim, so the previously designed suspension arms must be brought closer together.

8.2 Final geometry

Starting from the geometry described in Chapter 7, all appropriate modifications shall be made according to the requirements described above.

8.2.1 Front suspension

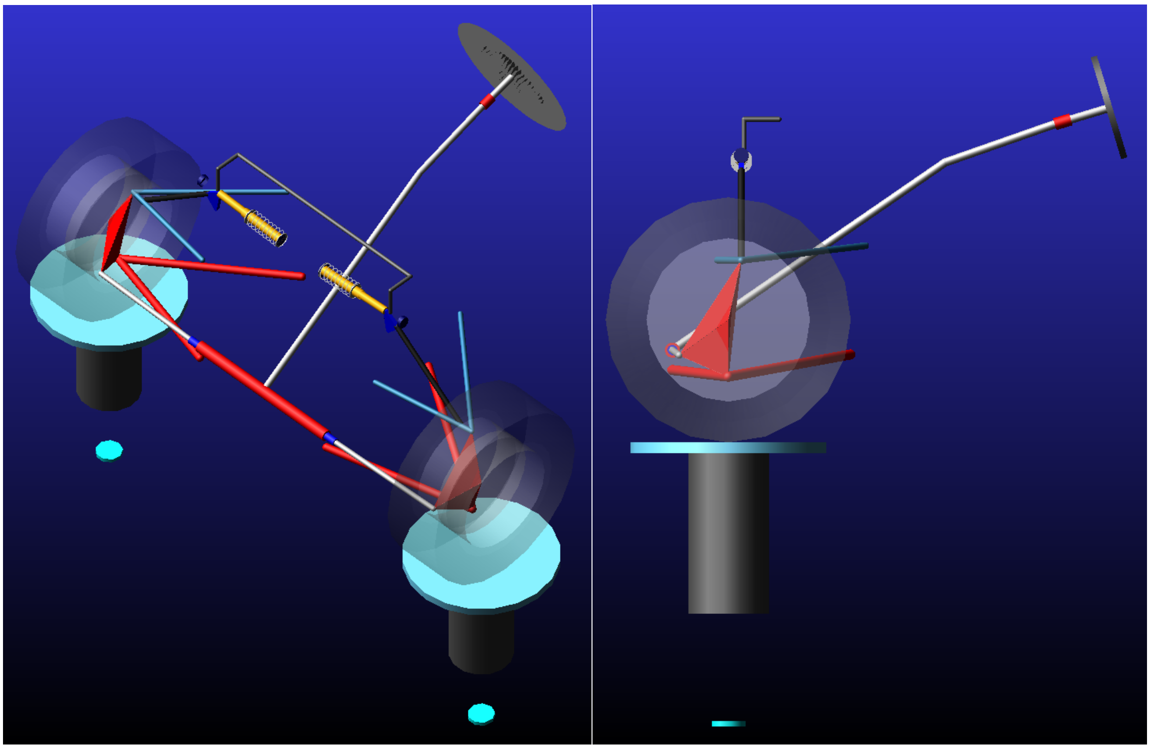

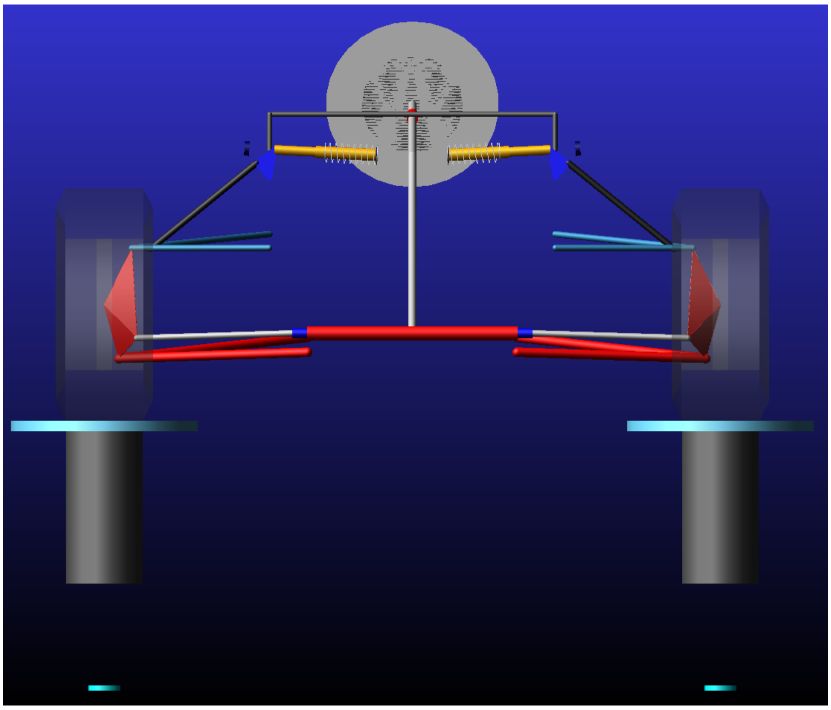

8.2.2 Rear suspension

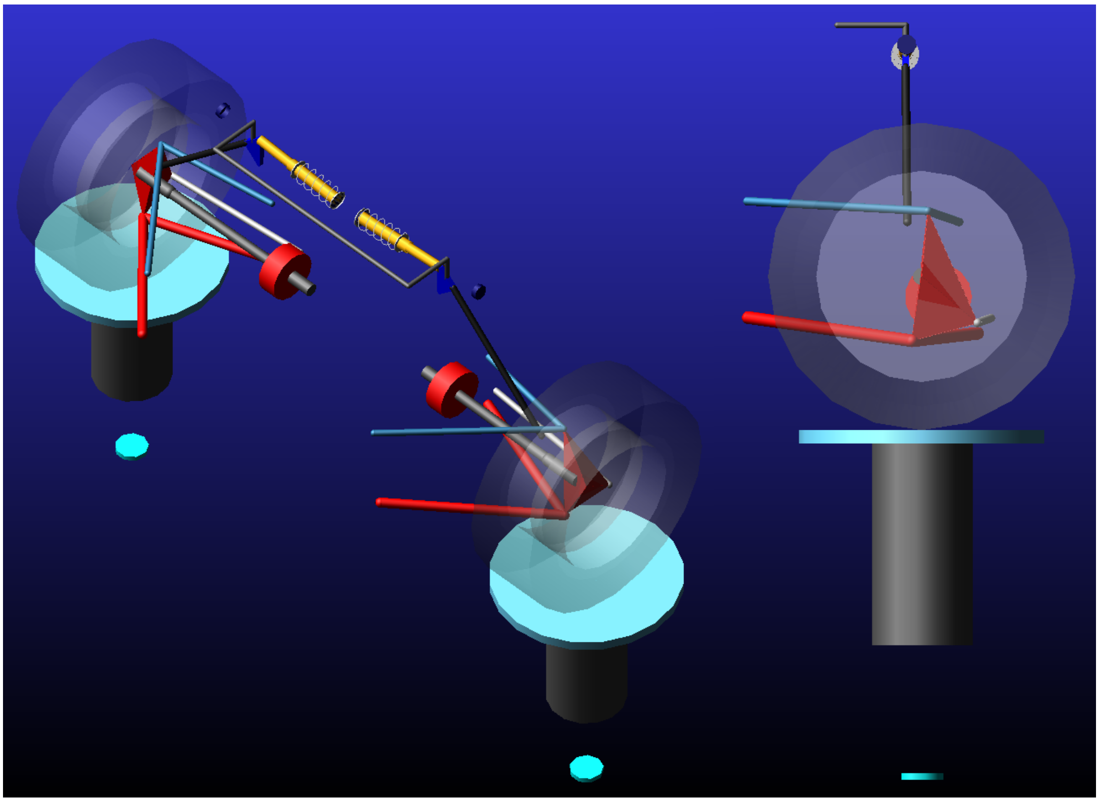

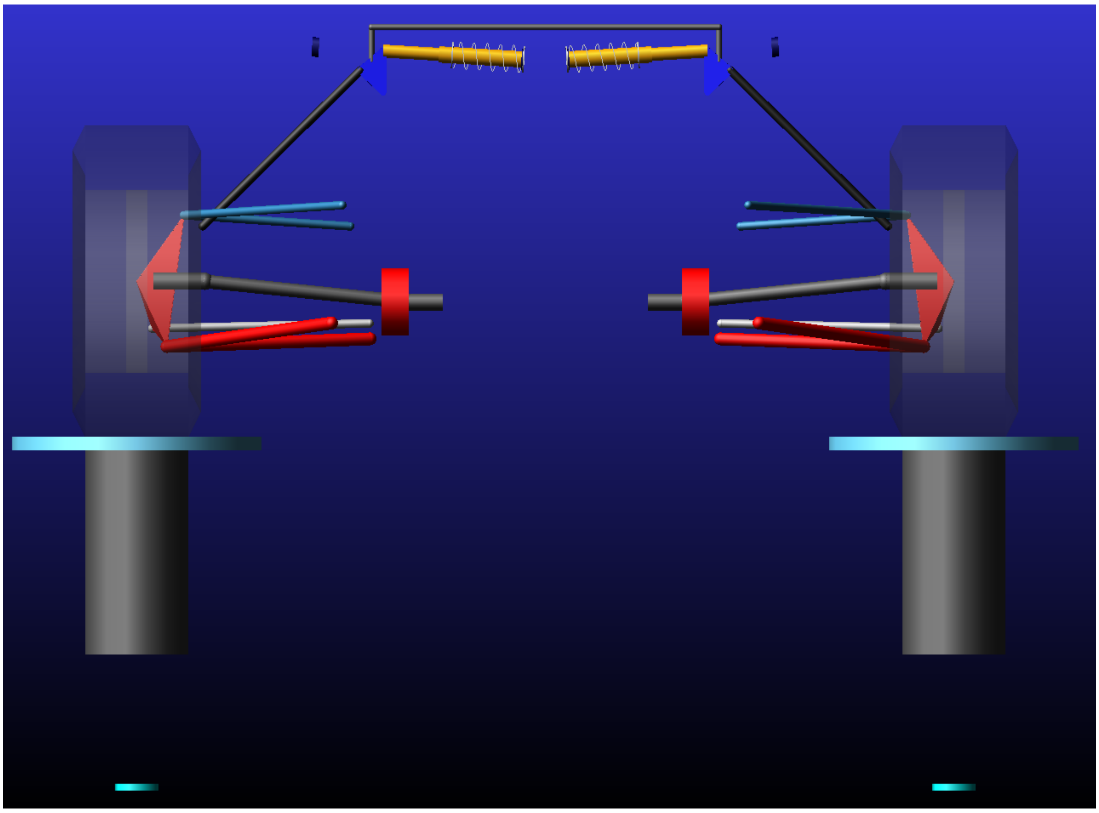

8.2.3 Full vehicle

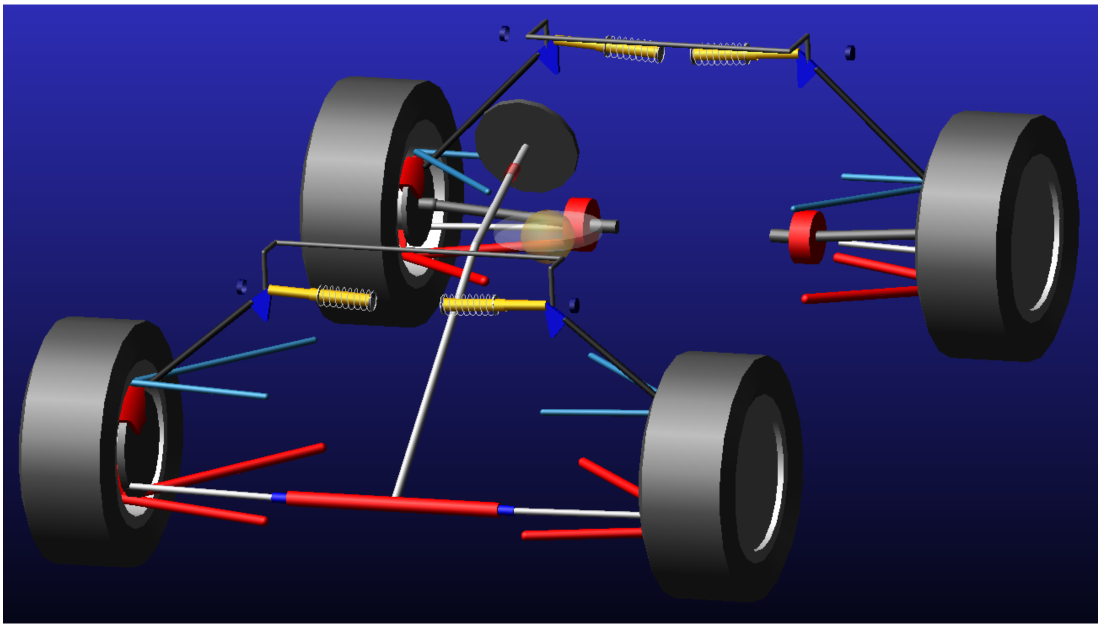

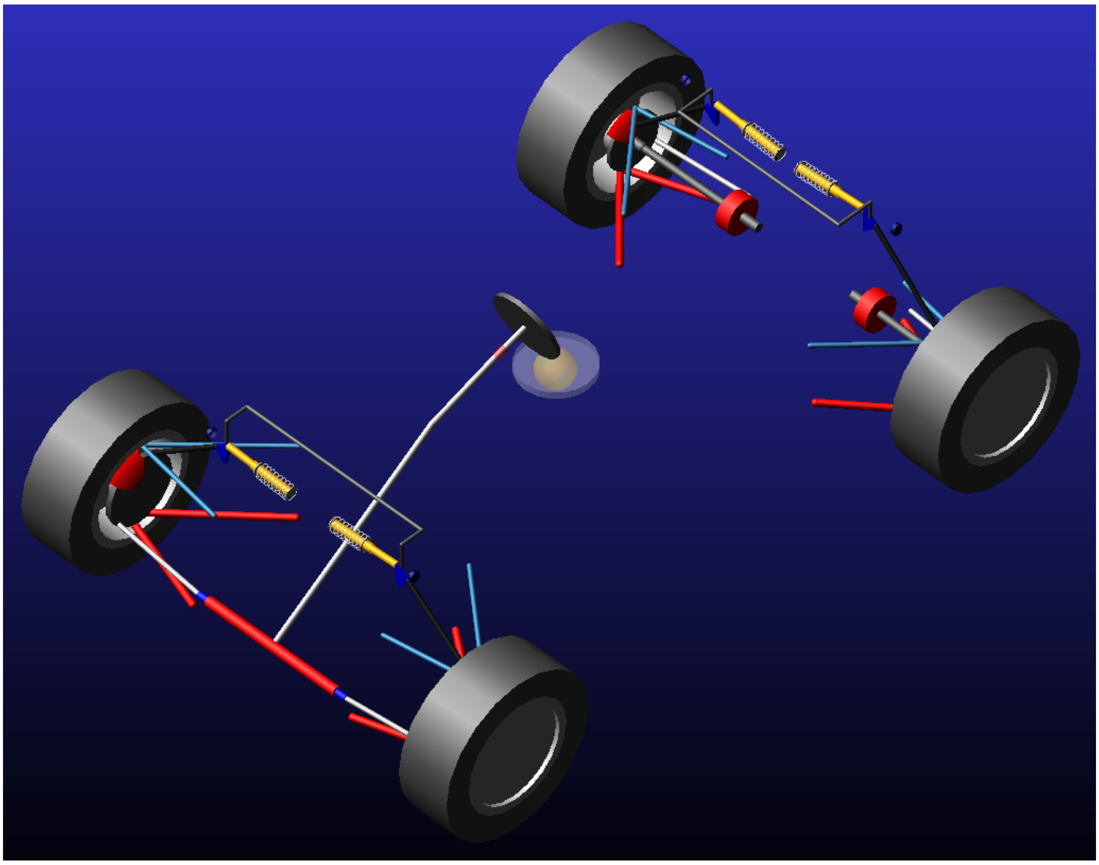

8.3 Kinematic behaviour

First, kinematic analysis is performed to get to the desired values for the suspension characteristics. In the following, the plots of all suspension parameters are shown.

8.3.1 Front suspension

8.3.1.1Parallel

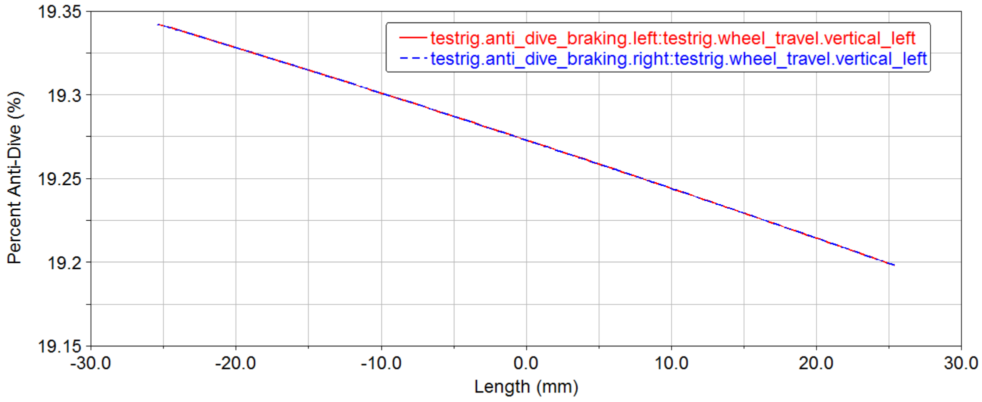

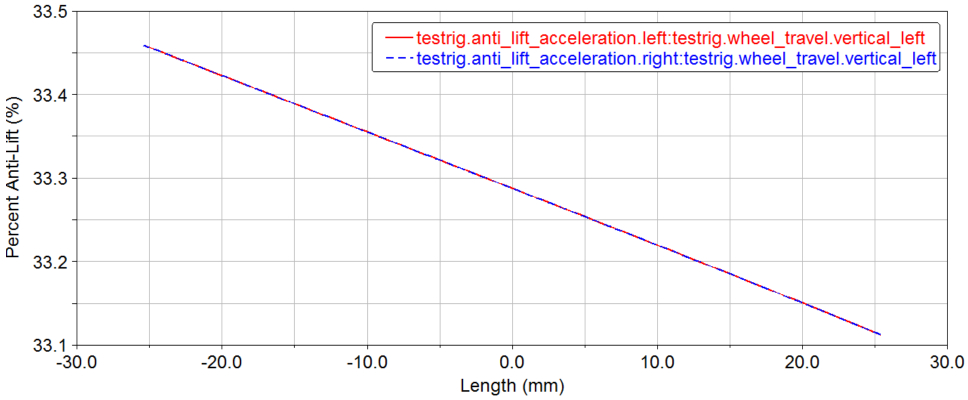

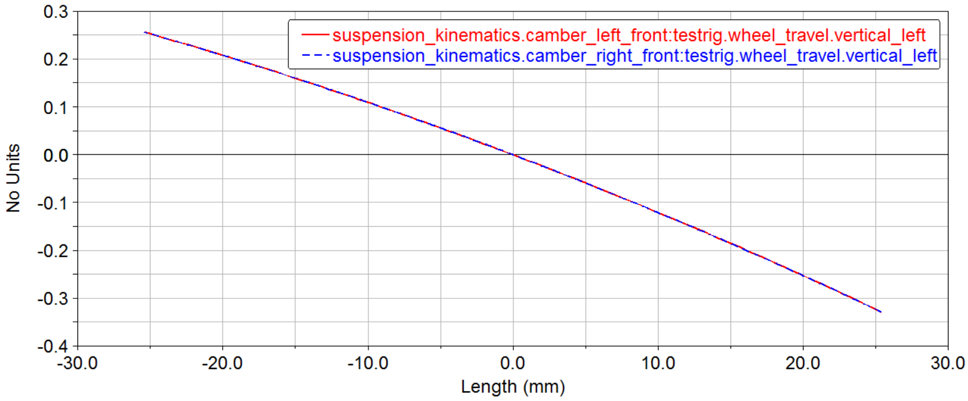

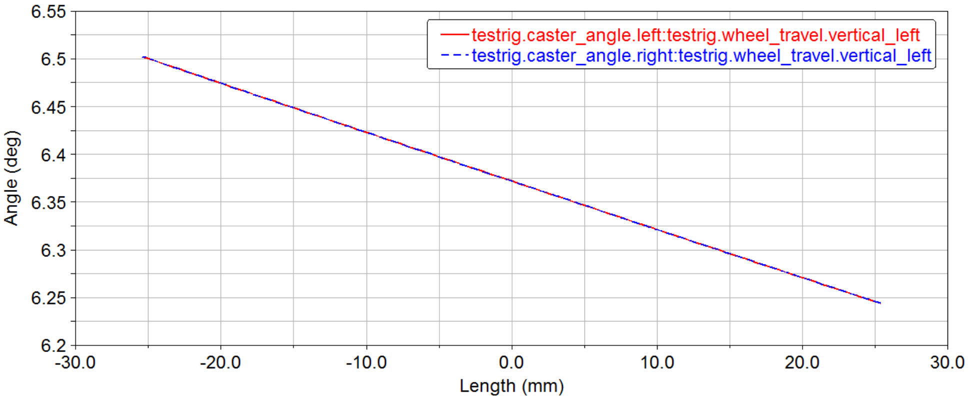
testrig.caster_angle.left:testrig.wheel_travel.vertical_left
testrig.caster_angle.right:testrig.wheel_travel.vertical_left
Angle (deg)
6.55
6.5
6.45
6.4
6.35
6.3
6.25
6.2
-30.0
-20.0
-10.0
0.0
10.0
20.0
30.0
Length (mm)

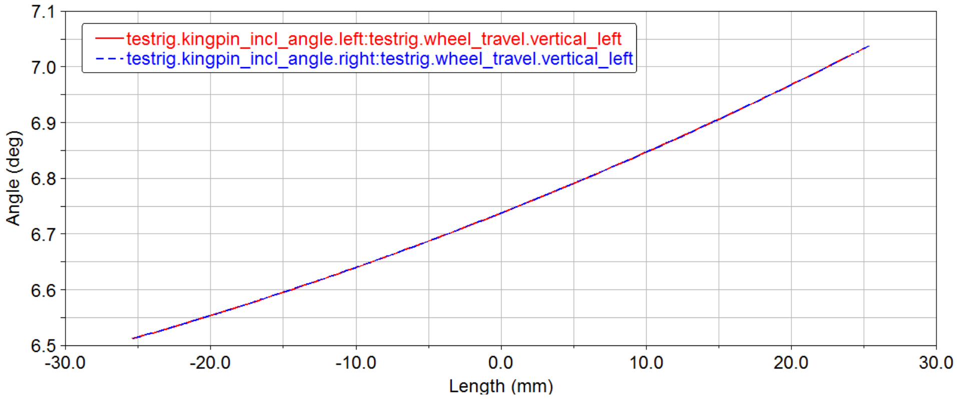
testrig.kingpin_incl_angle.left:testrig.wheel_travel.vertical_left
testrig.kingpin_incl_angle.right:testrig.wheel_travel.vertical_left
Angle (deg)
7.1
7.0
6.9
6.8
6.7
6.6
6.5
-30.0
-20.0
-10.0
0.0
10.0
20.0
30.0
Length (mm)

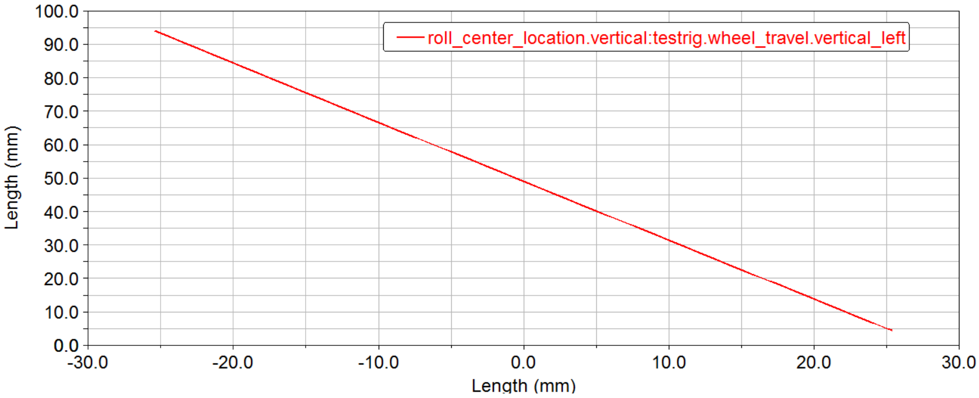
roll_center_location.vertical:testrig.wheel_travel.vertical_left
Length (mm)
100.0
90.0
80.0
70.0
60.0
50.0
40.0
30.0
20.0
10.0
0.0
-30.0
-20.0
-10.0
0.0
10.0
20.0
30.0
Length (mm)

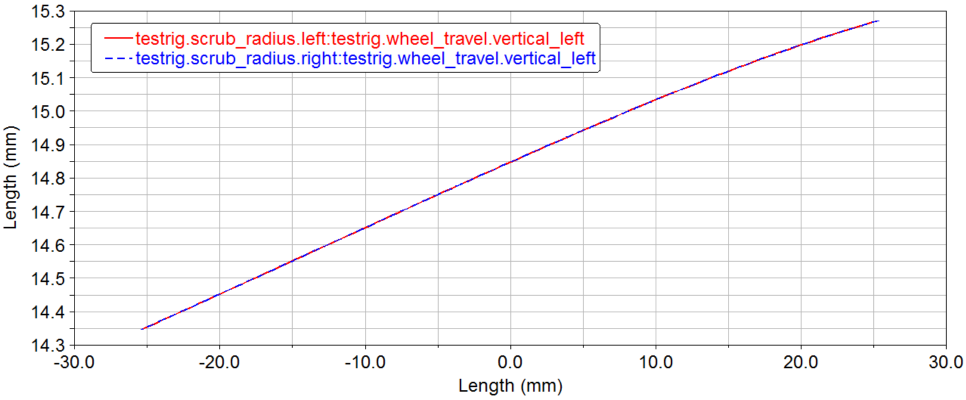
testrig.scrub_radius.left:testrig.wheel_travel.vertical_left
testrig.scrub_radius.right:testrig.wheel_travel.vertical_left
Length (mm)
15.3
15.2
15.1
15.0
14.9
14.8
14.7
14.6
14.5
14.4
14.3
-30.0
-20.0
-10.0
0.0
10.0
20.0
30.0
Length (mm)

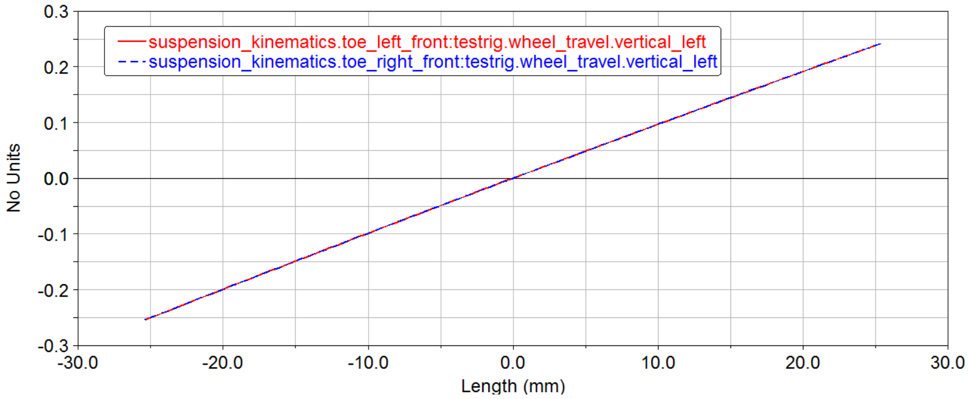

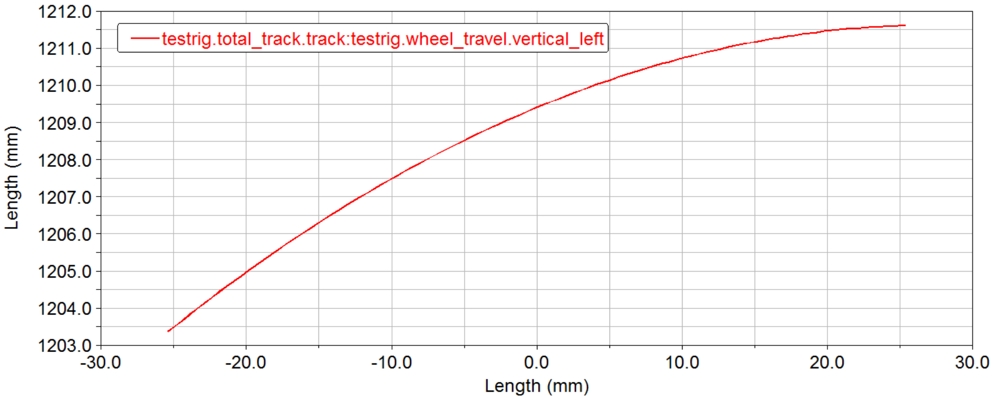

8.3.1.2 Opposite

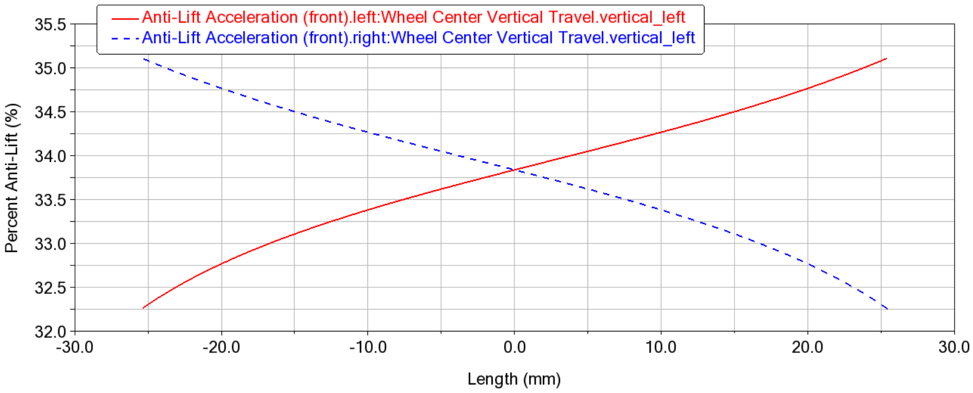

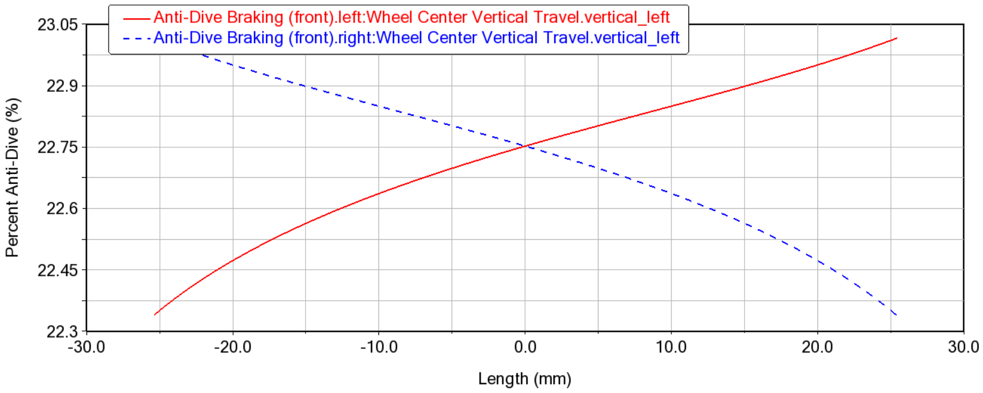

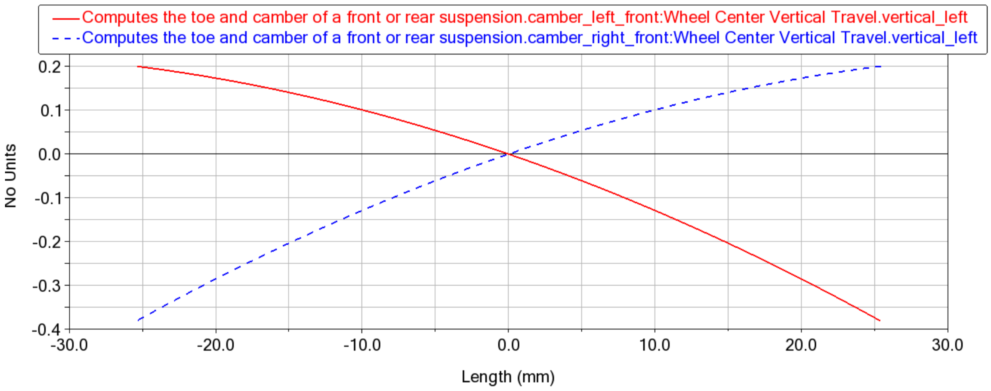
Computes the toe and camber of a front or rear suspension.camber_left_front:Wheel Center Vertical Travel.vertical_left
Computes the toe and camber of a front or rear suspension.camber_right_front:Wheel Center Vertical Travel.vertical_left
No Units
0.2
0.1
0.0
-0.1
-0.2
-0.3
-0.4
-30.0
-20.0
-10.0
0.0
10.0
20.0
30.0
Length (mm)

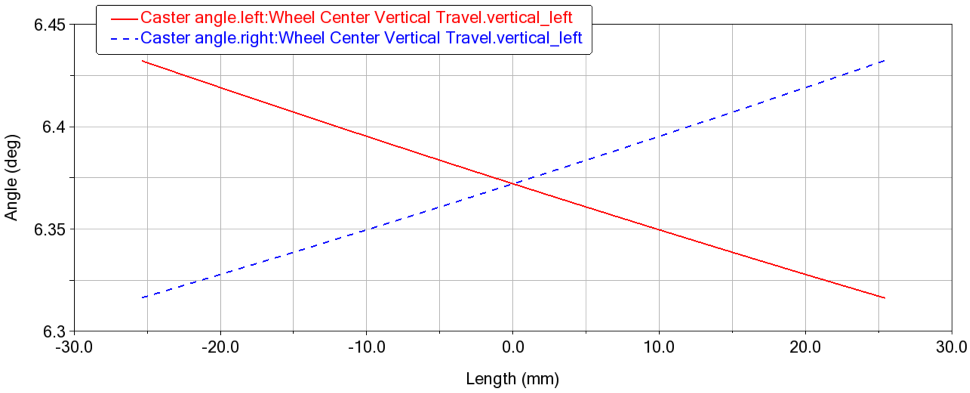
Caster angle.left:Wheel Center Vertical Travel.vertical_left
Caster angle.right:Wheel Center Vertical Travel.vertical_left
Angle (deg)
6.45
6.4
6.35
6.3
-30.0
-20.0
-10.0
0.0
10.0
20.0
30.0
Length (mm)

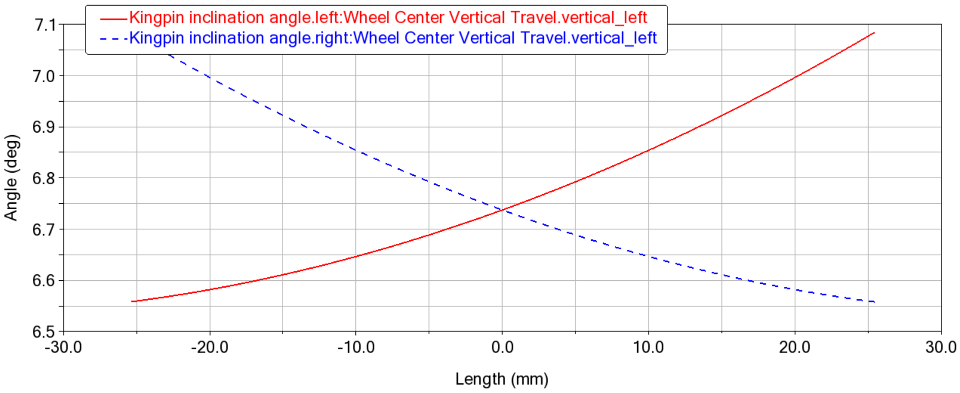
Kingpin inclination angle.left:Wheel Center Vertical Travel.vertical_left
Kingpin inclination angle.right:Wheel Center Vertical Travel.vertical_left
Angle (deg)
7.1
7.0
6.9
6.8
6.7
6.6
6.5
-30.0
-20.0
-10.0
0.0
10.0
20.0
30.0
Length (mm)

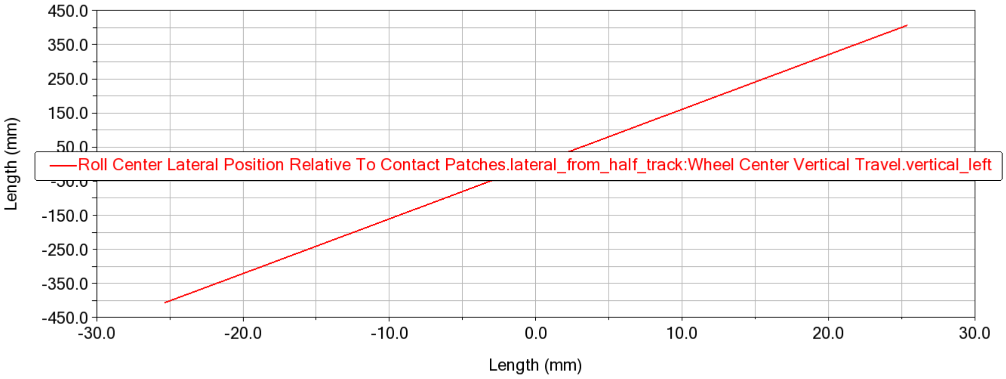
Roll Center Lateral Position Relative To Contact Patches.lateral_from_half_track:Wheel Center Vertical Travel.vertical_left
Length (mm)
450.0
350.0
250.0
150.0
50.0
-50.0
-150.0
-250.0
-350.0
-450.0
-30.0
-20.0
-10.0
0.0
10.0
20.0
30.0
Length (mm)

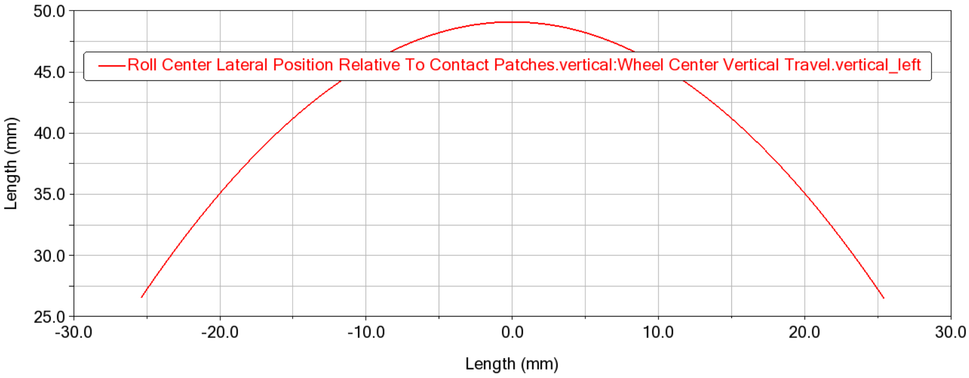
Roll Center Lateral Position Relative To Contact Patches.vertical:Wheel Center Vertical Travel.vertical_left
Length (mm)
50.0
45.0
40.0
35.0
30.0
25.0
-30.0
-20.0
-10.0
0.0
10.0
20.0
30.0
Length (mm)

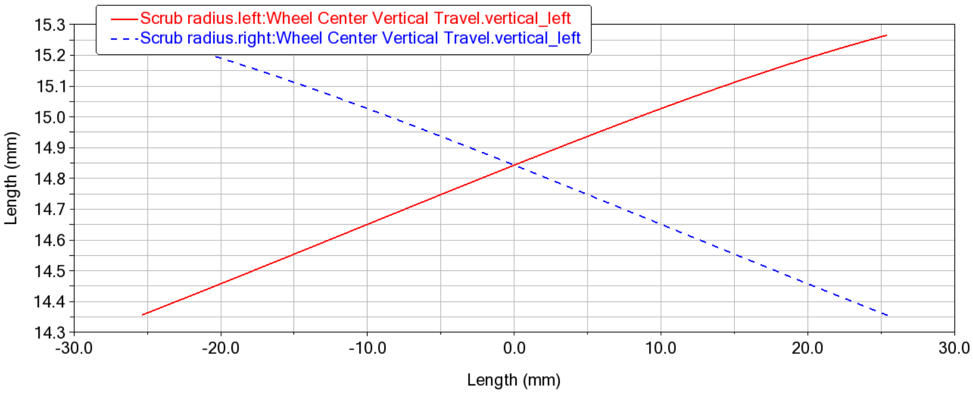
Scrub radius.left:Wheel Center Vertical Travel.vertical_left
Scrub radius.right:Wheel Center Vertical Travel.vertical_left
Length (mm)
15.3
15.2
15.1
15.0
14.9
14.8
14.7
14.6
14.5
14.4
14.3
-30.0
-20.0
-10.0
0.0
10.0
20.0
30.0
Length (mm)

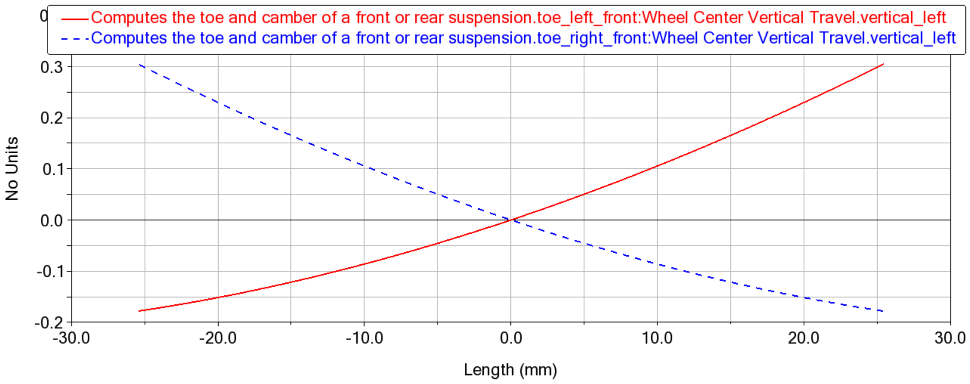
Computes the toe and camber of a front or rear suspension.toe_left_front:Wheel Center Vertical Travel.vertical_left
Computes the toe and camber of a front or rear suspension.toe_right_front:Wheel Center Vertical Travel.vertical_left
No Units
0
0.3
0.2
0.1
0.0
-0.1
-0.2
-30.0
-20.0
-10.0
0.0
10.0
20.0
30.0
Length (mm)

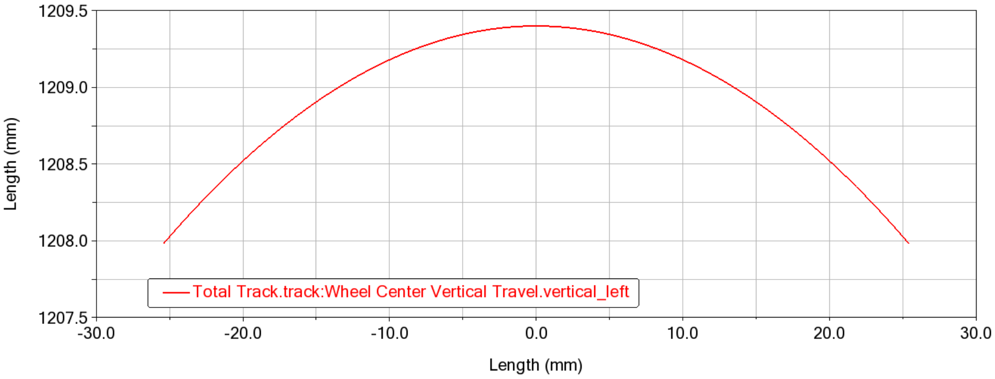
Total Track.track:Wheel Center Vertical Travel.vertical_left
Length (mm)
1209.5
1209.0
1208.5
1208.0
1207.5
-30.0
-20.0
-10.0
0.0
10.0
20.0
30.0
Length (mm)

8.3.2 Rear suspension

8.3.2.1 Parallel

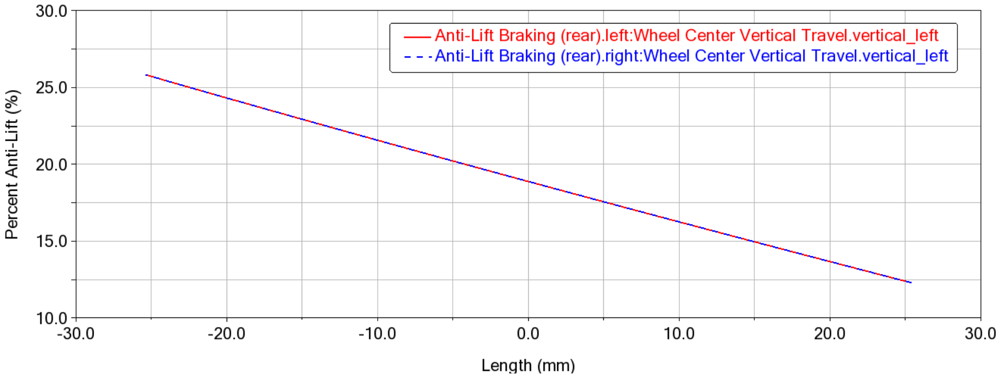

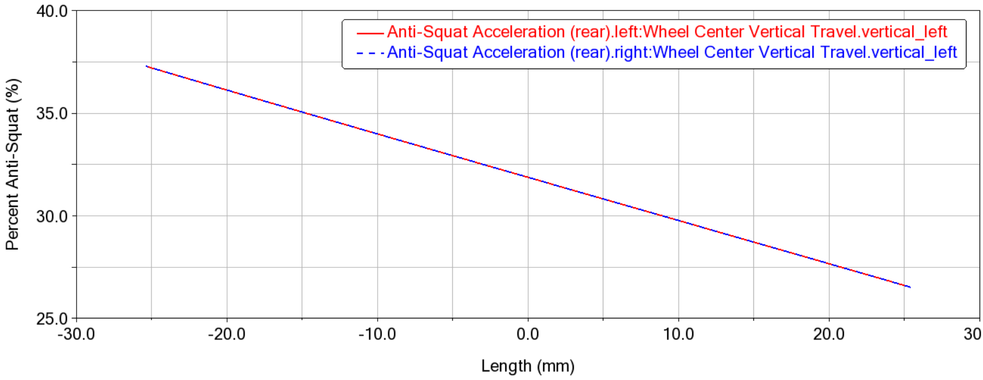

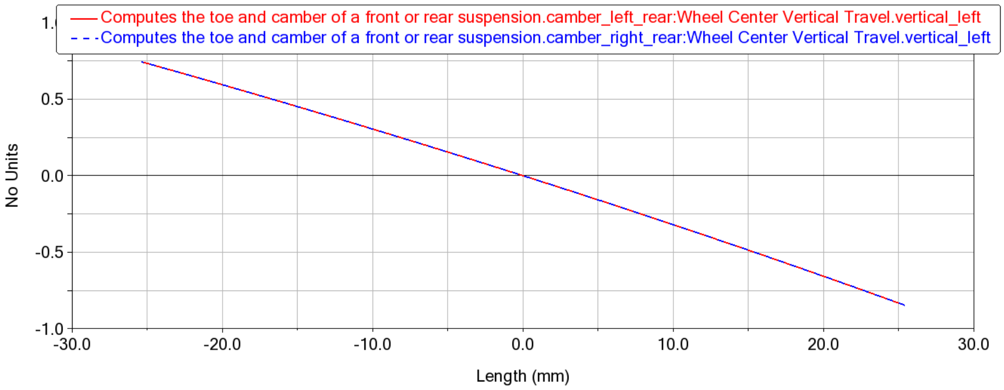

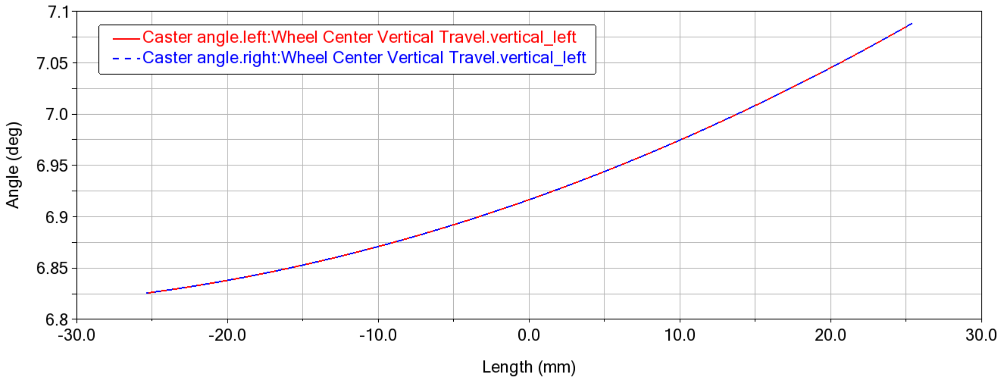

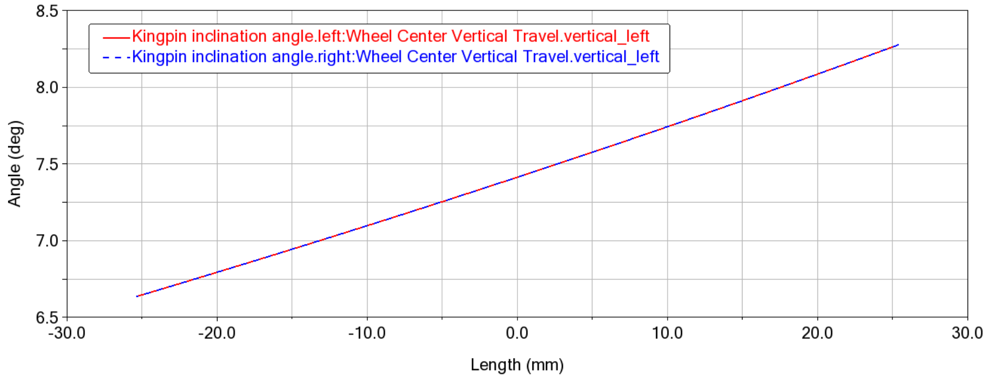
Kingpin inclination angle.left:Wheel Center Vertical Travel.vertical_left
Kingpin inclination angle.right:Wheel Center Vertical Travel.vertical_left
Angle (deg)
8.5
8.0
7.5
7.0
6.5
-30.0
-20.0
-10.0
0.0
10.0
20.0
30.0
Length (mm)

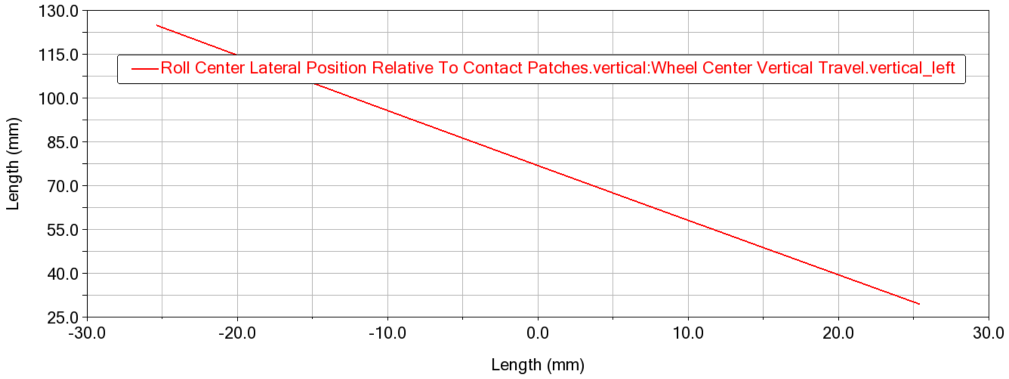
Roll Center Lateral Position Relative To Contact Patches.vertical:Wheel Center Vertical Travel.vertical_left
Length (mm)
130.0
115.0
100.0
85.0
70.0
55.0
40.0
25.0
-30.0
-20.0
-10.0
0.0
10.0
20.0
30.0
Length (mm)

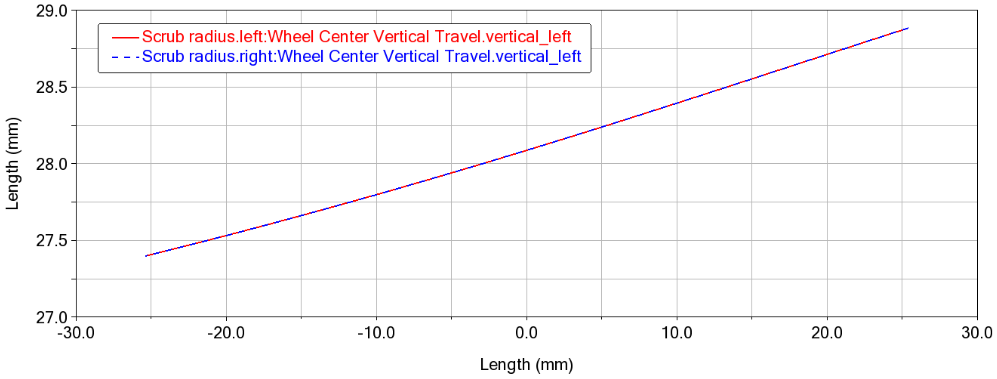
Scrub radius.left:Wheel Center Vertical Travel.vertical_left
Scrub radius.right:Wheel Center Vertical Travel.vertical_left
Length (mm)
29.0
28.5
28.0
27.5
27.0
-30.0
-20.0
-10.0
0.0
10.0
20.0
30.0
Length (mm)

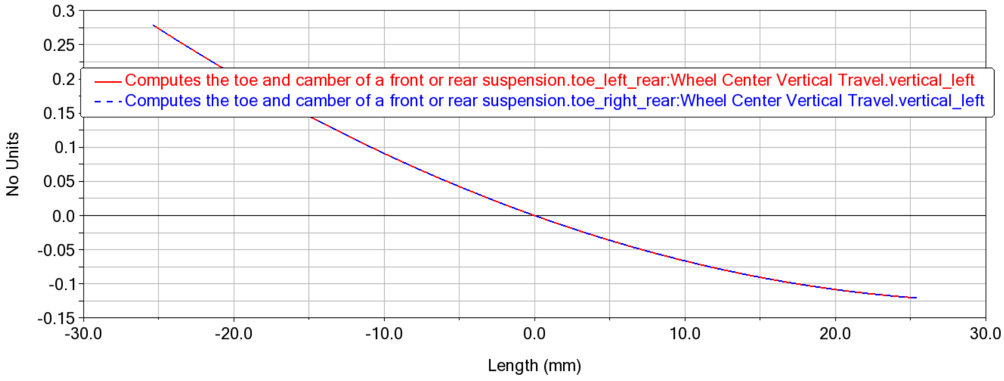
Computes the toe and camber of a front or rear suspension.toe_left_rear:Wheel Center Vertical Travel.vertical_left
Computes the toe and camber of a front or rear suspension.toe_right_rear:Wheel Center Vertical Travel.vertical_left
No Units
0.3
0.25
0.2
0.15
0.1
0.05
0.0
-0.05
-0.1
-0.15
-30.0
-20.0
-10.0
0.0
10.0
20.0
30.0
Length (mm)

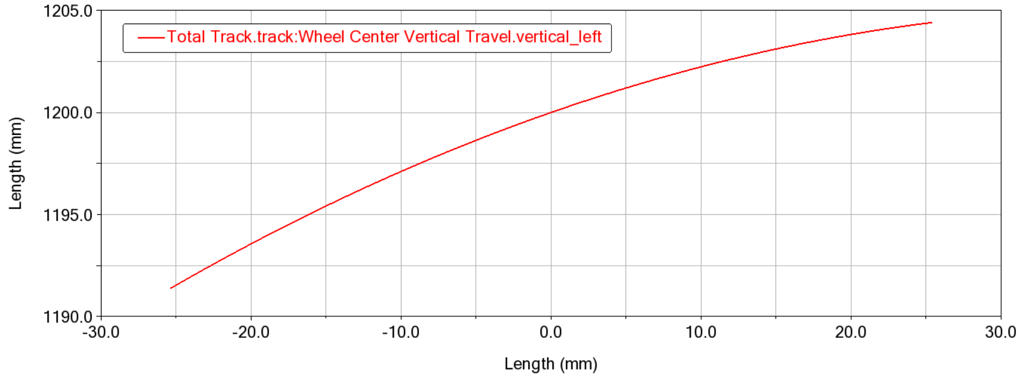

8.3.2.2 Opposite

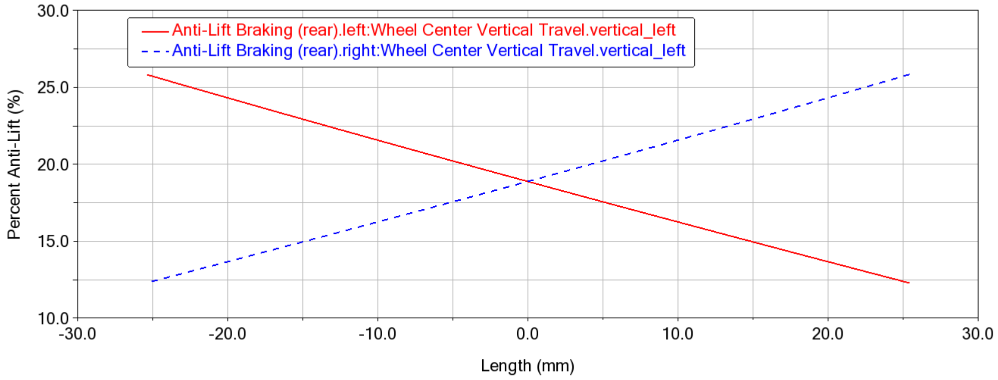

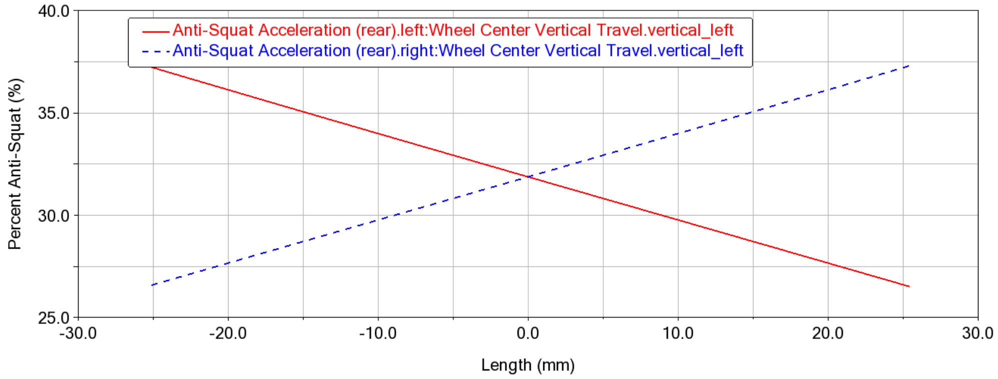

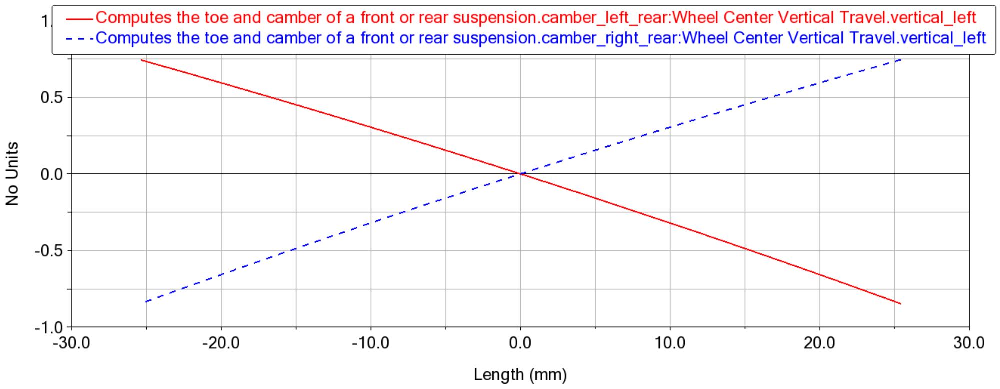

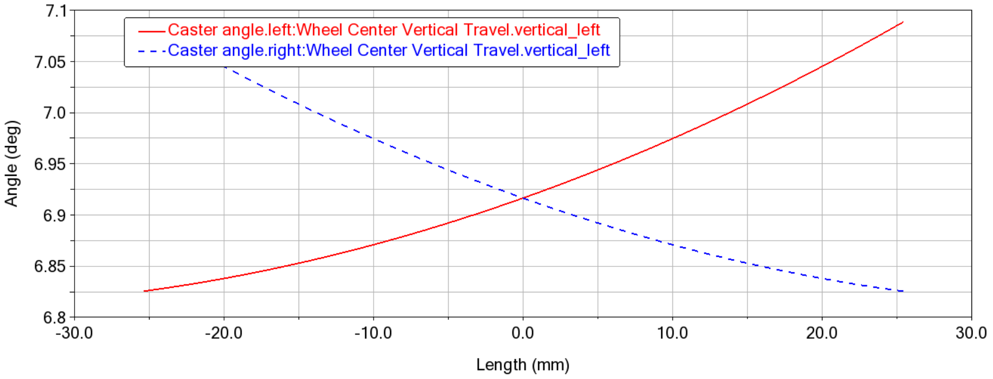
Caster angle.left:Wheel Center Vertical Travel.vertical_left
Caster angle.right:Wheel Center Vertical Travel.vertical_left
Angle (deg)
7.1
7.05
7.0
6.95
6.9
6.85
6.8
-30.0
-20.0
-10.0
0.0
10.0
20.0
30.0
Length (mm)

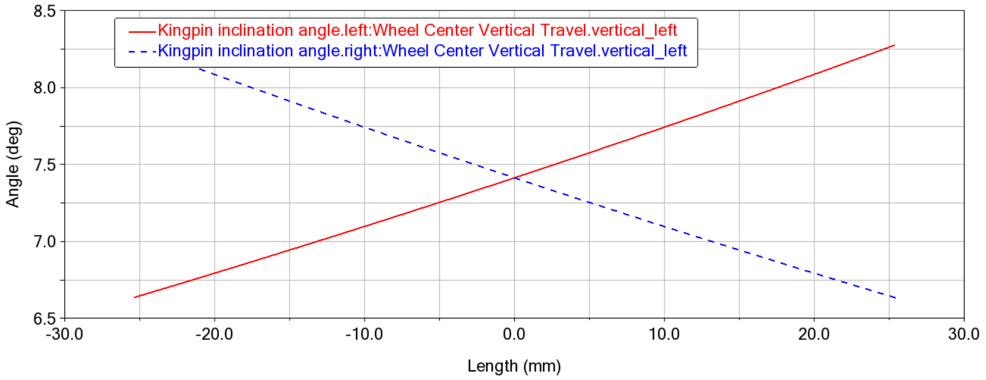
Kingpin inclination angle.left:Wheel Center Vertical Travel.vertical_left
Kingpin inclination angle.right:Wheel Center Vertical Travel.vertical_left
Angle (deg)
8.5
8.0
7.5
7.0
6.5
-30.0
-20.0
-10.0
0.0
10.0
20.0
30.0
Length (mm)

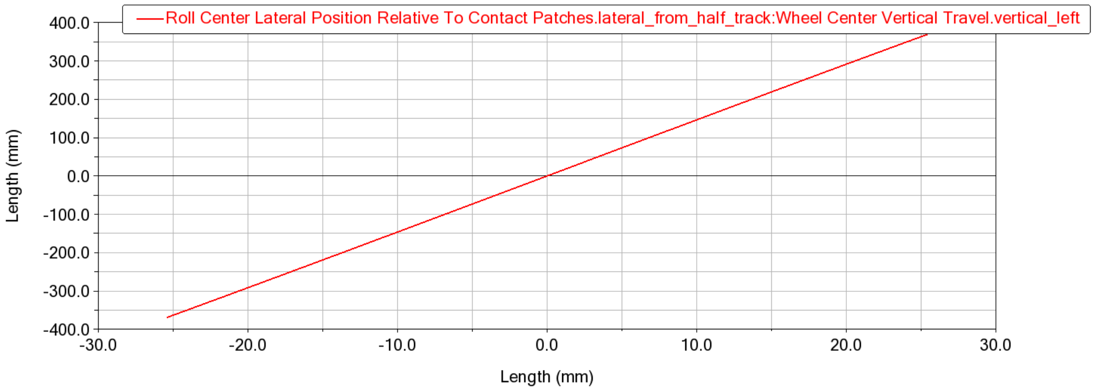
Roll Center Lateral Position Relative To Contact Patches.lateral_from_half_track:Wheel Center Vertical Travel.vertical_left
Length (mm)
400.0
300.0
200.0
100.0
0.0
-100.0
-200.0
-300.0
-400.0
-30.0
-20.0
-10.0
0.0
10.0
20.0
30.0
Length (mm)

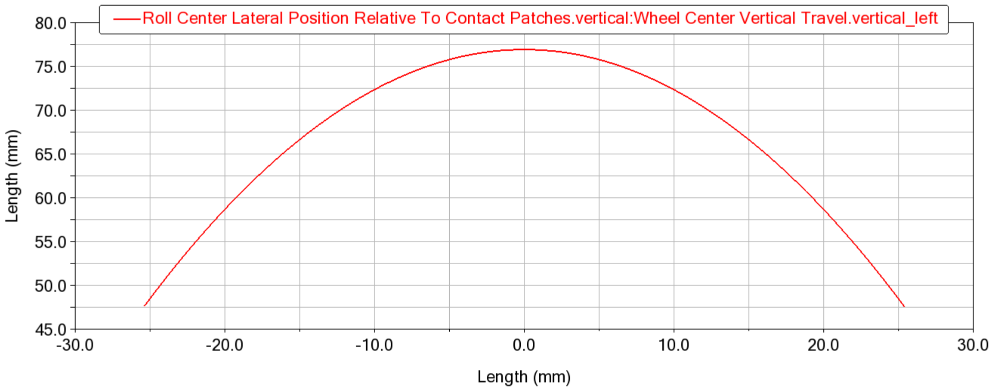
Roll Center Lateral Position Relative To Contact Patches.vertical:Wheel Center Vertical Travel.vertical_left
Length (mm)
80.0
75.0
70.0
65.0
60.0
55.0
50.0
45.0
-30.0
-20.0
-10.0
0.0
10.0
20.0
30.0
Length (mm)

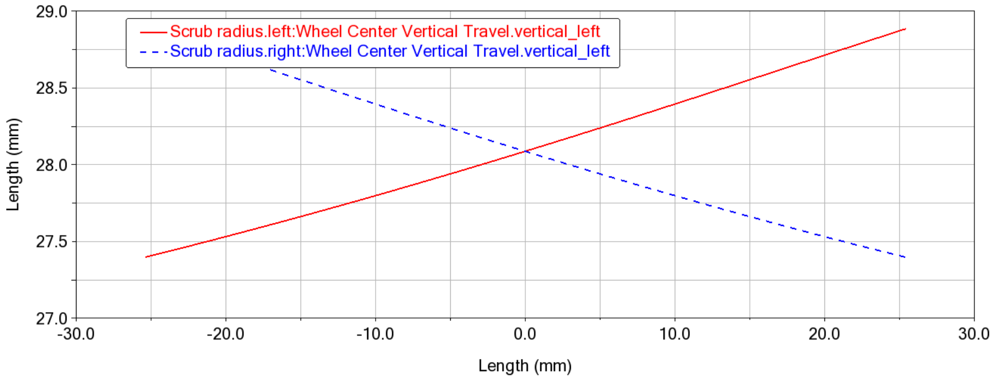

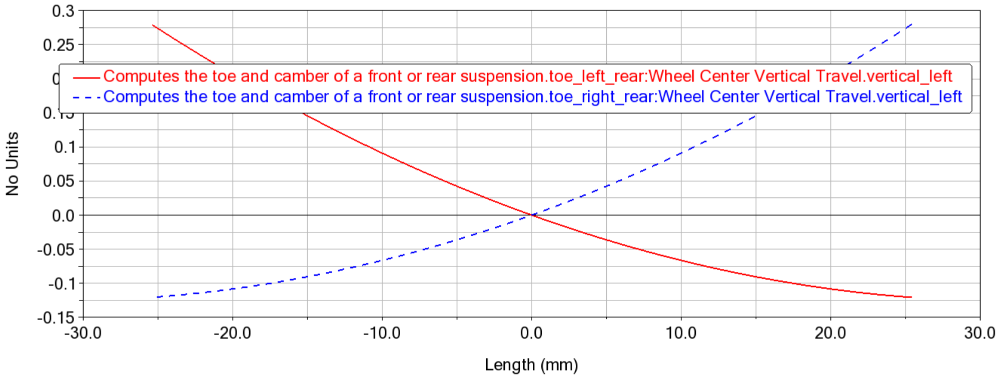

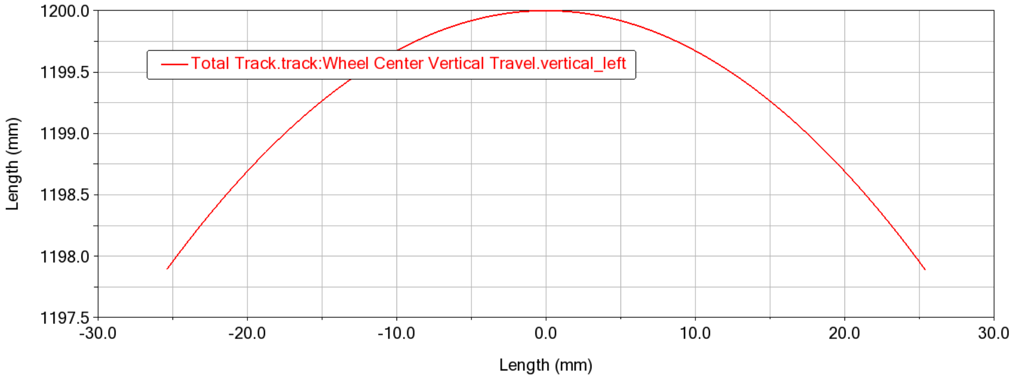

8.3.3 Comments

The modifications to the second geometry, according to the requirements specified above, produced modifications to the parameters of the two suspensions.

In both cases, the roll centre increased slightly and with it the evolution of the camber angle and toe angle.

The anti-dive is now more similar to that of the combustion vehicle geometry, while the other anti-features have the most reasonable values obtained with the second geometry.

The caster and kingpin angle have corrected values, according to the recommended ranges and according to the effects of longitudinal stability.

Due to the presence of the engine inside the wheel, it is impossible to obtain a small kingpin angle and at the same time negative scrub values for the front suspension: this requires greater skill on the part of the driver to control the vehicle. Appropriate wheel spacing could solve this problem.

A small improvement, compared to the second proposed geometry, is noticeable in the lateral displacement of the roll centre: this has been achieved by extending the lower arm towards the plane of symmetry of the vehicle, obviously worsening the evolution of the camper angle.

8.4 Dynamic behaviour

Unlike the kinematic part, the dynamic part is aimed to consider the forces generated by the elements that make up the suspension (elastic elements, tires, etc.).
Initially, the motion ratios are analysed and designed, consequently spring (stiffness and preload), shock absorber (strength-speed characteristic) and anti-roll bar (stiffness) are set.

In this paragraph, two solutions are proposed: the first one setting the spring stiffness on the basis of the designed motion ratio, while the second one propose the same spring characteristic (of the front), thus a change in the motion ratio is required to have the proper natural frequencies at the rear axle.

8.4.1 Motion ratios

The first step for the dynamic part is to understand which are the transmission ratios (so-called *motion ratios*) that involve the elastic parts of the suspension, to allow the definition of all subsequent parameters for the set-up. The two parts to be taken into consideration are the rocker and the anti-roll bar.

8.4.1.1 Rocker

Obviously, the rocker is the connecting piece between push-rod and shock-absorber, which plays a fundamental role in the "production" of the optimal stiffness at the wheel for the track and for the pilot. In fact, this piece defines the transmission ratio between the vertical movement of the wheel and the displacement of the spring element.

The value used by the team (and commonly by many others) is between 1.3 and 1.6 and takes into account two aspects: the displacement of the spring element cannot be as large as the wheel, so it is reduced; at the same time, the damper must avoid the stick-slip phenomenon, which would lead it to become a rigid element and thus worsen the behaviour of the single seater.

This transmission ratio depends both on the geometry of the rocker and on the inclination of the push-rod: as said before, it cannot be too inclined to avoid excessive stress. The rocker becomes, therefore, a corrective element of the motion ratio obtained with the sole inclination of the push-rod.

In fact, the driver can request different set-ups of the vehicle, according to his preferences, and the rocker can be one of the elements that can be modified.

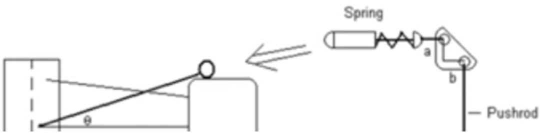

Figure 45. Second-type motion ratio simplification. (b)

The first type of motion ratio has been explained in Chapter 6, but what we generally deal with is the second type. The motion ratio can be approximated as $MR = {}^{a}/_{b} \cdot \sin(\theta)$, where a and b are the rocker sides and θ the push-rod inclination.

After setting the geometry of this element, its value can be proven by the slope of the plot wheel-to-spring displacements.

8.4.1.2 Anti-roll bar

Same goes for the anti-roll bar. Unlike the rocker, there is no optimal value that the team has considered.

It must be said that this value of motion ratio is indicative, as the bar will not be of the geometry designed on Adams Car, but a Z-bar, too difficult to be designed. The set value will refer to this bar, while with the geometry for the anti-roll bar that will actually be implemented you will look for the new motion ratio and therefore the relative torsional stiffness.

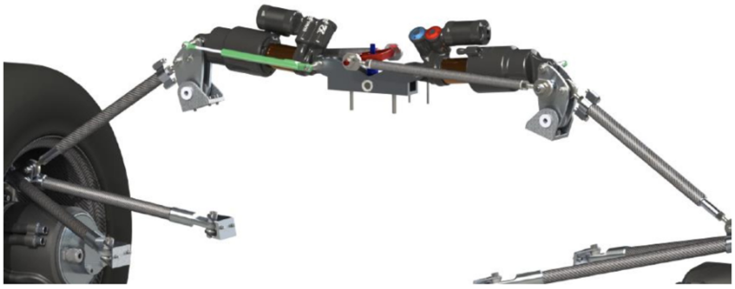

Figure 46. NTNU rear suspension layout, with the Z-type anti-roll bar.

The figure represents the layout of the rear suspension of the single seater designed and manufactured by the Norwegian University of Science and Technology (NTNU), reflecting the model of stabiliser bar that is incorporated in this axle. This model is similar to the one that will be incorporated to the UPM Racing single seater once the torsional study of the vehicle has been carried out and if it complies with the pertinent rolling limitations.

As explained in Chapter 6, the anti-roll bar intervenes to make up for the lack of vehicle roll stiffness that, with the only springs, might not be enough.

8.4.2 Stiffness

Once the motion ratios of these elastic elements have been identified, using the formulas explained in Chapter 6, it is possible to identify the stiffness required for $\mathbf{3\ Hz}$ as natural frequency of the sprung mass and, above all, a high natural frequency (between 7 and 10 Hz) for the wheel, necessary for the wheel to respond rapidly to obstacles (a kerb, for example). Also, the team decided to look for a roll gradient of **1° per each** $\boldsymbol{g}$ of lateral acceleration.

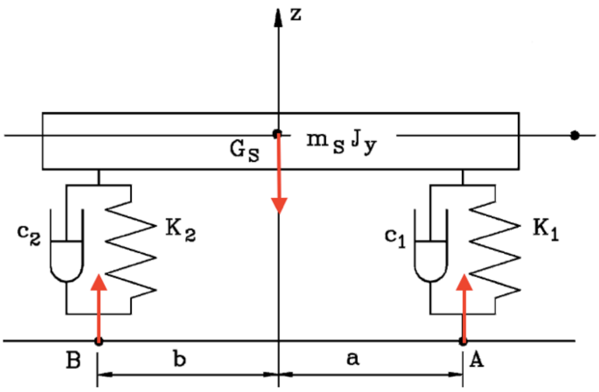

Figure 47. Static vehicle equilibrium.

Once a value has been calculated that is suitable to meet required natural frequencies and roll gradient, it is necessary to look for the suspension among those available to the team which is closest to this value

Then, while editing the suspension file in the software, you need to set the spring preload: for this reason, the equilibrium of the static forces of the vehicle is calculated. Making the equilibrium of forces, it results that the two reaction forces (the suspension preloads) are:

$$F_A = \frac{mgb}{a+b} \text{ and } F_B = \frac{mga}{a+b}.$$

At the individual wheels, these values must be divided by 2, being these equations referred to the axles: the preload at the front suspension is then $= 452\ N$, while at the rear is $= 729\ N$.

8.4.3 Damping

The shock-absorbers used in the design and assembly of the suspension in competition single seaters are adjustable both in their resistance to compression and extension. Their use has become widespread in this type of vehicles as they prevent the oscillation of the car, while allowing greater control and feeling of comfort.

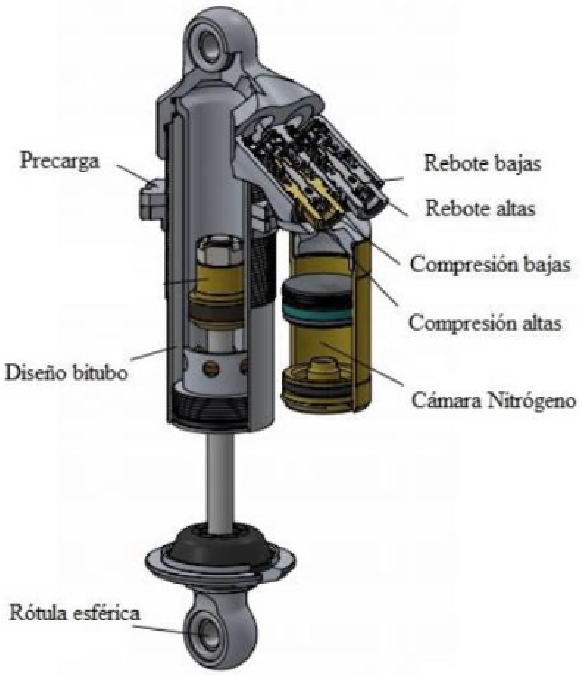

Figure 48. Internal view of the Ohlins TTX25 mk2 damper.

In the case of competition vehicles, the most commonly used type of shock absorber is hydraulic: the UPM Racing electric single seater will implement the use of ***Öhlins TTX25 mk2*** shock-absorbers on all four wheels, especially used in Formula Student competitions. This is due to the fact that they are sensitive to high speeds and lower displacements, characteristics necessary in this type of events. This hydraulic shock-absorber has a twin-tube design formed by four adjustable ways, which correspond to the different modes of action depending on whether it is in a process of compression or expansion, and whether the displacement is made at high or low speed. It also consists of a concentric spring and a secondary oil chamber.

Technical specifications:

- Total length: $200\,mm$ (from centre to centre of spherical plain bearings, fully extended);
- Stroke: 57 or 90 mm;
- Weight:
  - 394 g without spring (57 mm stroke);
  - 446 g without spring (90 mm stroke).
- Width of the kneecap: 8 mm;
- Inner diameter of the ball-joint: 8 mm;
- Outer diameter of the ball-joint: 15 mm.

The characteristic of the shock-absorber that will be implemented in the model will be chosen from the several tests that were carried out by the team, under different conditions.

8.4.4 Analysis

8.4.4.1 Solution 1

As said before, the first solution consists in setting the correct spring stiffnesses once the motion ratios have been fixed; by following the procedure explained in Chapter 6, this solution is a natural consequence.

The motion ratios that have been chosen in this case are 1.34 at the front axle and 1.33 at the rear, thus the respective stiffnesses are $44.659\,N/mm$ and $57.036\,N/mm$. As explained before, these values cannot be put directly because the list of available springs is given. For this reason, the chosen values are $43.705\,N/mm$ and $52.292\,N/mm$, that allow anyway to have the sprung natural frequencies of $2.95\,Hz$ and $3.27\,Hz$, lying in the desired range. Notice that these two values already consider the ***additional 10%*** required to recover the delay of the oscillations due to obstacles and/or the steering input (that propagates to the rear axle too).

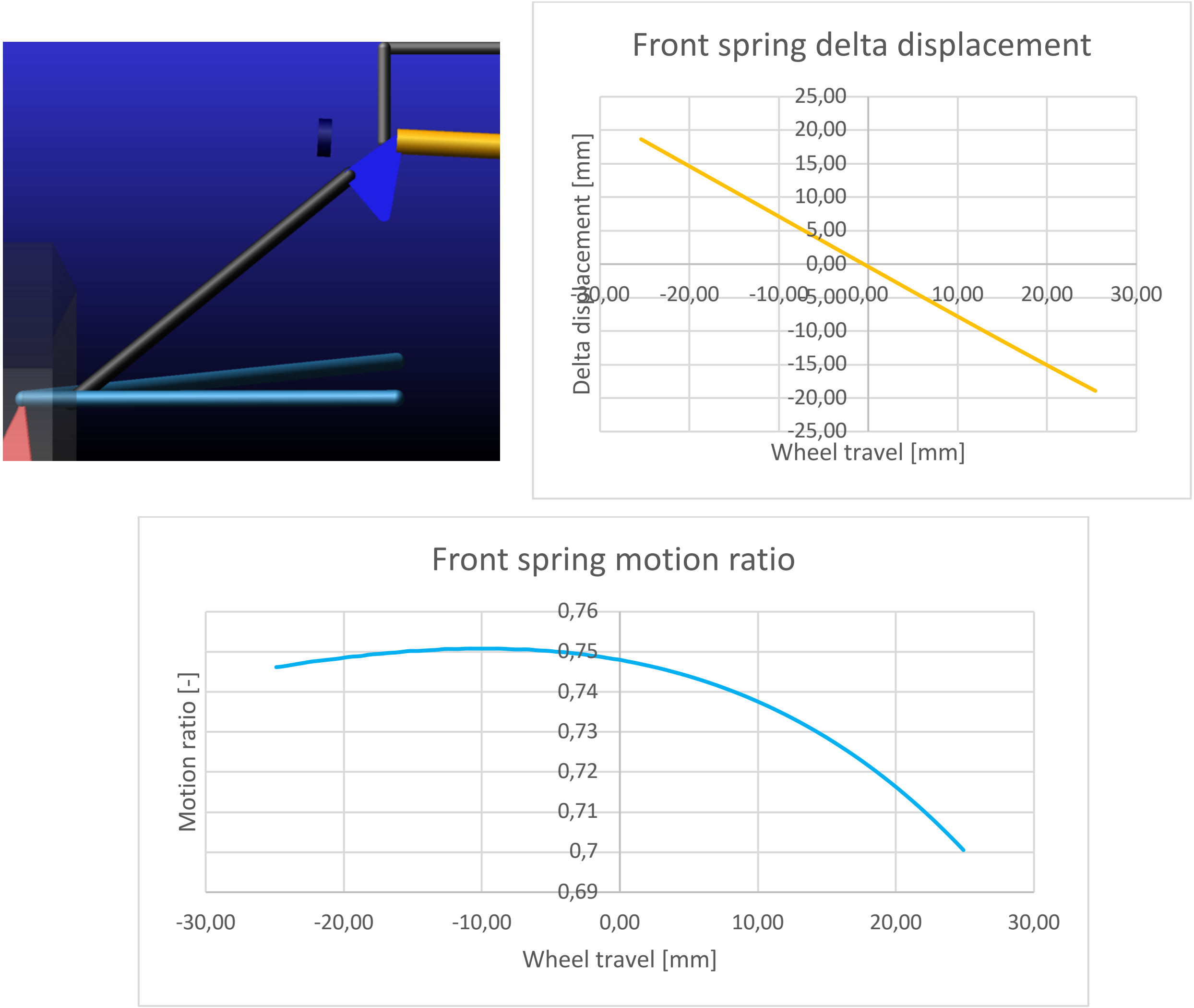

Figure 49. (a) Front rocker and push-rod geometry. (b) Front spring delta displacement. (c) Front motion ratio variation.

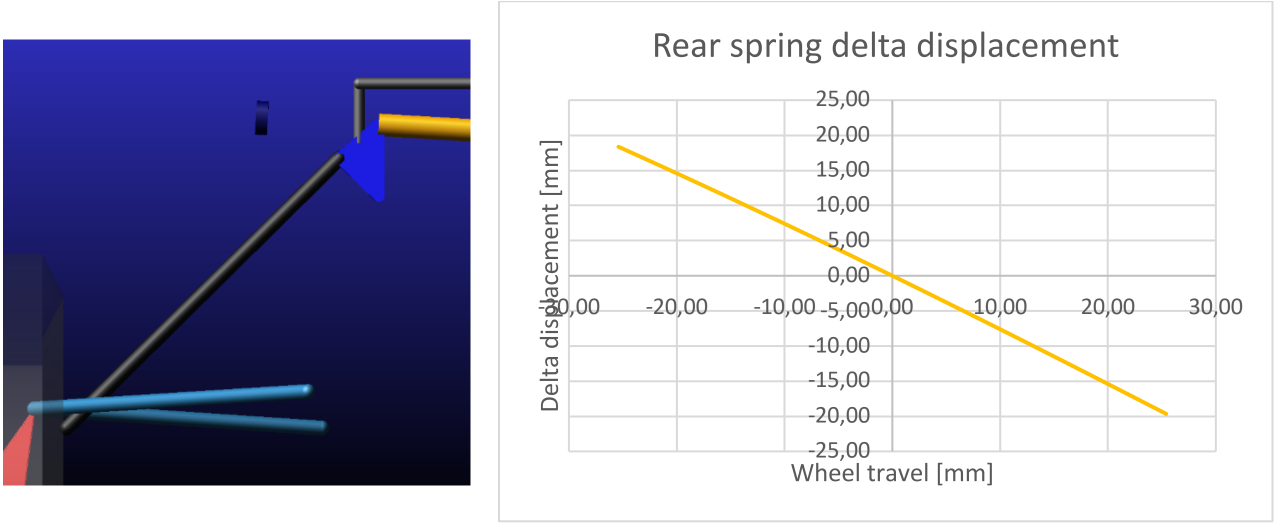

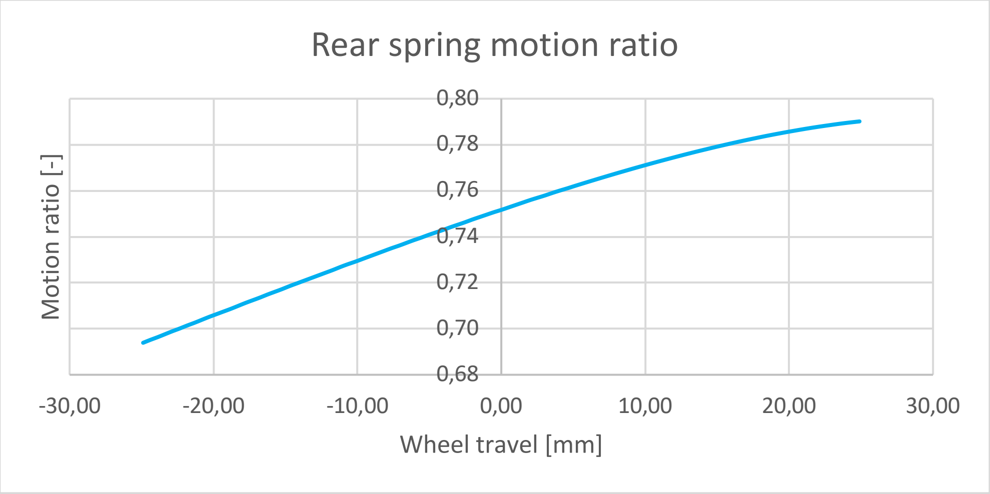

Figure 50. (a) Rear rocker and push-rod geometry. (b) Rear spring delta displacement. (c) Rear motion ratio variation.

To then obtain the preloads, it is necessary to put the values of the previous computations in the suspension settings: the software will evaluate the installed length on the basis of the desired preload, considering that the free-lengths are 126 mm for the front and 131.3 mm for the rear suspension

Due to the fact that a certain value of the roll stiffness is required, the stiffnesses of the anti-roll bars is computed as a consequence. Even though their value is not so large, they are respectively defined as 180 $\frac{N}{mm \cdot deg}$ at the front and 57 $\frac{N}{mm \cdot deg}$.

By looking at the following plot, it is noticeable that with the previous calculation, aimed at getting 1° per g of lateral acceleration, are more or less correct. Keep in mind that this is not an exact procedure, but a first good approximation.

8.4.4.2 Solution 2

In the second case, instead, is to change the motion ratio once the spring value is set. The value chosen for both springs is that of the front axle (43.705 N/mm) and so, to comply with the requirement of sprung natural frequency $> 3\ Hz$, the motion ratio at the rear must be changed: its new value is 1.5 approximately.

Again, the procedure allows to roughly obtain the desired roll gradient.

8.5 Analysis of forces

The maximum power delivered to the wheel, together with the corresponding reduction ratio introduced by the planetary system of each of them (that is 13.176), will allow estimating the maximum force that can be developed on the wheel. With this, the necessary calculations can be made to obtain the maximum available adherence value, and check whether this effort is the one that limits the traction of the vehicle.

The "load notebook" is then drawn up for the different suspension elements for four types of behaviour: ***traction***, ***braking***, ***lateral force*** + ***acceleration*** and ***lateral force*** + ***braking***. These types of situations are analysed due to the need to evaluate the forces and tensions supported by each of the elements of the geometry in some of the main events of the competition:

- The traction test limited by the adhesion imposed by the motor on the wheel, with the peak of maximum torque, is a record of the *Acceleration* dynamic test;
- The braking test with maximum grip makes it possible to evaluate the forces to which the whole suspension is subjected in the *Brake Test*;
- Also, lateral acceleration test is performed, aimed at evaluating the loads acting during a curve at constant speed;
- The combined lateral force and acceleration or braking tests are particular of tests such as *Endurance* or *Autocross*.

The necessary calculations will be made to estimate the vertical force supported by each wheel, taking into account the corresponding longitudinal and lateral load transfer.

Likewise, from these values, the longitudinal and lateral force in each wheel will be obtained, and the most critical one will be evaluated. The load notebook will be evaluated based on it, obtaining the components F_x, F_y, F_z and F_m, the latter as the value of the composition of efforts of the previous three.

8.5.1 Braking

The braking phase is the first of the most critical. In this case, a longitudinal deceleration of 1.75 g is considered, being it a reasonable value for vehicles with this mass.

$$m \cdot a = F_{x,total} = 4978.6\ N$$

To correctly divide the forces between tires, a $70/30$ braking split is considered to compute the longitudinal forces at tire level:

$$F_{x,front} = 0.7 \cdot F_{x,total} = 3485\ N \rightarrow F_{x,front\,wheel} = 1742.5\ N$$

$$F_{x,rear} = 0.3 \cdot F_{x,total} = 1493.6\ N \rightarrow F_{x,rear\,wheel} = 746.8\ N$$

Then, it is necessary to evaluate the transfer load, after computing the static weight acting on each axle:

$$F_{z,front} = m_{front} \cdot g = 140\ kg \cdot 9.81\ {}^{m}\!/_{s^2} = 1373.4\ N$$

$$F_{z,rear} = m_{front} \cdot g = 150\ kg \cdot 9.81\ {}^{m}\!/_{s^2} = 1471.5\ N$$

$$\Delta F_{z,front} = -\frac{m \cdot a \cdot h_{CG}}{l} = 1013.2\ N$$

$$\Delta F_{z,rear} = \frac{m \cdot a \cdot h_{CG}}{l} = -1013.2\ N$$

Therefore, the loads on the wheels are:

$$F_{z,front,left} = F_{z,front,right} = \frac{\left(F_{z,front} + \Delta F_{z,front}\right)}{2} = \frac{(1373.4\ N + 1013.2\ N)}{2} = 1242.4\ N$$

$$F_{z,rear,left} = F_{z,rear,right} = \frac{\left(F_{z,rear} + \Delta F_{z,rear}\right)}{2} = \frac{(1471.5\ N - 1013.2\ N)}{2} = 180.1\ N$$

8.5.2 Lateral acceleration

In this section, it is also necessary to calculate the lateral load transfer from the right wheel to the left wheel, motivated by the action of the centrifugal force applied in the centre of gravity when taking a curve to the right. In this way, the left wheel is taken as the outer one, being the right wheel the one that describes the curve of smaller radius.

A lateral acceleration of 1.75 g is considered. As in the previous paragraph, transfer load and lateral forces are computed.

The static load acting on each wheel is given by:

$$F_{z,front} = m_{front} \cdot g = 140\ kg \cdot 9.81\ {}^{m}/_{s^2} = 1373.4\ N$$

$$F_{z,rear} = m_{front} \cdot g = 150\ kg \cdot 9.81\ {}^{m}/_{s^2} = 1471.5\ N$$

While the lateral load transfer is simply an equilibrium of forces:

$$\Delta F_{z,lat} = \frac{m_{total} \cdot a_{lat} \cdot h_{CG}}{t} = \frac{\left(290\ kg \cdot 1.75 \cdot 9.81\ {}^{m}/_{s^2} \cdot 321.35\ mm\right)}{1200\ mm} = 1333.2\ N$$

As an approximation, it is possible to compute the load transfer on each wheel, depending on the values of spring stiffness previously assigned:

$$\Delta F_{z,lat,front,left} \approx \Delta F_{z,lat} \cdot \left(\frac{k_{front}}{k_{front} + k_{rear}}\right) = 607\ N$$

$$\Delta F_{z,lat,front,right} \approx \Delta F_{z,lat} \cdot \left(\frac{k_{front}}{k_{front} + k_{rear}}\right) = -607\ N$$

$$\Delta F_{z,lat,rear,left} \approx \Delta F_{z,lat} \cdot \left(\frac{k_{rear}}{k_{front} + k_{rear}}\right) = 726.2\ N$$

$$\Delta F_{z,lat,rear,right} \approx \Delta F_{z,lat} \cdot \left(\frac{k_{rear}}{k_{front} + k_{rear}}\right) = -726.2\ N$$

Therefore, the loads on the wheels are:

$$F_{z,front,left} = F_{z,front,left} + \Delta F_{z,lat,front,left} = \frac{1373.4}{2} + 607 = 1293.7\ N$$

$$F_{z,front,right} = F_{z,front,right} + \Delta F_{z,lat,front,right} = \frac{1373.4}{2} - 607 = 79.7\ N$$

$$F_{z,rear,left} = F_{z,rear,right} + \Delta F_{z,lat,rear,right} = \frac{1471.5}{2} + 726.2 = 1462\ N$$

$$F_{z,rear,right} = F_{z,rear,right} + \Delta F_{z,lat,rear,right} = \frac{1471.5}{2} - 726.2 = 9.55\ N$$

Finally, once computed the loads on each wheel, lateral force is calculated:

$$m \cdot a_{lat} = F_{y,total} = 4978.6\ N$$

The lateral forces generated on the wheels can be obtained again with an approximation:

$$F_{y,front,left} = F_{y,total} \cdot \left(\frac{F_{z,front,left}}{F_{z,total}}\right) = 2264\ N$$

$$F_{y,front,right} = F_{y,total} \cdot \left(\frac{F_{z,front,right}}{F_{z,total}}\right) = 139.5\ N$$

$$F_{y,rear,left} = F_{y,total} \cdot \left(\frac{F_{z,rear,left}}{F_{z,total}}\right) = 2558.5\ N$$

$$F_{y,rear,right} = F_{y,total} \cdot \left(\frac{F_{z,rear,right}}{F_{z,total}}\right) = 16.7\ N$$

8.5.3 Accelerating in a curve

The longitudinal and the lateral accelerations considered are of 1 g and 1.1 g respectively. All the calculations are clearly the same as in the previous paragraphs.

Therefore, longitudinal force has to be:

$$m \cdot a = F_{x,total} = 2844.9\ N$$

The traction split considered for this analysis is a common 30/70, to correctly divide the longitudinal force between all wheels:

$$F_{x,front} = 0.3 \cdot F_{x,total} = 853.5\ N \rightarrow F_{x,front\ wheel} = 426.7\ N$$

$$F_{x,rear} = 0.7 \cdot F_{x,total} = 1991.4\ N \rightarrow F_{x,rear\ wheel} = 995.7\ N$$

Then, the transfer load is given by:

$$F_{z,front} = m_{front} \cdot g = 140\ kg \cdot 9.81\ {}^{m}/_{s^2} = 1373.4\ N$$

$$F_{z,rear} = m_{front} \cdot g = 150\ kg \cdot 9.81\ {}^{m}/_{s^2} = 1471.5\ N$$

$$\Delta F_{z,front} = \frac{m \cdot a \cdot h_{CG}}{l} = -578.8\ N$$

$$\Delta F_{z,rear} = -\frac{m \cdot a \cdot h_{CG}}{l} = 578.8\ N$$

Therefore, the loads on the wheels are:

$$F_{z,front,left} = F_{z,front,right} = \frac{\left(F_{z,front} + \Delta F_{z,front}\right)}{2} = \frac{(1373.4\ N - 578.8\ N)}{2} = 397.3\ N$$

$$F_{z,rear,left} = F_{z,rear,right} = \frac{\left(F_{z,rear} + \Delta F_{z,rear}\right)}{2} = \frac{(1471.5\ N + 578.8\ N)}{2} = 1025.2\ N$$

In the lateral direction, the transfer load is given again by:

$$\Delta F_{z,lat} = \frac{m_{total} \cdot a_{lat} \cdot h_{CG}}{t} = \frac{\left(290\ kg \cdot 1.1 \cdot 9.81\ {}^{m}/_{s^2} \cdot 321.35\ mm\right)}{1200\ mm} = 838\ N$$

As an approximation:

$$\Delta F_{z,lat,front,left} \approx \Delta F_{z,lat} \cdot \left(\frac{k_{front}}{k_{front} + k_{rear}}\right) = 381.5\ N$$

$$\Delta F_{z,lat,front,right} \approx \Delta F_{z,lat} \cdot \left(\frac{k_{front}}{k_{front} + k_{rear}}\right) = -381.5\ N$$

$$\Delta F_{z,lat,rear,left} \approx \Delta F_{z,lat} \cdot \left(\frac{k_{rear}}{k_{front} + k_{rear}}\right) = 456.5\ N$$

$$\Delta F_{z,lat,rear,right} \approx \Delta F_{z,lat} \cdot \left(\frac{k_{rear}}{k_{front} + k_{rear}}\right) = -456.5\ N$$

From the load transfers, it is possible to estimate the vertical force on each wheel, as well as the longitudinal and lateral stress that each one suffers, and there may be a lifting effect on some of them.

$$F_{z,front,left} = \frac{\left(F_{z,front} + \Delta F_{z,front}\right)}{2} + \Delta F_{z,lat,front,left} = \frac{(1373.4\ N - 468.3\ N)}{2} + 381.5$$
$$= 778.8\ N$$

$$F_{z,front,right} = \frac{\left(F_{z,front} + \Delta F_{z,front}\right)}{2} + \Delta F_{z,lat,front,right} = \frac{(1373.4\ N - 468.3\ N)}{2} - 381.5$$
$$= 15.8\ N$$

$$F_{z,rear,left} = \frac{\left(F_{z,rear} + \Delta F_{z,rear}\right)}{2} + \Delta F_{z,lat,rear,right} = \frac{(1471.5\ N + 468.3\ N)}{2} + 456.5$$
$$= 1481.7\ N$$

$$F_{z,rear,right} = \frac{\left(F_{z,rear} + \Delta F_{z,rear}\right)}{2} + \Delta F_{z,lat,rear,right} = \frac{(1471.5\ N + 468.3\ N)}{2} - 456.5$$
$$= 568.7\ N$$

The total lateral force is computed:

$$m \cdot a_{lat} = F_{y,total} = 3129.4\ N$$

And so, lateral forces generated on the wheels are:

$$F_{y,front,left} = F_{y,total} \cdot \left(\frac{F_{z,front,left}}{F_{z,total}}\right) = 856.7\ N$$

$$F_{y,front,right} = F_{y,total} \cdot \left(\frac{F_{z,front,right}}{F_{z,total}}\right) = 17.4\ N$$

$$F_{y,rear,left} = F_{y,total} \cdot \left(\frac{F_{z,rear,left}}{F_{z,total}}\right) = 1629.9\ N$$

$$F_{y,rear,right} = F_{y,total} \cdot \left(\frac{F_{z,rear,right}}{F_{z,total}}\right) = 625.6\ N$$

8.5.4 Braking in a curve

The longitudinal and the lateral accelerations considered in this case are $-1\ g$ and $1\ g$ respectively.

$$m \cdot a = F_{x,total} = 4267.4\ N$$

Again, braking split is a 70/30:

$$F_{x,front} = 0.7 \cdot F_{x,total} = 2987.1\ N \rightarrow F_{x,front\ wheel} = 1493.6\ N$$
$$F_{x,rear} = 0.3 \cdot F_{x,total} = 1280.2\ N \rightarrow F_{x,rear\ wheel} = 640.1\ N$$

Static load, as always:

$$F_{z,front} = m_{front} \cdot g = 140\ kg \cdot 9.81\ {}^{m}/_{s^2} = 1373.4\ N$$
$$F_{z,rear} = m_{front} \cdot g = 150\ kg \cdot 9.81\ {}^{m}/_{s^2} = 1471.5\ N$$

And then longitudinal transfer load:

$$\Delta F_{z,front} = \frac{m \cdot a \cdot h_{CG}}{l} = 578.8\ N$$
$$\Delta F_{z,rear} = -\frac{m \cdot a \cdot h_{CG}}{l} = -578.8\ N$$

Therefore, the vertical loads, due to longitudinal load transfer, acting on the wheels are:

$$F_{z,front,left} = F_{z,front,right} = \frac{\left(F_{z,front} + \Delta F_{z,front}\right)}{2} = \frac{(1373.4\ N + 578.8\ N)}{2} = 976.1\ N$$
$$F_{z,rear,left} = F_{z,rear,right} = \frac{\left(F_{z,rear} + \Delta F_{z,rear}\right)}{2} = \frac{(1471.5\ N - 578.8\ N)}{2} = 446.4\ N$$

The lateral load transfer is evaluated:

$$\Delta F_{z,lat} = \frac{m_{total} \cdot a_{lat} \cdot h_{CG}}{t} = \frac{\left(290\ kg \cdot 9.81\ {}^{m}/_{s^2} \cdot 321.35\ mm\right)}{1200\ mm} = 761.8\ N$$

As an approximation, on each wheel there is the following lateral load transfers:

$$\Delta F_{z,lat,front,left} \approx \Delta F_{z,lat} \cdot \left(\frac{k_{front}}{k_{front} + k_{rear}}\right) = 346.8\ N$$

$$\Delta F_{z,lat,front,right} \approx \Delta F_{z,lat} \cdot \left(\frac{k_{front}}{k_{front} + k_{rear}}\right) = -346.8\ N$$

$$\Delta F_{z,lat,rear,left} \approx \Delta F_{z,lat} \cdot \left(\frac{k_{rear}}{k_{front} + k_{rear}}\right) = 415\ N$$

$$\Delta F_{z,lat,rear,right} \approx \Delta F_{z,lat} \cdot \left(\frac{k_{rear}}{k_{front} + k_{rear}}\right) = -415\ N$$

Therefore, the overall vertical loads acting on the wheels are:

$$F_{z,front,left} = \frac{\left(F_{z,front} + \Delta F_{z,front}\right)}{2} + \Delta F_{z,lat,front,left} = \frac{(1373.4\ N + 578.8\ N)}{2} + 346.8$$
$$= 1322.9\ \ N$$

$$F_{z,front,right} = \frac{\left(F_{z,front} + \Delta F_{z,front}\right)}{2} + \Delta F_{z,lat,front,right} = \frac{(1373.4\ N + 578.8\ N)}{2} - 346.8$$
$$= 629.3\ N$$

$$F_{z,rear,left} = \frac{\left(F_{z,rear} + \Delta F_{z,rear}\right)}{2} + \Delta F_{z,lat,rear,right} = \frac{(1471.5\ N - 578.8\ N)}{2} + 415 = 861\ N$$

$$F_{z,rear,right} = \frac{\left(F_{z,rear} + \Delta F_{z,rear}\right)}{2} + \Delta F_{z,lat,rear,right} = \frac{(1471.5\ N - 578.8\ N)}{2} - 415 = 31.4\ N$$

Lateral force:

$$m \cdot a_{lat} = F_{y,total} = 2844.9\ N$$

The lateral forces generated on the wheels are:

$$F_{y,front,left} = F_{y,total} \cdot \left(\frac{F_{z,front,left}}{F_{z,total}}\right) = 1322.9\ N$$

$$F_{y,front,right} = F_{y,total} \cdot \left(\frac{F_{z,front,right}}{F_{z,total}}\right) = 629.3 N$$

$$F_{y,rear,left} = F_{y,total} \cdot \left(\frac{F_{z,rear,left}}{F_{z,total}}\right) = 2210.4\ N$$

$$F_{y,rear,right} = F_{y,total} \cdot \left(\frac{F_{z,rear,right}}{F_{z,total}}\right) = 31.4\ N$$

8.5.5 Forces on components

Once the different conditions are analysed, it is necessary to evaluate which of the conditions, which wheel, is the worst, to evaluate the load acting on the components. This computation is made directly by the software, given the worst condition as input.

As it can be deduced: in the braking scenario, the front wheels are equally loaded; in the lateral acceleration and combined acceleration-cornering conditions, the most critical is the rear left since the curvature is towards the right and the load transfer increase on the left side and on the rear due to the acceleration; in the combined braking-cornering, on the contrary, the most critical is the front left, being loaded the most.

In the following tables, the load on the suspension joints are reported.

BRAKING SCENARIO

Joint	F_x	F_y	F_z	F_m
UCA-to-frame	826.55	1274.67	202.15	1532.59033
UCA-to-knuckle	−816.23	336.92	985.05	1322.90211
LCA-to-frame	−2549.71	104.67	−218.96	2561.23415
LCA-to-knuckle	−2549.71	104.67	−225.12	2561.76812
Pushrod-to-rocker	−10.33	−1611.58	−1184.01	1999.79411
Pushrod-to-UCA	−10.33	−1611.58	−1185.23	2000.51667
Rocker-to-frame	−9.41	−124.62	−1223.53	1229.89607
Tierod-to-frame	−9.01	238.56	−1.34	238.733846
Tierod-to-knuckle	9.01	−238.56	12.69	239.067124

PURE CORNERING SCENARIO

Joint	F_x	F_y	F_z	F_m
UCA-to-frame	−70.02	−121.12	404	427.538133
UCA-to-knuckle	39.12	2119.93	1455.23	2571.63915
LCA-to-frame	0.26	3495.19	67.11	3495.83423
LCA-to-knuckle	0.26	3495.19	61.72	3495.73491
Pushrod-to-rocker	30.9	−1998.8	−1856.08	2727.85432
Pushrod-to-UCA	30.9	−1998.8	−1857.36	2728.72542
Rocker-to-frame	9.24	70.84	−1967.55	1968.84654
Tierod-to-frame	23.04	888.68	−32.27	889.564127
Tierod-to-knuckle	−23.04	−888.68	42.54	889.995863

COMBINED ACCELERATION-CORNERING SCENARIO

Joint	F_x	F_y	F_z	F_m
UCA-to-frame	438.3	65.7	309.79	540.733968
UCA-to-knuckle	−464.94	1787.79	1439.41	2341.85043
LCA-to-frame	488.23	2190.63	33.27	2244.62363
LCA-to-knuckle	488.23	2190.63	27.87	2244.55008
Pushrod-to-rocker	26.64	−1853.5	−1746.05	2546.53933
Pushrod-to-UCA	26.64	−1853.5	−1747.33	2547.41714
Rocker-to-frame	6.74	77.1	1852.62	1854.23588
Tierod-to-frame	−9.01	238.56	−1.34	238.733846
Tierod-to-knuckle	9.01	−238.56	12.69	239.067124

COMBINED BRAKING-CORNERING SCENARIO

Joint	F_x	F_y	F_z	F_m
UCA-to-frame	677.59	816.52	215.58	1082.73166
UCA-to-knuckle	−662.01	1018.77	1085.09	1628.97816
LCA-to-frame	−2147.97	2325.57	−204.89	3172.38567
LCA-to-knuckle	−2147.97	2325.57	−211.05	3172.78947
Pushrod-to-rocker	−15.58	−1835.28	−1297.44	2247.63119
Pushrod-to-UCA	−15.58	−1835.28	−1298.65	2248.32988
Rocker-to-frame	−14.98	−135.18	−1392.14	1398.76796
Tierod-to-frame	0.86	23.71	4.13	24.0823711
Tierod-to-knuckle	0.86	−23.71	7.22	24.7998407

It can be seen that the greatest stresses are achieved in the coupling of the lower arm, especially in the y-direction (axle direction), as a result of lateral load transfer. In general, most of the maximum load values occur as a result of the acceleration curve process, as the vertical load carried by each wheel is greater than in the rest of the tests.

9. CONCLUSIONS

The design and conception of the final geometry of the rear suspension model of a single seater vehicle requires the acquisition of a series of technical skills necessary in the world of automotive, and more specifically, in the world of competition. To do this, it is necessary to start from a preconceived scheme of vehicle skeleton, able to bring together the main components of the car and reference planes and to delimit areas of the monocoque for each branch of design.

Moreover, this project is not understood as an individual purpose, but is managed in such a way that forces can be joined with the rest of the UPM Racing division to reach the commitment to design and manufacture a vehicle with the best possible kinematic and dynamic performance, and that is capable of performing the different events of the Formula Student competition.

Under this assumption, it is important to highlight the importance of intercommunication between all team members. This is because some requirements in three-dimensional design are strictly related, especially the planes and distances between them and between some points.

Many improvements of this project can be made, starting from reducing the centre of gravity height. This led to the major problems of overestimating the spring elastic constants and, furthermore, the acceleration capabilities of the vehicle, that are quite low, compared to other race vehicles. Then, it is necessary to evaluate if the suspension hardpoints are correct for the frame structure, integrity and stress levels, even though its structure will be produced on the basis of the optimal suspension geometries.

The fact of having a software such as ADAMS/Car makes it possible to evaluate the different kinematic parameters of the vehicle, as well as the evolution and state of loads that act on some of the anchors of the geometry. Having a simulator with this multifunctional analysis capability is a competitive advantage in terms of the design and integration of the different subsystems constituting the vehicle, as it is a relatively simple tool that allows conclusive data to be obtained on real tests.

One of the main advantages of using ADAMS/Car is the possibility of providing a simpler and more intuitive working environment than other commercial software, with a post-processing screen that shows graphic representations that make it easier to analyse the model in the tests. This is why ADAMS/Car was chosen, which also offers a learning platform on its website especially oriented to the design of vehicle models for students belonging to FSAE teams. another of the main advantages of ADAMS compared to other similar programs is the greater accuracy and more detailed output of data from dynamic analysis, as well as the possibility of configuring an asymmetric suspension on an axis (that is, the arrangement of the hardpoints is not symmetrical with respect to the median plane transverse to the corresponding axis).

10. BIBLIOGRAPHY

10.1 Books

Genta, G., *Motor vehicle dynamics*. Singapore, World Scientific Publishing Co. , 2008

Genta, G., Morello, L., *The automotive chassis, Volume 1: components design*, Springer 2009.

Genta, G., Morello, L., *The automotive chassis, Volume 2: system design*, Springer 2009.

Milliken, William F. and Douglas L., *Race Car Vehicle Dynamics*. Warrendale, Pennsylvania. SAE INTERNATIONAL (1995)

Smith, Carroll (1978). *Tune to win: the art and science of race car development and tuning*. 329 Aviston Road, Faltbrook. AERO PUBLISHERS, INC.

10.2 Thesis projects and documents

Amati, N., Notes of *Chassis Design* course at Politecnico di Torino, 2018.

Del Castro Graziano, D., *Modelo de suspensión de vehículo monoplaza mediante Adams/Car. Propuesta de mejoras*, 2017. Escuela Técnica Superior de Ingenieros Industriales, UPM, Madrid.

Fernández-Pedraza, M. C., *Ajuste del modelo de Pacejka '89 implementado en ADAMS/CAR a las curvas reales del neumático Hoosier 6.0/18.0 -10 LCO 6 (ancho de llanta 6')*, 2018. Universidad Politécnica de Madrid, Máster de Ingeniería Industrial.

Giaraffa, M., *Tech tip: Springs & Dampers, Part One*. OptimumG. (http://www.optimumg-.com/docs/Springs&Dampers_Tech_Tip_1.pdf)

Giaraffa, M., *Tech tip: Springs & Dampers, Part Two*. OptimumG. (http://www.optimumg-.com/docs/Springs&Dampers_Tech_Tip_2.pdf)

Giaraffa, M., *Tech tip: Springs & Dampers, Part Three*. OptimumG. (http://www.optimumg-.com/docs/Springs&Dampers_Tech_Tip_3.pdf)

Grazioso, A., Di Maria, E., Gallone, R., Margheriti, S., Prete, G., *Guida all'utilizzo di Adams/Car. Modellazione della sospensione anteriore del veicolo di Formula SAE "SRT15"*. Università del Salento.

Losada Arias, A., *Diseño de la suspensión trasera del vehículo Fórmula Student eléctrico 2018*, 2018. Escuela Técnica Superior de Ingenieros Industriales, UPM, Madrid.

10.3 Internet sites and videos

FSAE rules:
https://www.fsaeonline.com/page.aspx?pageid=c4c5195a-60c0-46aa-acbf-2958ef545b72
https://www.fsaeonline.com/cdsweb/gen/DownloadDocument.aspx?DocumentID=64b861c2-980a-40fc-aa88-6a80c43a8540
http://fsaeonline.com/cdsweb/gen/DownloadDocument.aspx?DocumentID=d9fa3638-59f8-411c-a487-e27abc2d9022
Ohlins TTX25 mk2:
https://www.ohlinsusa.com/suspension-products/Automotive/Auto+Racing/Shock+Absorber/70/TTX25+MkII
Tyre information: alignment. *https://www.tirerack.com/tires/tiretech/techpage.jsp?techid=4&*

Camber gain: *https://www.youtube.com/watch?v=c4AU7222nTk&t=321s*
Roll centre: *https://www.youtube.com/watch?v=tiq9NzKDtd4&t=19s*
Kick up and caster angle: *https://www.youtube.com/watch?v=EBzO6y8IYEg*
Ackermann: *https://www.youtube.com/watch?v=lXNxfTwmQSc*
Bump steer: *https://www.youtube.com/watch?v=tH7WgzXpk4Q&t=26s*
Anti-squat: *https://www.youtube.com/watch?v=BeuNZnZSm60*

11. ANNEX

11.1 Suspension hardpoints

11.1.1 Petrol vehicle

Front suspension

-583.2	-325	263.7	bellcrankpivotorient
-569.6	-326.3	263.2	bellcrankpivot
-550	-246.2	424.3	shocktochassis
-568.9	-386.5	302.5	shocktobellcrank
-618.5	-232.9	78.8	(none)
-612.4	-573.9	60.7	(none)
-346.9	-230.7	77.5	(none)
-564	-388.7	267.2	prodtobellcrank
-590.3	-534.3	85.4	prodouter
-766.0	-219.1	21.85	(none)
-661.9	-247	116.2	(none)
-675.1	-570.2	103.7	(none)
-609.8	-286	239.8	(none)
-577.7	-544.2	272.4	(none)
-343.5	-300.6	227	(none)
-604.5	-604.7	156.5	(none)
-512.0	0.0	27.4	(none)

Rear suspension

891.8	-213.3	284.2	(none)
901.8	-213.3	284.2	(none)
899.8	-33	326.8	(none)
901.8	-218.2	358.1	(none)
1000.0	-200.66	126.06	(none)
587.1	-348.8	75.3	(none)
933.7	-515.6	46.8	(none)
936.9	-192.5	62	(none)
901.2	-261.4	306.6	(none)
903.6	-508.1	77.6	(none)
1000.0	-381.0	63.5	(none)
935.5	-193.4	82.7	(none)
1028.2	-512.2	42.3	(none)
685.5	-313.4	201.4	(none)
954.1	-475.5	273.7	(none)
931.9	-231.7	244.4	(none)
945	-535.3	156.5	(none)
-900	0.0	-100	(none)

Steering

-661.9	247.0	116.2	(none)
-661.9	247.0	116.2	(none)
-100.0	0.0	450.0	(none)
0.0	0.0	500.0	(none)
-661.9	0.0	116.2	(none)
100.0	0.0	550.0	(none)

Front anti-roll bar

-515.6	388.7	220.0	(none)
-564.0	388.7	267.2	(none)
-564.0	388.7	220.0	(none)
-515.6	0.0	220.0	(none)

Rear anti-roll bar

850.0	-250.0	256.4	(none)
901.2	-250.0	306.6	(none)
850.0	-250.0	308.0	(none)
850.0	0.0	256.4	(none)

11.1.2 Electric vehicle

Front suspension

-600.0	-280.5	405.0	"bellcrankpivotorient"
-580.0	-280.3	405.2	"bellcrankpivot"
-580.0	-70.0	450.5	"shocktochassis"
-580.0	-270.5	460.5	"shocktobellcrank"
-708.5	-205.9	63.0	"lca"
-604.5	-575.9	50.7	"lca"
-376.9	-205.7	92.0	"lca"
-580.0	-305.7	435.0	"prodtobellcrank"
-580.0	-514.3	265.4	"prodouter"
-766.0	-219.1	21.85	"(none)"
-708.5	-235.9	100.2	"tr"
-695.5	-540.2	90.7	"tr"

Rear suspension

941.8	-238.3	434.2	(none)
951.8	-238.3	434.2	(none)
949.8	-33.0	482.8	(none)
951.8	-238.2	495.1	(none)
1000.0	-200.66	126.06	(none)
717.1	-313.8	95.3	(none)
960.7	-555.6	60.8	(none)
1058.2	-257.5	72.0	(none)
951.2	-271.4	466.6	(none)
953.6	-503.1	237.6	(none)
1000.0	-381.0	63.5	(none)
1078.2	-258.4	94.7	(none)

-624.8	-280.9	268.0	"uca"
-580.3	-550.3	267.4	"uca"
-348.5	-280.7	294.8	"uca"
-604.5	-604.7	156.5	"wheelcenter"
-512.0	0.0	27.4	(none)

1058.2	-577.2	87.3	(none)
715.5	-298.4	268.4	(none)
984.1	-530.5	253.7	(none)
1030.9	-286.7	237.4	(none)
975.0	-600.0	156.5	(none)
-900.0	0.0	-100.0	(none)

Steering			
-708.5	-205.9	55.2	"tr"
-708.5	-225.9	55.2	"tr"
-200.0	0.0	400.0	(none)
0.0	0.0	500.0	(none)
-708.5	0.0	55.2	(none)
100.0	0.0	550.0	(none)

Front anti-roll bar			
-510.0	-270.0	570.4	(none)
-575.0	-270.0	500.4	(none)
-575.0	-270.0	570.4	(none)
-510.0	0.0	570.4	(none)

Rear anti-roll bar			
850.0	-255.0	550.0	(none)
951.2	-255.0	500.0	(none)
951.2	-255.0	550.0	(none)
850.0	0.0	550.0	(none)

11.1.3 Final model – 2020 single seater

Front suspension			
-600.0	-280.5	405.0	"bellcrankpivotorient"
-580.0	-280.3	405.2	"bellcrankpivot"
-580.0	-70.0	450.5	"shocktochassis"
-580.0	-270.5	460.5	"shocktobellcrank"
-708.5	-255.9	60.8	"lca"
-604.5	-575.9	50.7	"lca"
-376.9	-255.7	87.5	"lca"
-580.0	-305.7	435.0	"prodtobellcrank"
-580.0	-514.3	265.4	"prodouter"
-766.0	-219.1	21.85	(none)
-708.5	-235.9	100.2	"tr"
-695.5	-540.2	90.7	"tr"
-624.8	-270.9	268.0	"uca"
-580.3	-550.3	267.4	"uca"
-348.5	-270.7	295.8	"uca"
-604.5	-604.7	156.5	"wheelcenter"
-512.0	0.0	27.4	(none)

Rear suspension			
941.8	-238.3	434.2	(none)
951.8	-238.3	434.2	(none)
949.8	-33.0	482.8	(none)
951.8	-238.2	495.1	(none)
1000.0	-200.66	126.06	(none)
717.1	-313.8	95.3	(none)
960.7	-555.6	60.8	(none)
1058.2	-257.5	72.0	(none)
951.2	-271.4	466.6	(none)
953.6	-503.1	237.6	(none)
1000.0	-381.0	63.5	(none)
1078.2	-258.4	94.7	(none)
1058.2	-577.2	87.3	(none)
715.5	-298.4	268.4	(none)
984.1	-530.5	253.7	(none)
1030.9	-286.7	237.4	(none)
975.0	-600.0	156.5	(none)
-900.0	0.0	-100.0	(none)

Steering			
-708.5	-205.9	100.2	"tr"
-708.5	-235.9	100.2	"tr"
-200.0	0.0	450.0	(none)
0.0	0.0	520.0	(none)
-708.5	0.0	100.2	(none)
100.0	0.0	550.0	(none)

Front anti-roll bar			
-510.0	-280.0	530.4	(none)
-575.0	-280.0	460.4	(none)
-575.0	-280.0	530.4	(none)
-510.0	0.0	530.4	(none)

Rear anti-roll bar			
850.0	-255.0	530.0	(none)
951.2	-255.0	480.0	(none)
951.2	-255.0	530.0	(none)
850.0	0.0	530.0	(none)

11.2 MATLAB scripts

```
%% *** SUSPENSION STIFFNESS COMPUTATIONS ***

clc
close all
clear all

%% EDITABLE
mf =                %front mass kg
```

```
mr =                %rear mass kg
m_sprung =          %sprung mass considering driver
fn = 3;             %natural frequency sprung (1.4 - 7.6 Hz)

Gfi = 1;            %1 deg per g (required roll angle per lateral
                    %acceleration)
Kt = 100000;        %tire stiffness

hcg =               %centre of gravity height
tf =                %front track
tr =                %rear track
rcf =               %front roll centre height
rcr =               %rear roll centre height
a =                 %distance between front axle and cg
b =                 %distance between rear axle and cg
cgx =               %horizontal displacement of cg to get correct mf and mr
MR_fa =             %motion ratio front arb
MR_ra =             %motion ratio rear arb


%% FRONT SUSPENSION
M = mf + mr;        %vehicle mass kg

MR_f =              %front rocker motion ratio

Kw = mf*(2*pi*fn)^2     %required wheel stiffness (at the axle level)
Ks = Kw*0.5*MR_f^2      %required suspension stiffness (at the single
                        %corner)

Ks_f =              % CHOSEN FRONT SUSPENSION STIFFNESS

Kw_f = Ks_f/MR_f^2                    %actual wheel stiffness
freq_nat_f = sqrt(2*Kw_f/mf)/(2*pi)   %actual front sprung natural
                                      %frequency

fn_unf = sqrt(Kw_f/((M-m_sprung)/4))/(2*pi)    %actual unsprung natural
                                               %frequency

%% REAR SUSPENSION
MR_r =              %rear rocker motion ratio

Kw = mr*(2*pi*fn)^2     %required wheel stiffness (at the axle level)
Ks = Kw*0.5*MR_r^2      %required suspension stiffness (at the single
                        %corner)

Ks_r =              % CHOSEN REAR SUSPENSION STIFFNESS

Kw_r = Ks_r/MR_r^2                    %actual wheel stiffness
freq_nat_r = sqrt(2*Kw_r/mr)/(2*pi)   %actual rear sprung natural
                                      %frequency

fn_unr = sqrt(Kw_r/((M-m_sprung)/4))/(2*pi)    %actual unsprung natural
                                               %frequency

%% CG HEIGHT

H = 1e-3*(hcg - ((rcf-rcr)*cgx/(a-b)+(-b*(rcf-rcr)+rcr*(a-b))/(a-b)))
                    %distance between cg and roll axis
```

```
%% ROLL STIFFNESS
t = (tf+tr)/2;                %average track
Kw = (Kw_f+Kw_r)*2;           %total wheel stiffness

Kfi_obj = M*9.81*H/Gfi        %required vehicle roll stiffness

Kfi_arb = (pi/180)*((Kfi_obj*Kt*(t^2/2))/(Kt*(t^2/2)*pi/180-Kfi_obj)-
Kw*(t^2/2))       %required arb stiffness
Kfi_arb_f = (180/pi)*(mf/M + 0.05)*Kfi_arb*MR_fa^2
                  %front arb stiffness
Kfi_arb_r = (180/pi)*(1 - mf/M - 0.05)*Kfi_arb*MR_ra^2
                  %rear arb stiffness
```

11.3 Tire model

```
$---------------------------------------------------------------------DIMENSION
[DIMENSION]
 UNLOADED_RADIUS        = 228.6
 WIDTH                  = 152.4
 ASPECT_RATIO           = 0.47
$---------------------------------------------------------------------PARAMETER
[PARAMETER]
 VERTICAL_STIFFNESS     = 150
 VERTICAL_DAMPING       = 9.0
 LATERAL_STIFFNESS      = 190.0
 ROLLING_RESISTANCE     = 0.01
$-------------------------------------------------------------------------shape
[SHAPE]
{radial width}
 1.0   0.0
 1.0   0.2
 1.0   0.4
 1.0   0.5
 1.0   0.6
 1.0   0.7
 1.0   0.8
 1.0   0.85
 1.0   0.9
 0.9   1.0
$----------------------------------------------------------LATERAL_COEFFICIENTS
[LATERAL_COEFFICIENTS]
 a0  =  1.661
 a1  = -34.0
 a2  =  2261.586
 a3  =  3036.00
 a4  =  12.80
 a5  =  0.00501
 a6  = -0.02103
 a7  =  0.77394
 a8  =  0.0022890
 a9  =  0.013442
 a10 =  -0.595051
 a11 =  19.1656
 a12 =  1.21356
 a13 =  6.26206
$------------------------------------------------------------------longitudinal
[LONGITUDINAL_COEFFICIENTS]
 b0  =    380.2
 b1  =    1075.96
 b2  =    1400
 b3  =    0
 b4  =    175
 b5  =    0.1
 b6  =    0.005
 b7  =    -0.1
 b8  =    27580.06
 b9  =    0
 b10 =    0
$--------------------------------------------------------------------aligning
[ALIGNING_COEFFICIENTS]
 c0  =  2.34000
 c1  =  1.4950
 c2  =  31.9536
 c3  = -3.57403
 c4  = -0.087737
 c5  =  0.098410
 c6  =  0.0027699
 c7  = -0.0001151
 c8  =  0.1000
 c9  =     228.153
 c10 =  0.025501
 c11 = -0.02357
 c12 =  0.03027
 c13 = -0.0647
 c14 =  0.0211329
 c15 =  0.89469
 c16 = -0.099443
 c17 = -1.65574
```

11.4 Electric engine technical drawings

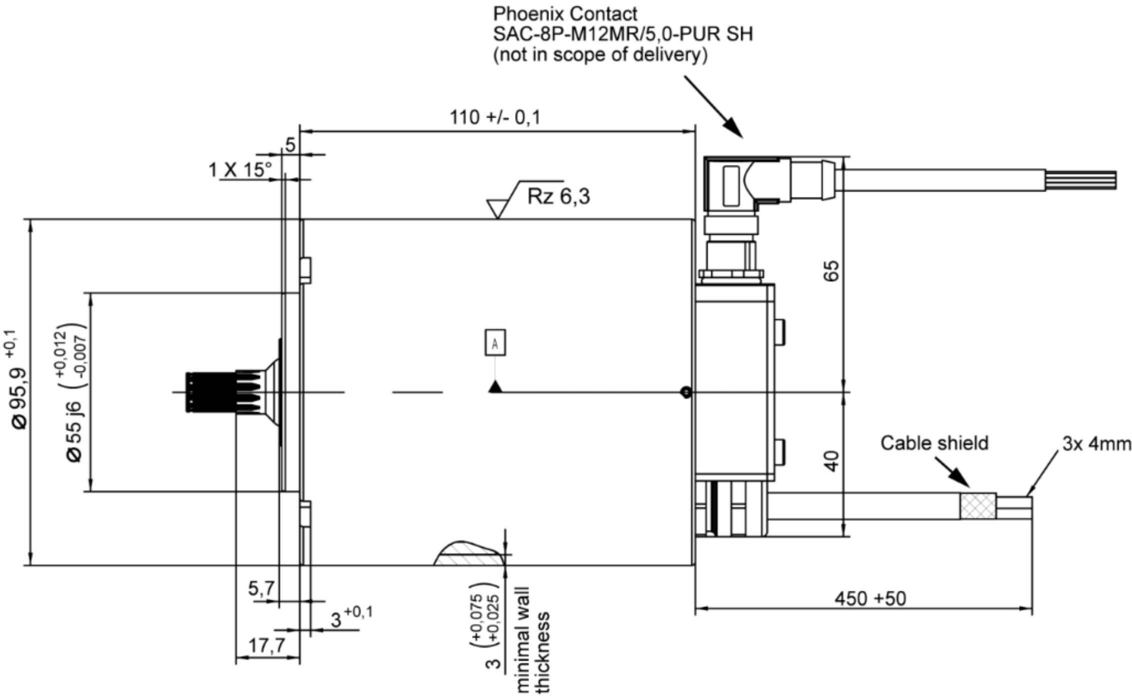

Phoenix Contact
SAC-8P-M12MR/5,0-PUR SH
(not in scope of delivery)
110 +/- 0,1
5
1 X 15°
Rz 6,3
A
65
40
Ø95,9 +0,1
Ø55 j6 (+0,012 / -0,007)
Cable shield
3x 4mm²
5,7
3 +0,1
17,7
3 (+0,075 / +0,025)
minimal wall thickness
450 +50

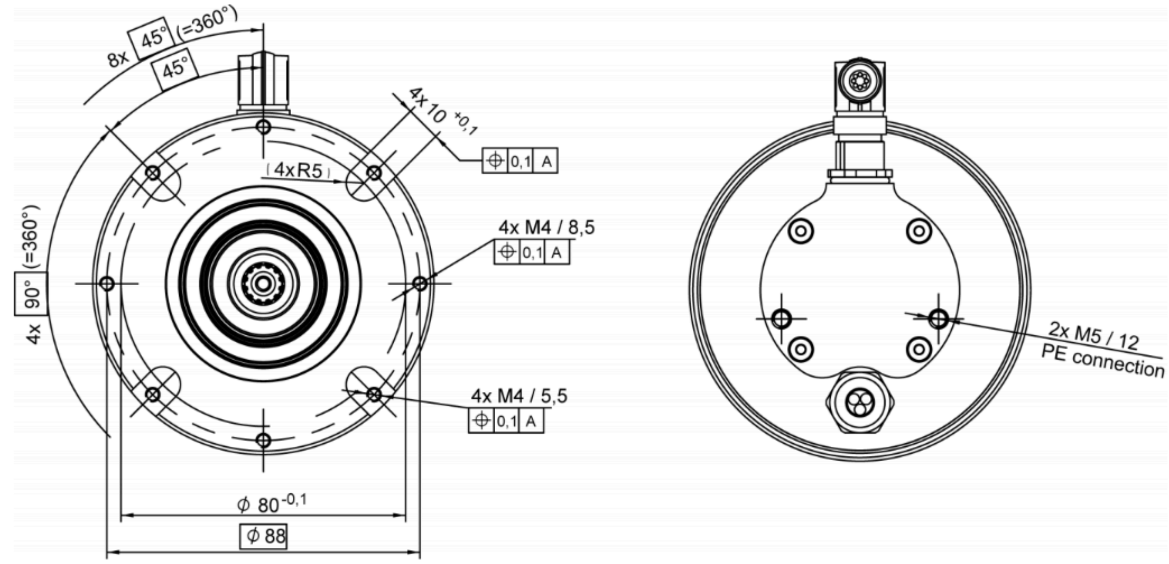
8x 45° (=360°)
45°
4x 10 +0,1
⌖ 0,1 A
4xR5
4x M4 / 8,5
⌖ 0,1 A
4x 90° (=360°)
4x M4 / 5,5
⌖ 0,1 A
ϕ 80 -0,1
ϕ 88
2x M5 / 12
PE connection